Chiral Chemistry

Science Exploration

Open Access Review

Recent advances in the construction of C-N axial chirality via asymmetric C-H activation

Junlian Ji, Jun Wang*

Key Laboratory of Bioinorganic and Synthetic Chemistry of Ministry of Education, School of Chemistry, and Guangdong Key Laboratory of Chiral Molecule and Drug Discovery, Sun Yat-sen University, Guangzhou 510006, Guangdong, China.

***Correspondence to:** Jun Wang, Key Laboratory of Bioinorganic and Synthetic Chemistry of Ministry of Education, School of Chemistry, and Guangdong Key Laboratory of Chiral Molecule and Drug Discovery, Sun Yat-sen University, Guangzhou 510006, Guangdong, China. E-mail: wangjun23@mail.sysu.edu.cn

Received: July 27, 2026 **Accepted:** October 28, 2026 **Published:** October 28, 2026

Cite this article: Ji J, Wang J. Recent advances in the construction of C-N axial chirality via asymmetric C-H activation. Chiral Chem. 2027;3:202635. https://doi.org/10.70401/cc.2026.0046

Abstract

C-N chiral axes are prevalent in natural products, bioactive molecules, and chiral ligands. The development of synthetic methodologies for constructing C-N chiral axes has attracted considerable interest among chemists. Herein, we review advances in the construction of C-N axial chirality via asymmetric C-H activation, a strategy with high atom- and step-economy. This review covers the literature from 2019 to 2026, categorizing the transformations into annulation, alkynylation, alkenylation, alkylation, arylation, borylation and imidoylation. The representative products, reaction mechanisms, and the application of products are demonstrated. We hope this review will serve as a useful guide for chemists interested in this field and stimulate further progress in this area.

Keywords: C-N Axial chirality, C-H activation, asymmetric catalysis

1. Introduction

C-N axially chiral frameworks are increasingly recognized as structurally intriguing and synthetically valuable motifs, which can be widely found in natural products[1-3], chiral ligands[4-6] and bioactive molecules[7-9] (Figure 1a). Notably, their C-N chiral axes require a sufficiently high rotational energy barrier to maintain configurational stability. According to the stability of such chiral axes, they could be categorized into three types: Type1 ($\Delta G^{\ddagger}_{rac}$ < 20 kcal/mol), highly unstable, with a half-life of mere seconds, rendering it of no practical value; Type2 ($\Delta G^{\ddagger}_{rac}$ = 20-30 kcal/mol), moderately stable, with axial chirality persisting from hours to months; and Type3 ($\Delta G^{\ddagger}_{rac}$ > 30 kcal/mol), very stable, with a half-life of years, making these atropisomers the most suitable candidates for chiral ligands and bioactive molecules[10-14]. Compared with biaryl counterparts, C-N atropisomers exhibit more flexible conformations and greater rotational freedom, which makes the enantioselective control of the C-N chiral axis formation more challenging[15]. In the early 2000s, the groups of Taguchi[16] and Curran[17] independently reported the asymmetric synthesis of C-N axially chiral anilides via Pd-catalyzed *N*-allylation of achiral N-H anilides, albeit with enantiomeric excesses (ee) of 33-44% and 12-53%, respectively. Subsequently, various strategies, including chiral resolution and asymmetric synthesis, have been developed to obtain chiral compounds with C-N axial chirality.

Transition metal-catalyzed asymmetric C-H activation has emerged as a powerful tool for accessing enantioenriched molecules from simple and readily available starting materials, featuring high step- and atom-economy. In 2019, the groups of Shi[18], Wang[19] and Xie[20] independently reported the asymmetric C-H activation to construct C-N chiral axes via alkynylation, [2+2+2] annulation, and alkenylation, respectively. Since then, studies on the construction of C-N axial chirality via asymmetric C-H activation have advanced rapidly, and a variety of transition-metal catalysts have been employed (e.g., Co, Pd, Rh, Ru, Ir and Fe) (Figure 1b).

Several reviews have appeared on the synthesis of C-N axially chiral compounds. Some are organized by catalyst type[21], synthetic strategy[15,22-24], or reaction type[25,26], whereas others focus on a specific class of catalyst[27,28], strategy[29] or reaction[30,31]. To date, a comprehensive review focusing on asymmetric C-H activation strategy for C-N axis construction is still lacking. The present review aims to fulfil this purpose and summarizes the advances from 2019 to 2026. It is organized by reaction type, including asymmetric C-H activation/annulation, alkynylation, alkenylation, alkylation, arylation, borylation and imidoylation (Figure 1b). We hope this review could serve as a useful guide for chemists interested in this field and stimulate further progress in this area.

© The Author(s) 2026. This is an Open Access article licensed under a Creative Commons Attribution 4.0 International License (https://creativecommons.org/licenses/by/4.0/), which permits unrestricted use, sharing, adaptation, distribution and reproduction in any medium or format, for any purpose, even commercially, as long as you give appropriate credit to the original author(s) and the source, provide a link to the Creative Commons license, and indicate if changes were made.

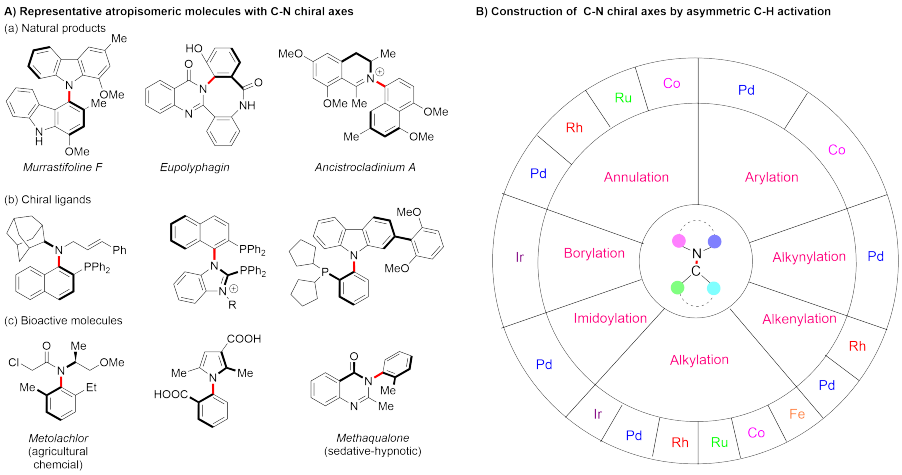

Figure 1. (a) Representative atropisomeric molecules with C-N chiral axes[1-9]; (b) Construction of C-N chiral axes by asymmetric C-H activation.

2. Asymmetric C-H Activation/Annulation Reactions

Asymmetric C-H activation/annulation reactions have been widely applied in the construction of axial chirality. In 2019, Wang and coworkers reported the construction of C-N axial chirality via asymmetric C-H activation/annulation[19]. Subsequently, numerous chemists have further advanced this strategy, establishing it as one of the most effective methods for constructing C-N axial chirality. Based on the annulation mode, these reactions can be classified into [2+2+2], [4+2], [3+2], [4+1], and [3+3] annulations.

2.1 [2+2+2] annulation reaction

In 2008, Satoh and Miura disclosed a Rh^{III}-catalyzed aromatic homologation reaction that proceeds via chelation-assisted dual C-H activation in a [2+2+2] annulation mode[32]. This transformation has garnered significant attention from chemists due to its ability to rapidly construct polycyclic aromatic and heteroaromatic compounds. Afterwards, a diverse range of C-H activation substrates and alkynes have been explored, and the catalyst has been extended from Rh to Pd, Ni, Co, and others[33,34].

However, the asymmetric Satoh-Miura reaction remained elusive until 2019. In that year, Wang and coworkers achieved the first asymmetric Satoh-Miura-type reaction employing You's chiral spiro-CpRh catalyst **C1** in combination with an indolinone directing group (Figure 2a)[19]. This reaction furnished the C-N axially chiral products **3** from *N*-aryloxindoles **1** and alkynes **2** in 17-99% yield and 8-99% ee. Mechanistically, under the catalysis of Rh complex **C1**, substrate **1** undergoes twofold C-H activation, each followed by coordination and migratory insertion of an alkyne. Final reductive elimination furnishes the target axially chiral product **3**.

In 2022, the same group developed a new catalyst **C2** for the above asymmetric Satoh-Miura-type reaction. The C-N axially chiral products **3** were obtained in 45-95% yield with 78-94% ee (Figure 2b)[35]. Compared with the former study, this reaction proceeded with reduced catalyst loadings (2.5 mol%) and an extended reaction time (72 h) at a lower temperature (45 °C).

By using a chiral transient directing group (TDG) strategy, Xie and coworkers developed a Pd-catalyzed asymmetric Satoh-Miura-type reaction for the construction of C-N axial chirality from *N*-arylindole-based aldehydes **4** and alkynes **2** (Figure 3)[36]. Four products **5** were successfully prepared in 25-40% yield with 95-98% ee.

2.2 [4+2] annulation reaction

The asymmetric C-H activation/[4+2] annulation reaction has been extensively investigated. Its reaction mechanism involves directing group-assisted C-H activation, migratory insertion of an unsaturated bond, and subsequent reductive elimination to close the 6-menbered ring to afford the target product (Figure 4). This transformation represents a powerful tool for constructing C-N axial chirality. Typical reactants employed in such annulations include alkynes, allenes and alkenes. The following discussions are organized accordingly. However, the Catellani reaction, which uses aryl halides as starting materials, does not follow this mechanism (Section 2.2.4).

2.2.1 Using alkynes as reactants

2.2.1.1 Products only with C-N axial chirality

One of the facile ways to generate C-N axially chiral products is the C-H activation/[4+2] annulation reaction with properly designed C-N containing reactants. The originally rotationally flexible C-N bond in the reactants becomes rotationally restricted in the products, thus generating a C-N chiral axis. Under chiral induction by a chiral catalyst, this axis would preferentially adopt one configuration during its formation.

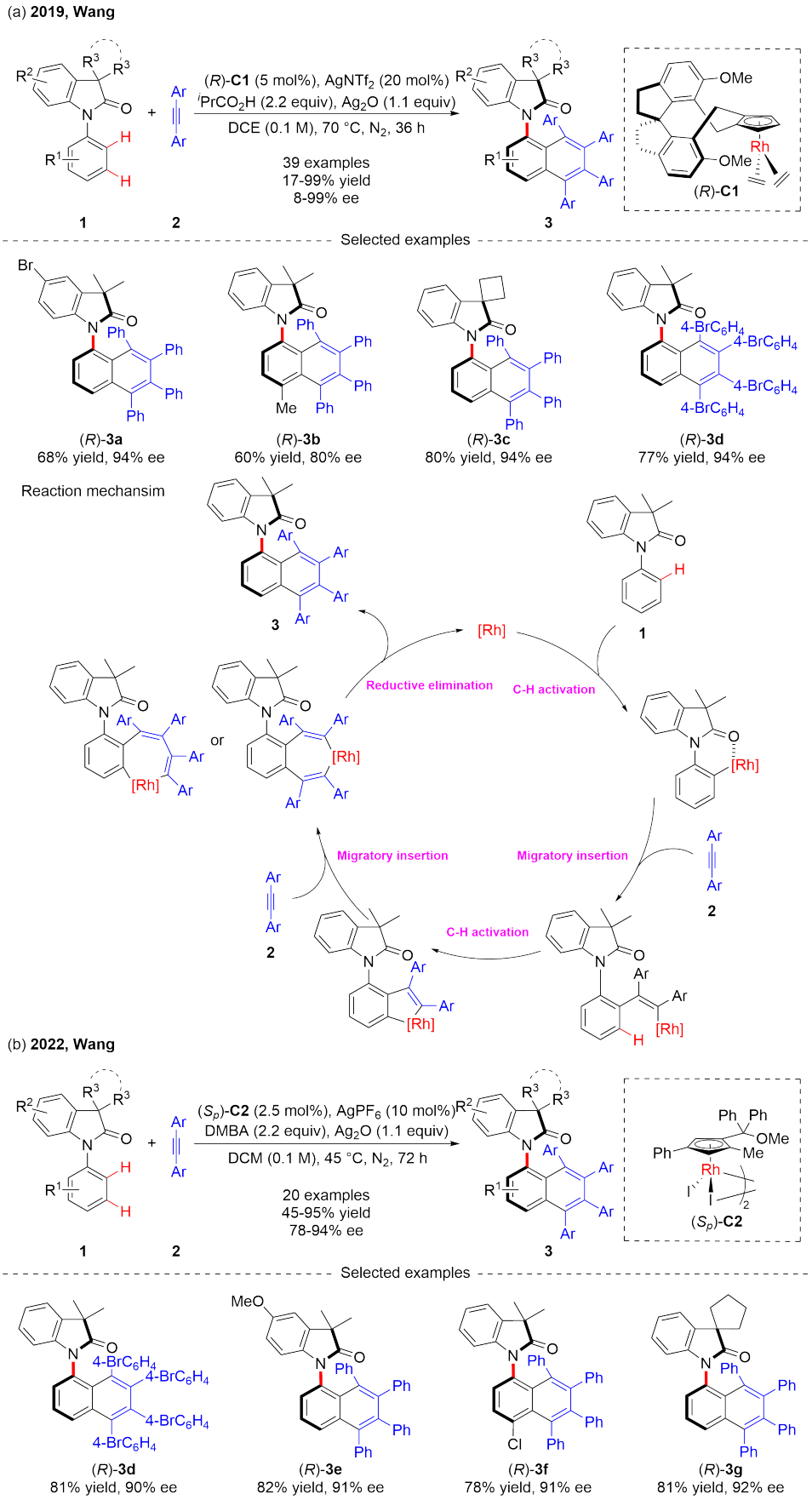

Figure 2. [2+2+2] annulation of *N*-aryloxindoles with alkynes[19,35]. DCM: dichloromethane; DCE: 1,2-dichloroethane; DMBA: dimethylbarbituric acid.

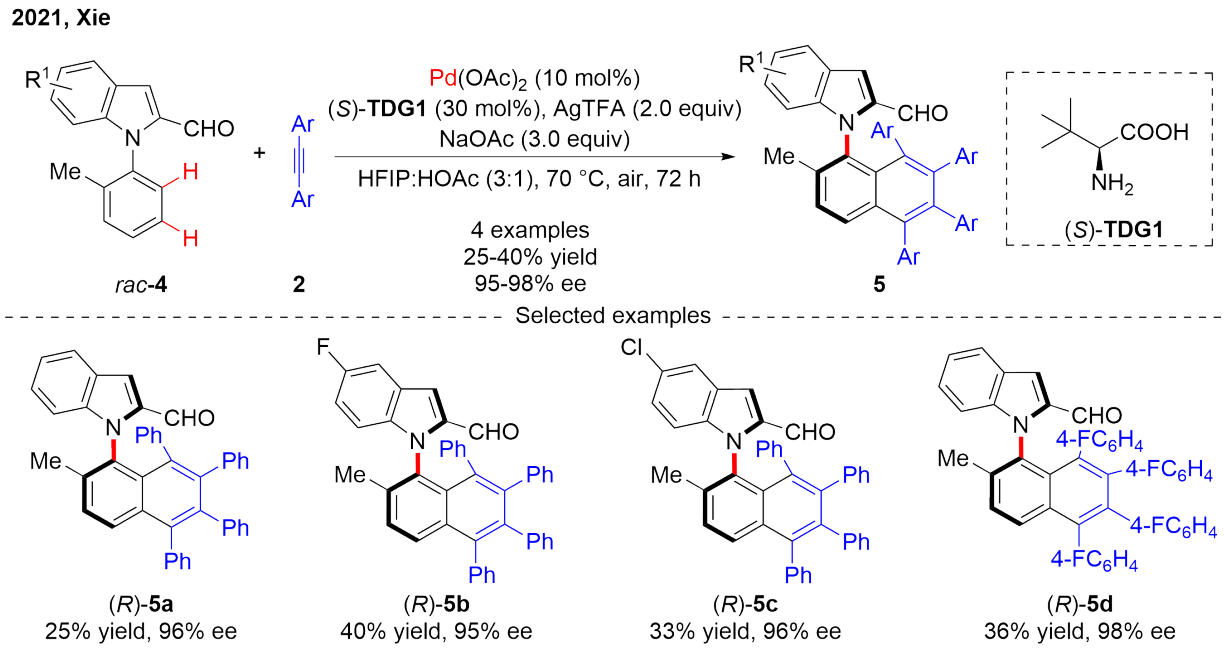

Figure 3. [2+2+2] annulation of *N*-arylindole-based aldehydes with alkynes[36]. HFIP: hexafluoroisopropanol; TDG: transient directing group.

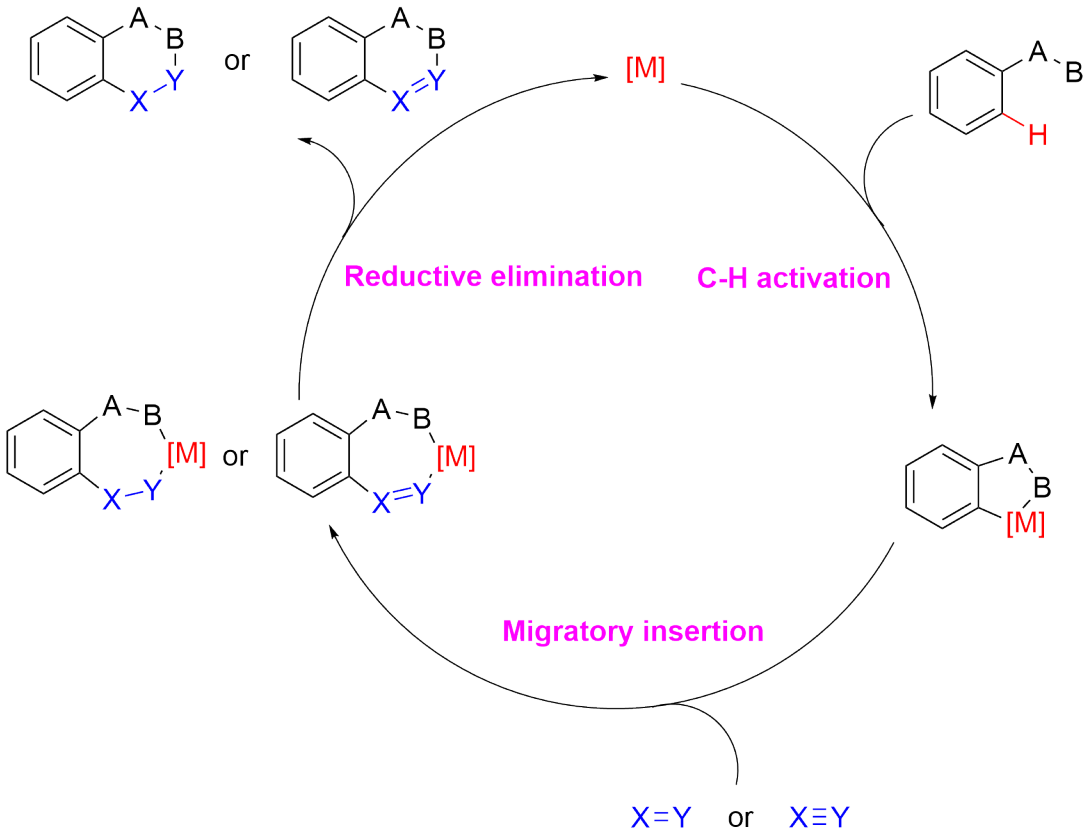

Figure 4. General mechanism for C-H activation/[4+2] annulation reactions.

In 2022, Li and coworkers constructed a C-N chiral axis from sulfonium ylides **6** with alkynes **7** or **8** bearing an amine or indole motif (Figure 5)[37]. Using Cramer's chiral $CpRh^{III}$ catalyst **C3** in combination with chiral acid **A1**, sulfoxonium ylides **6** and alkynes **7** were converted into C-N axially chiral naphthylamines **9** in 54-85% yield with 77-98% ee. In contrast, products **10** could be obtained in high yields and excellent enantioselectivities (80-97% yield and 80-99% ee) using chiral $CpRh^{III}$ catalyst **C3** alone, without adding chiral acids. Notably, products **10** exhibit a high rotational barrier ($\Delta G^{\ddagger}_{rac}$ > 34.1 kcal/mol in toluene at 100 °C).

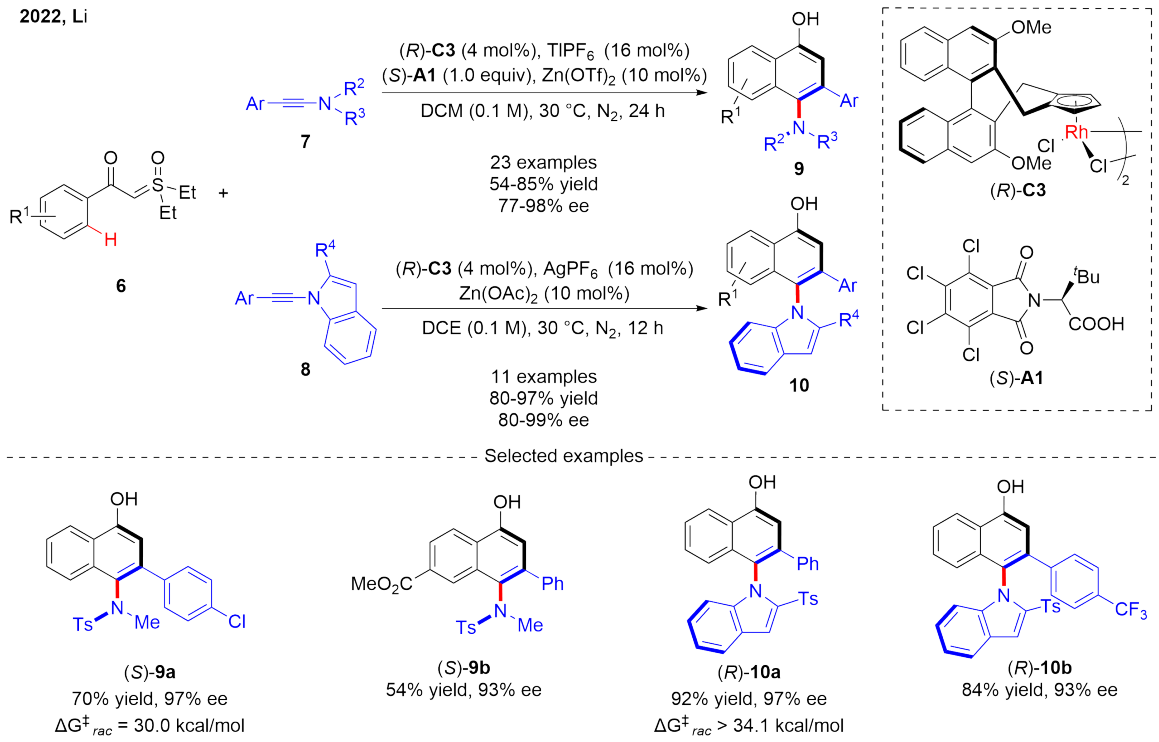

Figure 5. Synthesis of C-N axially chiral naphthylamines or indoles via [4+2] annulation[37]. DCM: dichloromethane; DCE: 1,2-dichloroethane.

In 2022, Niu and coworkers achieved a C-H activation/[4+2] annulation, utilizing *N*-(quinolin-8-yl)benzamide **11** and alkynes **12** as starting materials (Figure 6a)[38]. Using Co^{II}/salicyloxazoline (Salox) **L1** as the catalyst, the C-N axially chiral products **13** were obtained in 7-98% yield with 86-98% ee. Density functional theory (DFT) calculations revealed that reductive elimination was the enantiodetermining step. The *R*-configured transition states including (*R*)-**TS1** and (*R*)-**TS2** are both energetically preferred over their *S*-configured counterparts. And (*R*)-**TS1** is the most favored. It is worth noting that, following this work[38] as well as those by Shi[39,40], the Co^{II}/Salox-catalyzed enantioselective C-H functionalization has garnered significant attention and witnessed great progress, largely owing to its low cost and ready availability.

Subsequently, Ackermann and coworkers applied electrocatalysis to the [4+2] annulation of *N*-(quinoline-8-yl)benzamide **11** with 4-hydroxyalkynoate **14**, followed by transesterification (Figure 6b)[41]. Using Co^{II}/Salox **L2** as the catalyst, the corresponding C-N axially chiral lactone products **15** were obtained in 81-95% yield with 99% ee. Only eight examples were reported. Electrocatalysis could avoid stoichiometric oxidants and operate at lower temperatures. But it required ionic liquid as reaction media.

In 2026, Lu and coworkers reported the [4+2] annulation of *N*-(quinoline-8-yl)benzamides **11** with alkynes **12** at room temperature using Co^{II}/Salox catalyst **L1** (Figure 6c)[42]. This reaction delivered C-N axially chiral isoquinolinones **13** in 6-95% yield with 77-97% ee under conventional conditions (**Condition A**). Although the conditions were milder than those reported by Niu[38], many substrates only gave low yields. Lu found that light irradiation could improve the yields of less reactive substrates without compromising enantioselectivity (30-99% yield and 73-98% ee under **Condition B** or **Condition C**). Notably, **Conditions B** and **C** were suitable for different substrates.

In 2023, Niu and coworkers expanded the substrate scope of the Co-catalyzed asymmetric [4+2] annulation from *N*-(quinoline-8-yl)benzamide **11** to sulfonamide substrates **16** and successfully synthesized C-N axially chiral *S*-heteroisoquinolinone products **17** (Figure 7)[43]. With Co^{II}/Salox **L3** as the optimal catalyst and $Mn(OAc)_3{\cdot}2H_2O$ as the oxidant, products **17** were obtained in 20-96% yield with 91-99% ee under conventional conditions (**Condition A**). In an effort to circumvent the use of a stoichiometric oxidant, they introduced electrocatalysis into this reaction and found that certain products could be obtained in higher yields under milder reaction conditions (35-99% yield and 93-99% ee under **Condition B**).

Niu and coworkers also extended the reaction to the benzamide substrates derived from 2-aminopyridine 1-oxide (PyO-amine), constructing a series of C-N axially chiral pyridine *N*-oxides **19** (Figure 8)[44]. High enantioselectivity is considered difficult to achieve for this reaction, since the pyridine *N*-oxide (PyO) directing group is less sterically demanding than the quinolinyl group and forms a weaker π-π interaction with the Salox ligand. Through evaluation of various ligands, Niu found that only sterically hindered Salox ligands such as **L3** could deliver high enantioselectivity. Moreover, this reaction also exhibited excellent regioselectivity for unsymmetrical alkynes **12**, affording products **19** in 35-97% yield and 88-98% ee.

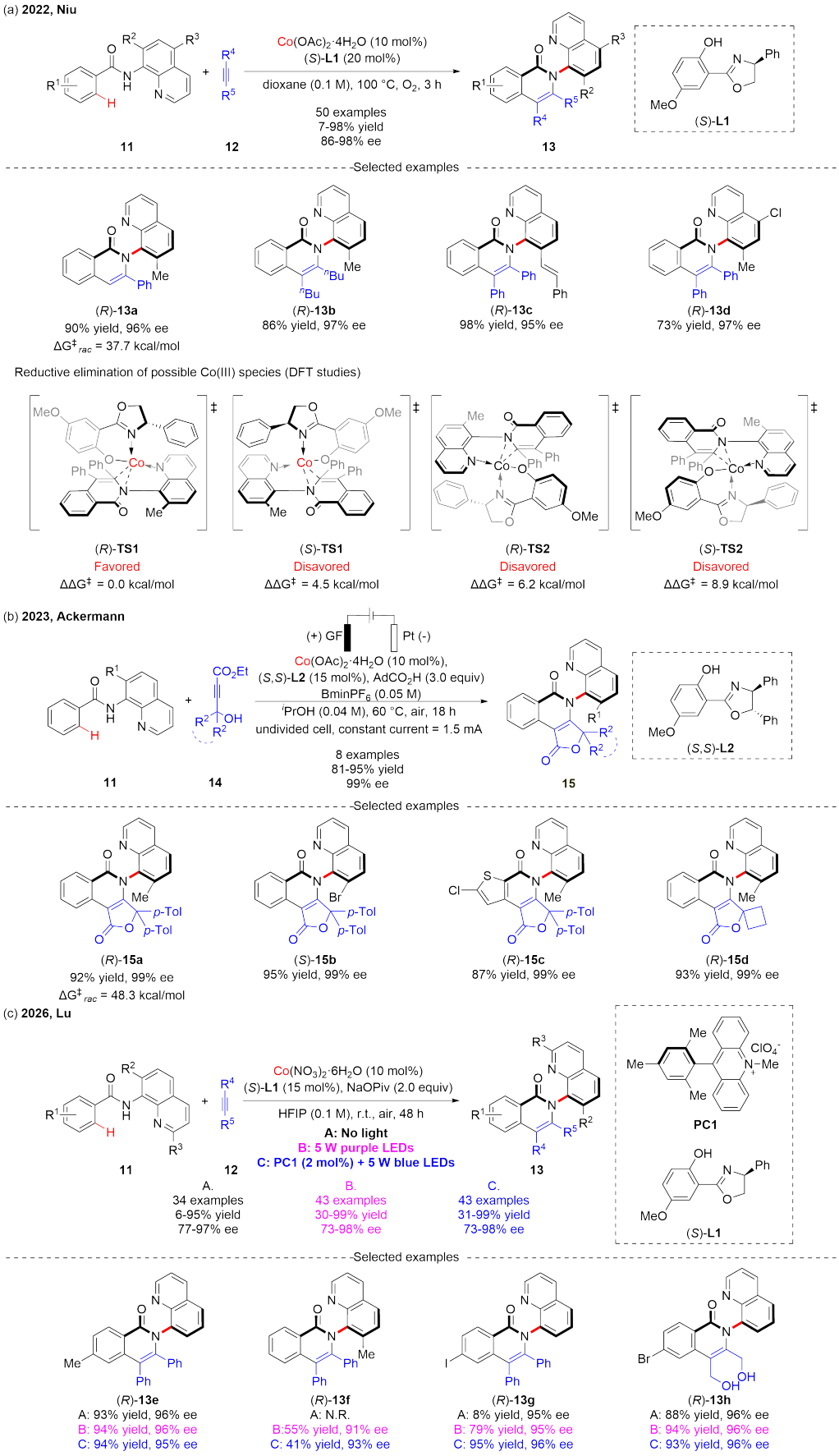

Figure 6. Synthesis of C-N axially chiral isoquinolinone frameworks with *N*-(quinolin-8-yl)benzamides and alkynes via [4+2] annulation[38,41,42]. HFIP: hexafluoroisopropanol.

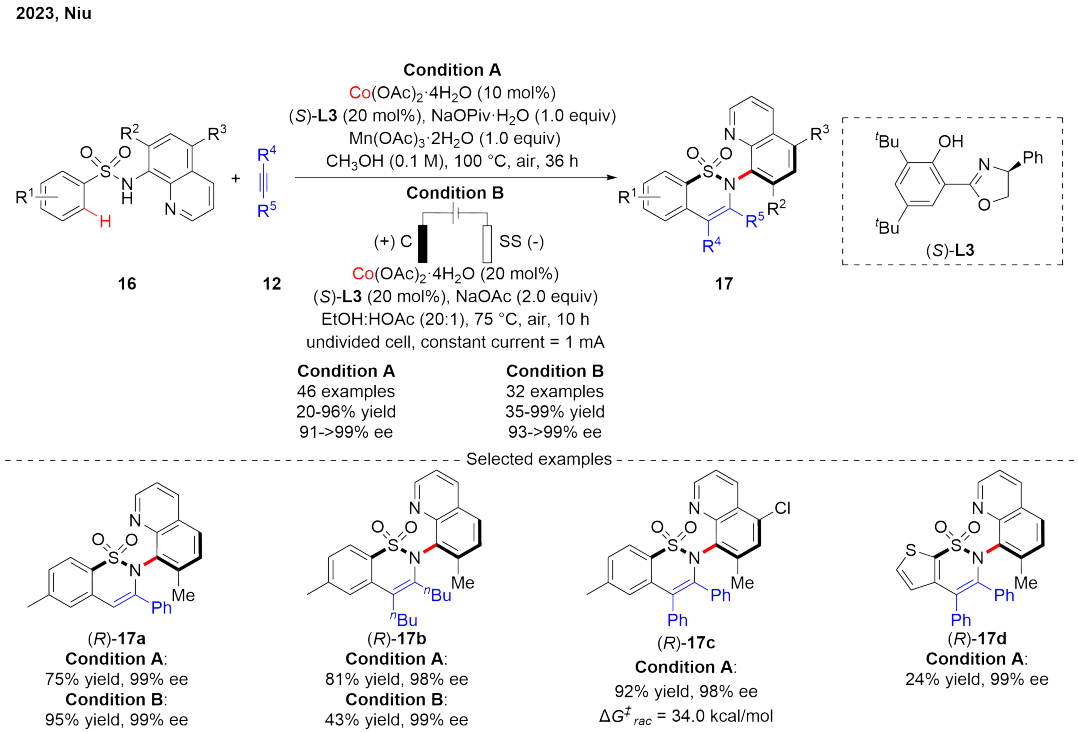

Figure 7. Synthesis of C-N axially chiral *S*-heteroisoquinolinones with aryl sulfonamides and alkynes via [4+2] annulation[43]. HOAc: acetic acid; EtOH: ethanol.

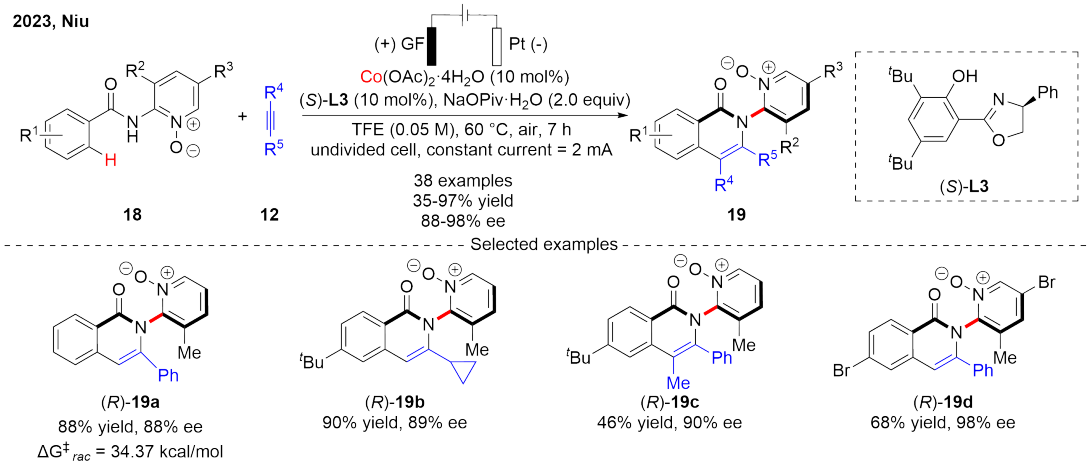

Figure 8. Synthesis of C-N axially chiral pyridine *N*-oxides from benzamides and alkynes via [4+2] annulation[44]. TFE: 2,2,2-trifluoroethanol.

2.2.1.2 Products with C-N axial chirality and other chiral elements

Synthesis of products possessing C-N axial chirality along with other chiral elements has also been reported. In 2022, Shi and coworkers developed an intramolecular [4+2] annulation for the construction of both C-N and C-C axial chirality using the Co^{II}/Salox **L4** catalyst (Figure 9)[40]. Despite the high steric hindrance, the reaction of benzamides **20** bearing an 8-aminoquinolinyl (8-AQ) directing group proceeded smoothly, affording products **21** with 24-99% yield, 41 -> 99% ee and 1.2:1-70:1 dr. It was found that products with extended π-conjugated aryl substituents at the C8 position, such as **21b**, displayed significant circularly polarized luminescence (CPL) activity, rendering them suitable candidates for potential CPL applications.

In 2023, Li and coworkers developed the simultaneous construction of C-N and N-N axial chirality through a Rh-catalyzed [4+2] annulation of *N*-(7-azaindol-1-yl)benzamides **22** with alkynes **8** (Figure 10)[45]. The two distal axes exhibit weak interactions, which may render it challenging to achieve high enantioselectivity and diastereoselectivity. With Cramer's $CpRh^{III}$ catalyst, a range of products **23** was obtained in varied yields with excellent enantioselectivities and high diastereoselectivities (32-82% yield, 88-99% ee and > 20:1 dr). Solvent screening identified heavily halogenated haloarenes as beneficial for enantio- and diastereoselectivity, with **S1** being optimal.

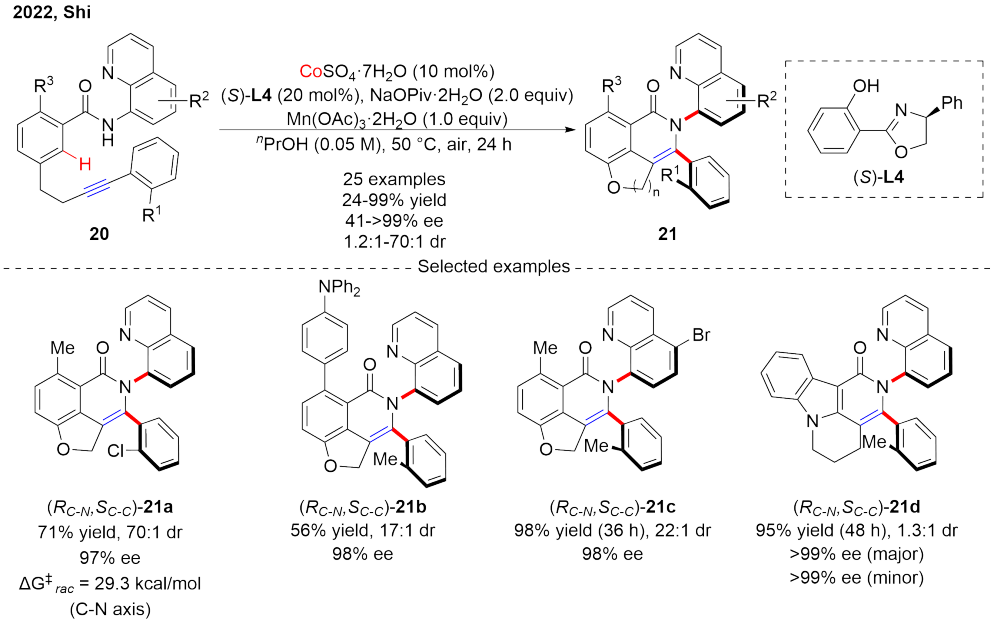

Figure 9. Synthesis of chiral isoquinolinones bearing both C-N and C-C chiral axes via intramolecular [4+2] annulation[40].

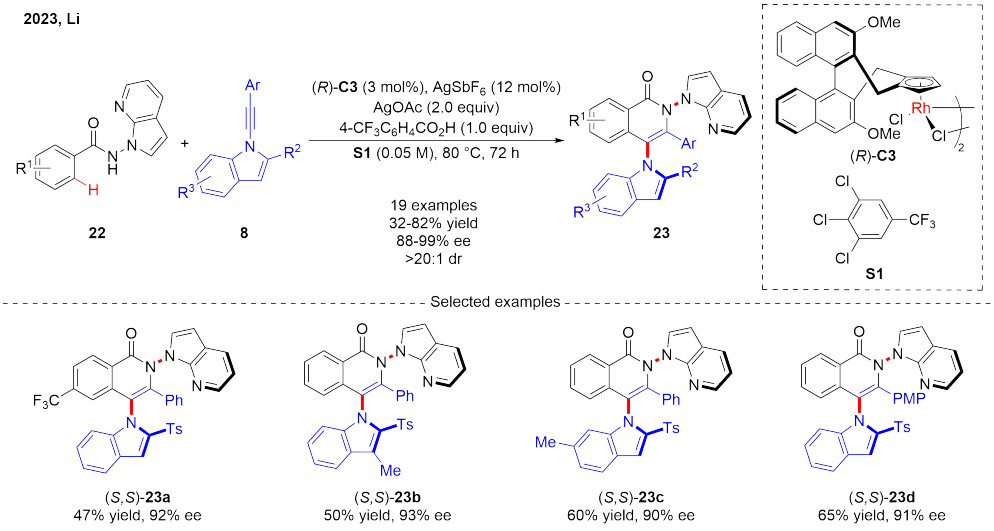

Figure 10. Synthesis of chiral isoquinolinones bearing both C-N and N-N chiral axes via intermolecular [4+2] annulation[45].

In 2024, Niu reported the reaction of substrates **24** derived from calix[4]arene with alkynes **25** in the presence of the Co^{II}/Salox **L5** catalyst, enabling the concurrent construction of C-N axial chirality and inherent chirality (Figure 11a)[46,47]. Due to the considerable steric congestion of the substrates, the reaction was confined to terminal alkynes, producing inherently chiral calix[4]arenes **26** bearing an additional C-N chiral axis in 40-94% yield with 81-96% ee and > 20:1 dr.

Concurrently, Shi also reported a similar transformation, using substrate **26** derived from calix[4]arenes with 8-AQ directing groups to react with alkynes **25** (Figure 11b)[46,47]. With the Co/Salox **L6** catalyst, this reaction exhibited excellent regioselectivity, affording the products **28** in 60-99% yield with 99 -> 99% ee and 16:1-20:1 dr. Different from Niu's work, in this case a stoichiometric amount of oxidant $Mn(OAc)_3{\cdot}2H_2O$ was used as the oxidant.

In 2025, Ackermann and coworkers reported the construction of two C-N chiral axes via C-H activation/[4+2] annulation using the Co^{II}/Salox catalytic system. They developed a multivariate linear regression (MVLR) model to quantitatively probe the key electronic, steric, and geometric parameters governing the cooperative steric effects of the substrate and ligand on enantioselectivity. The model was experimentally validated for its successful extrapolation from single to dual atroposelectivity, demonstrating the value of computation-aided prediction in guiding experimental design. Using Co/Salox **L7** as the catalyst, the reaction of amide substrates **11** and alkynes **8** afforded dual C-N chiral products **27** in 37-82% yield with 16-99% ee under electrocatalytic conditions (Figure 12a)[48].

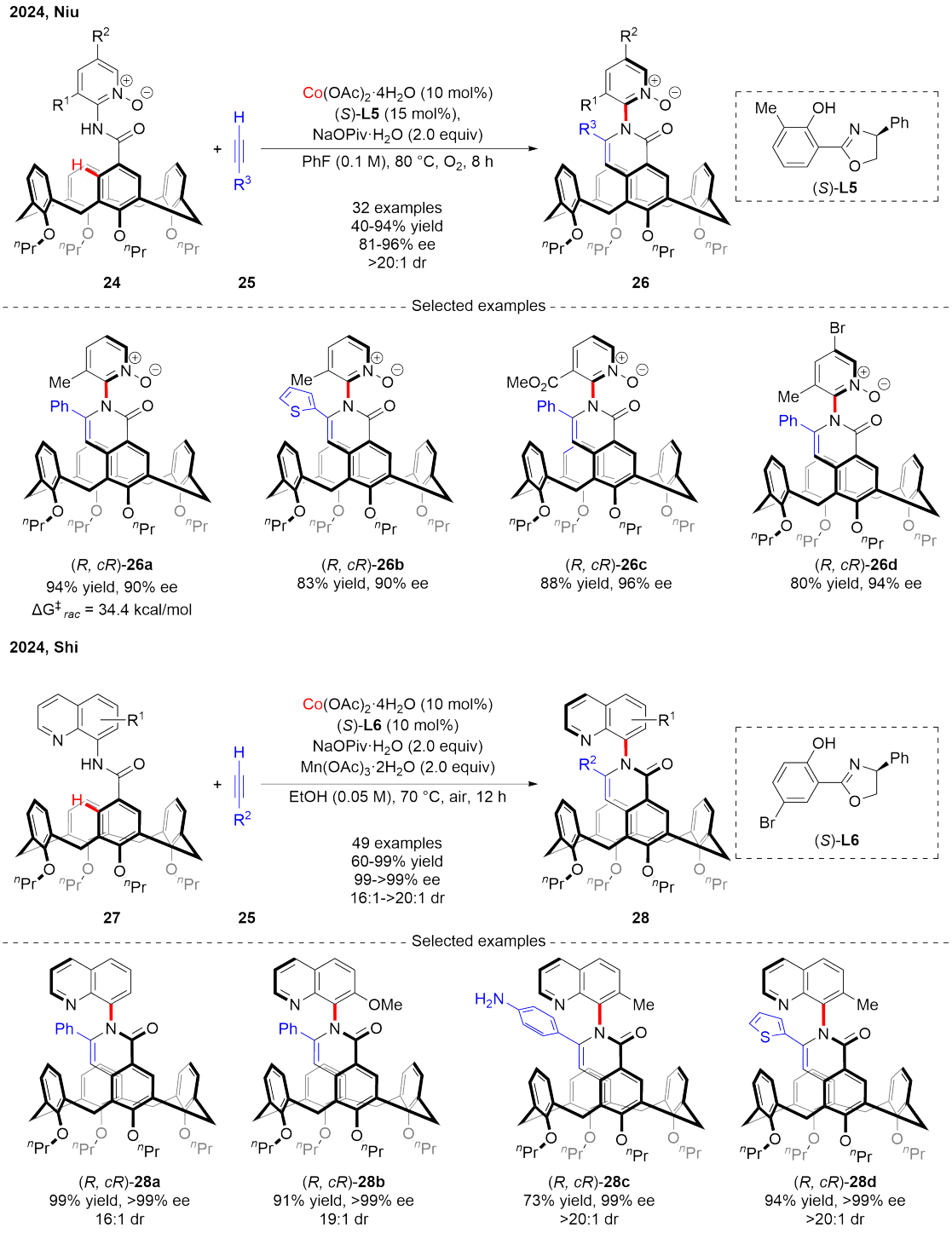

Figure 11. Synthesis of chiral isoquinolinone frameworks with C-N axial chirality and inherent chirality via intermolecular [4+2] annulation[46,47]. EtOH: ethanol.

In the same year, Niu and coworkers achieved the same reaction using O_2 as the oxidant rather than electricity (Figure 12b)[49,50]. With Co/Salox **L1** catalyst, the chiral products **27** were obtained in 32-93% yield with 96 to > 99% ee and 11.1:1-1:0 dr.

Moreover, Sundararaju and coworkers also successfully achieved this reaction using Co/Salox **L8** as catalyst, affording chiral products **27** in 72-98% yield with 93-99% ee and 16:1-27:1 dr (Figure 12c)[49,50]. However, this protocol required a higher catalyst loading of 20 mol%.

In 2026, Wang and coworkers subjected alkynes **7** to asymmetric [4+2] annulation with substrates **11**, affording dual C-N chiral products **29** in 73-93% yield with 80-98% ee and 5:1 -> 20:1 dr (Figure 12d)[51]. Notably, in this case, one end of a C-N chiral axis is non-cyclic.

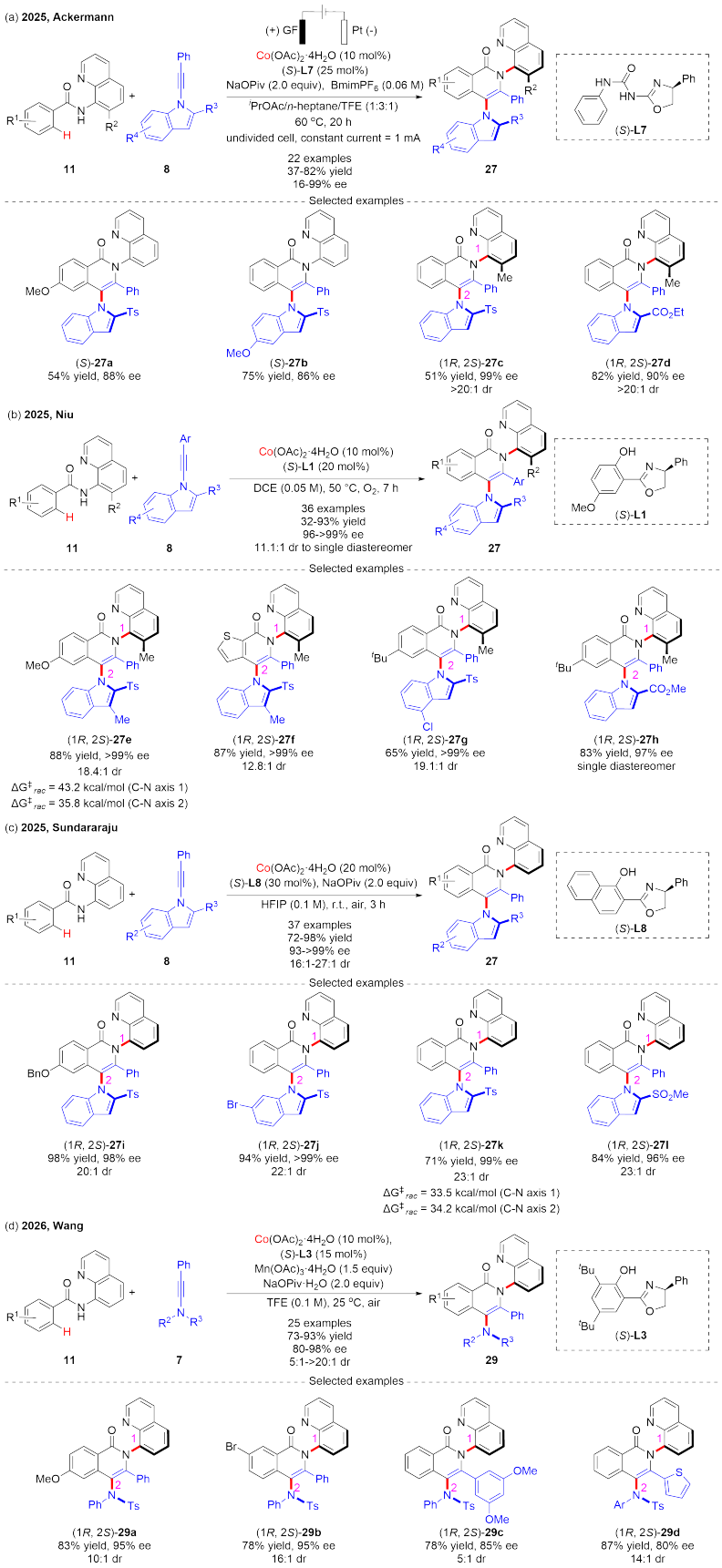

Figure 12. Synthesis of chiral isoquinolinone frameworks with dual C-N axial chirality via intermolecular [4+2] annulation[48-51]. TFE: 2,2,2-trifluoroethanol; DCE: 1,2-dichloroethane; HFIP: hexafluoroisopropanol.

In 2025, Shi and coworkers reported the construction of two remote C-N chiral axes from substrates **30** and terminal alkynes **25** via C-H activation with Co/Salox catalyst (Figure 13)[52]. The phenyl group in the oxazoline ring proved critical for high reactivity; replacing it with a *tert*-butyl group abolished the reaction. The para weakly electron-withdrawing Br substituent benefits stereocontrol. With catalyst Co^{II}/Salox **L6**, substrate **30** reacted with terminal alkyne **25** to afford dual C-N axially chiral product **31** in 23-99% yield with 96-99% ee and 2.6:1-20:1 dr. The stereocontrol model was elucidated by X-ray diffraction analysis of a pyridine-stabilized octahedral cobaltacycle single crystal. Notably, the photoluminescence quantum yield (PLQY) of product **31d** is 0.99 (10^{-5} M in dichloromethane (DCM)), highlighting its potential applications in fluorescent uses.

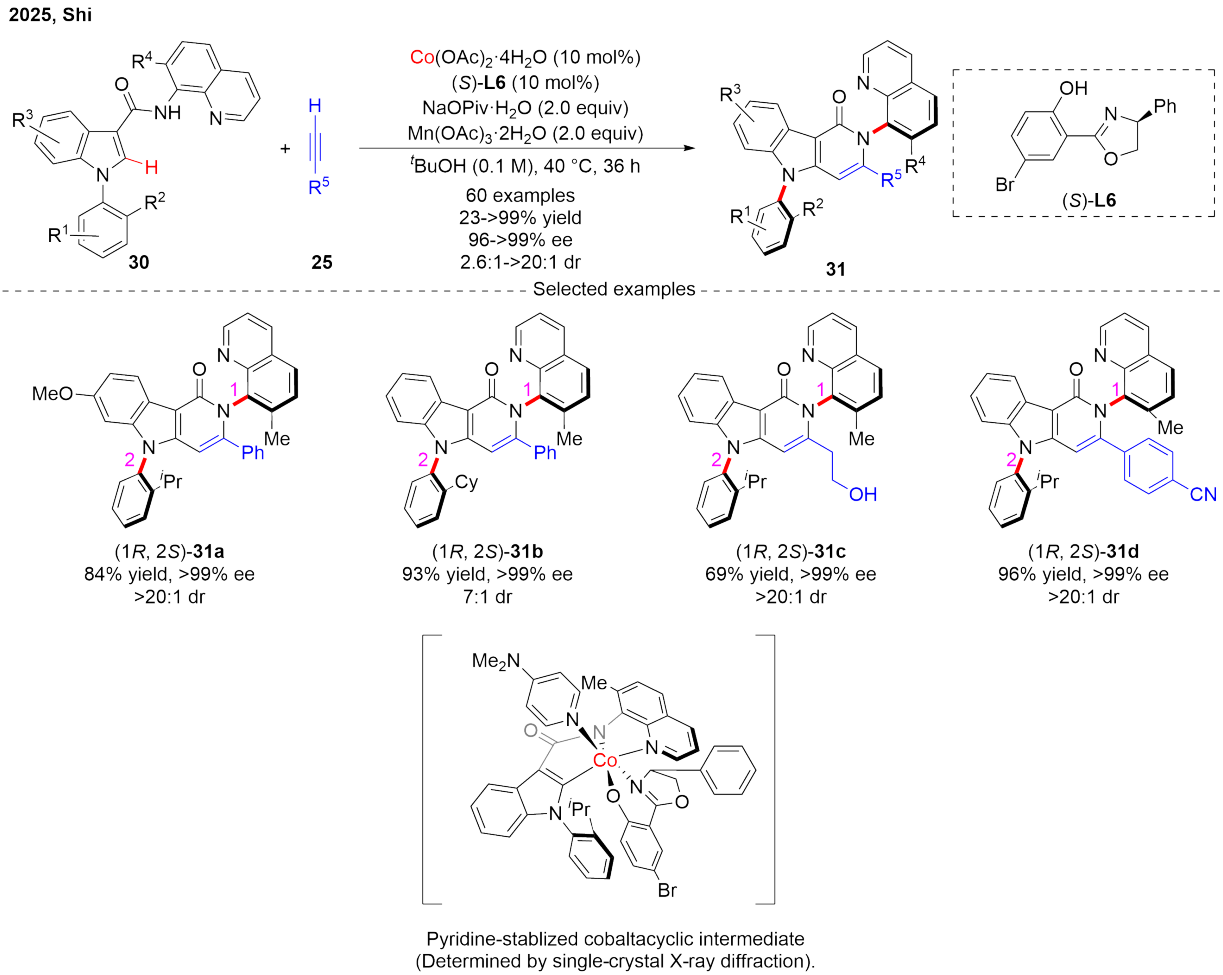

Figure 13. Synthesis of chiral isoquinolinones with remote dual C-N axial chirality via intermolecular [4+2] annulation[52].

In 2026, Sahoo and coworkers disclosed the simultaneous construction of three chiral elements, including C-N axial chirality, C-C axial chirality and *P*-chirality, via a C-H activation/[4+2] annulation (Figure 14)[53]. With catalyst Co^{II}/Salox **L9**, diphenylphosphinamide **32** reacted with ynamide **33** to afford chiral products **34** in good yields and excellent enantioselectivities and good diastereoselectivities (56-87% yield, 88-99% ee and ~5:1-20:1 dr). The configuration of the C-N chiral axis was influenced by the substituent on the naphthyl moiety of alkyne **33**. DFT calculations of the transition states for the concerted metalation-deprotonation (CMD) step show that the transition states with *S*-configured phosphine, P^S-**A** and P^S-**A**′, are substantially lower in energy than their *R*-configured counterparts P^R-**A** and P^R-**A**′, indicating the CMD step is the enantiodetermining event for the *P*-stereocenter. Furthermore, the subsequent migratory insertion and reductive elimination steps proceed with lower barriers from P^S-**A** than from P^S-**A**′, which not only confirms the coordination mode of the ligand as depicted for P^S-**A**, but also fixes the configurations of the C-C and C-N axes during the later stages.

In 2026, Niu and coworkers developed a Co^{II}/Salox-catalyzed enantioselective C-H activation/[4+2] annulation for the efficient assembly of helical heterohelicenes bearing a chiral C-N axis (Figure 15)[54]. With Co/Salox **L3** as catalyst and O_2 as the oxidant, diverse benzamides **35** featuring a benzo-3,4-phenanthrene framework reacted smoothly with alkynes **12**, furnishing the chiral products **36** in 25-92% yield with 90 -> 99% ee and 2:1-86:1 dr. However, this reaction requires a high catalyst loading of 20 mol%. Interestingly, the *N*-oxide derivative **37** of product **36e** could serve as a chiral ligand in palladium-catalyzed asymmetric carbene insertion reaction, affording the chiral product **38** in 50% yield with 60% ee.

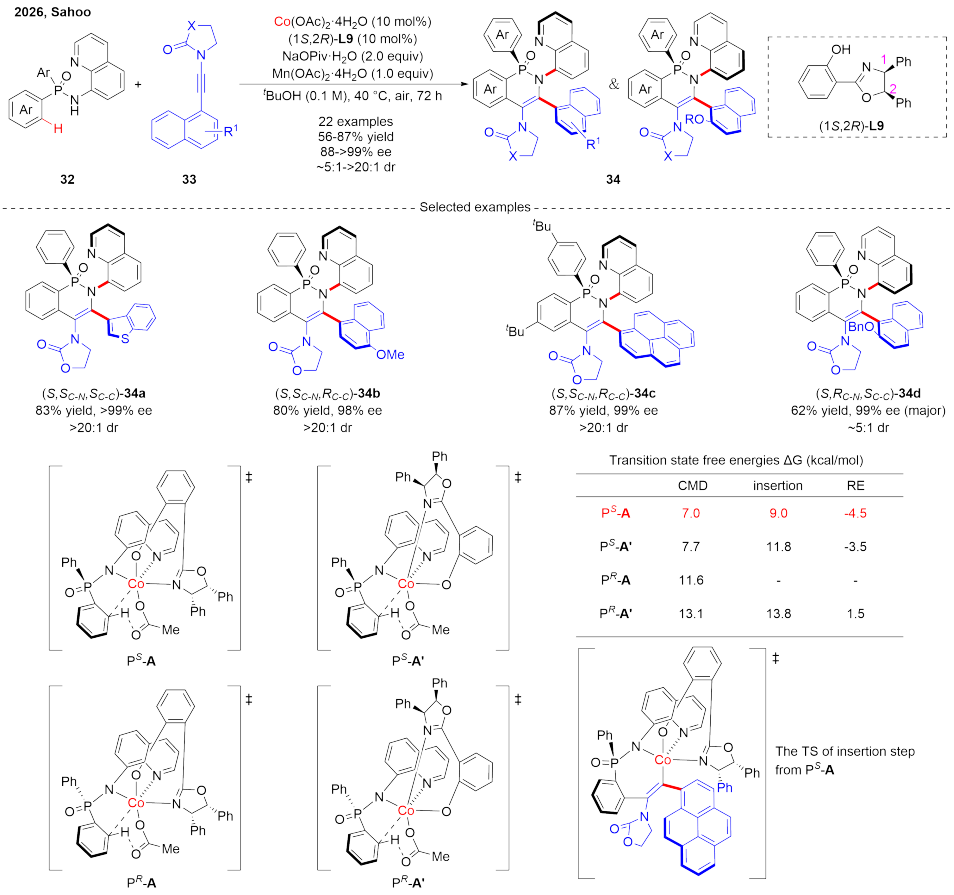

Figure 14. Synthesis of chiral *P*-heteroisoquinolinones with *P*-central, C-N axial and C-C axial chirality via intermolecular [4+2] annulation[53].

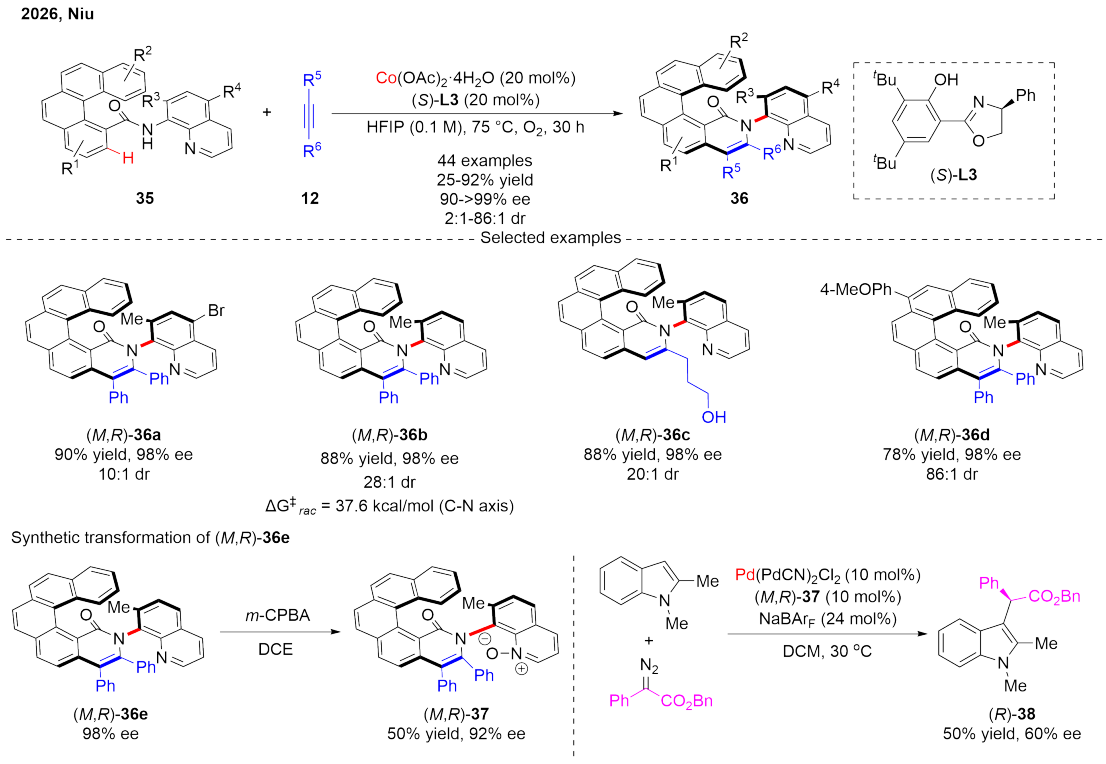

Figure 15. Synthesis of chiral heterohelicenes featuring both helical and C-N axial chirality via intermolecular [4+2] annulation[54]. HFIP: hexafluoroisopropanol.

2.2.2 Using allenes as reactants

Allenes are widely used in catalytic cycloaddition reactions[55]. In 2023, Niu and coworkers described an enantioselective Co^{II}/Salox **L3**-catalyzed C-H activation/[4+2] annulation of sulfonamides **16** and allenes **39** to afford C-N axially chiral sultams **40** (Figure 16)[43]. Various substituents on substrates **16** and allenes **39** were tolerated, giving the products in 32-95% yield with 77-98% ee. In the proposed mechanism, after migratory insertion of the allene into the C-Co bond, reductive elimination forms a cyclic intermediate, which is subsequently converted to product **40** through a 1,3-hydrogen migration.

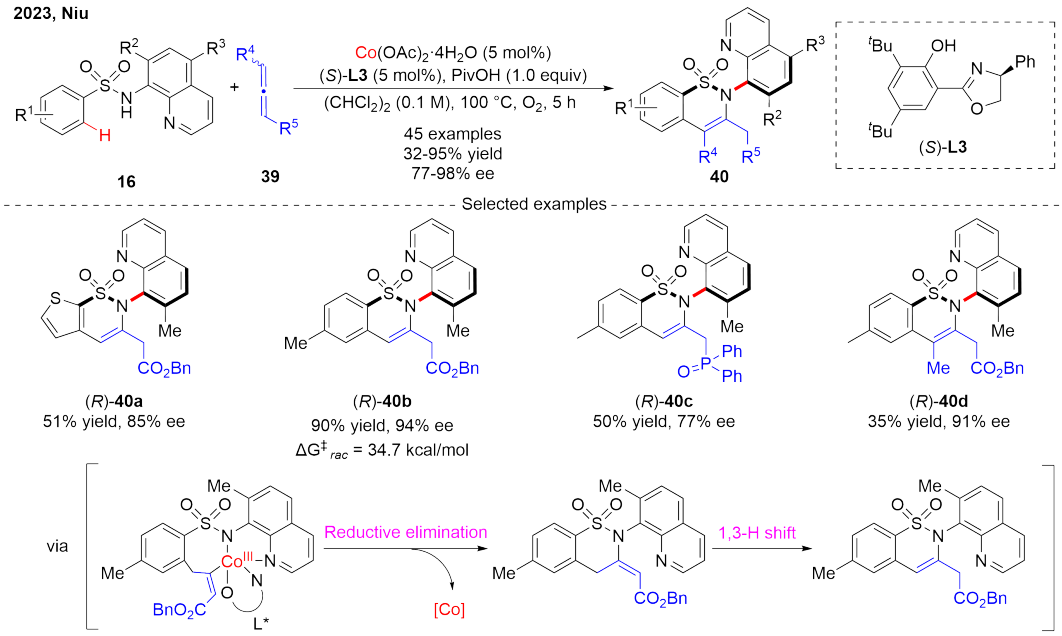

Figure 16. Synthesis of chiral *S*-heteroisoquinolinone frameworks with C-N axial chirality via intermolecular [4+2] annulation[43].

In 2023, Ackermann and coworkers described a Co^{II}/Salox **L3**-catalyzed enantioselective electrochemical [4+2] annulation of *N*-(quinoline-8-yl)benzamides **11** with allenes **41** at ambient temperature, affording product **42** in 44-98% yield with 82 -> 99% ee (Figure 17a)[56]. This method avoids the use of a stoichiometric oxidant, but requires ionic liquid and fluorinated solvent to facilitate electrocatalysis.

Niu and coworkers also realized the same reaction with Co^{II}/Salox **L1** as the catalyst and O_2 as the environmentally friendly oxidant. Both monosubstituted and disubstituted allenes **39** have been examined, delivering C-N axially chiral isoquinolinones **43** in 27-97% yield with 89 -> 99% ee (Figure 17b)[57]. Compared with Ackermann's work, it necessitated a higher reaction temperature (80 °C). This reaction was also tried under electrocatalysis in an air atmosphere. However, the yield decreased while the enantioselectivity remained unchanged.

In 2025, Baidya and coworkers reported the Co^{II}/Salox **L1**-catalyzed [4+2] annulation of *N*-(quinoline-8-yl)benzamide **11** with α-aryl-allenyl acetates **44** (Figure 18)[58]. A series of fused polycyclic products **45** bearing a C-N chiral axis were obtained in 50-84% yield with 82-98% ee. According to the proposed mechanism, intermediate **I** is formed via a [4+2] annulation followed by deacetylation. Intermediate **II** is then generated through *cis-trans* isomerization. Subsequent light-induced annulative π-extension (APEX) affords the final product **45**. This tandem [4+2] annulation/aromatization sequence provides a highly efficient strategy for the construction of fused polycyclic compounds.

2.2.3 Using alkenes as reactants

Transition metal-catalyzed heteroannulative difunctionalization of alkenes via C-H activation is an efficient strategy for the synthesis of heterocycles[59]. In 2023, Wang reported the Ru-catalyzed C-H activation/[4+2] annulation of chiral benzamides **46** with *N*-arylmaleimides **47** bearing a prochiral C-N axis to construct C-N axial chirality via a chiral directing group strategy (Figure 19)[60]. Isocoumarins **48** with C-N axial chirality were obtained in moderate yields and with high enantioselectivities (four examples, 42-61% yield and 80-92% ee). The reaction proceeded via a dihydroisocoumarin intermediate, which upon oxidation gave product **48**.

In 2024, Ackermann and coworkers achieved the [4+2] annulation of *N*-(quinoline-8-yl)benzamide **11** with alkenes **49** utilizing the Co^{II}/Salox **L3** catalyst under electrocatalytic conditions (Figure 20a)[61]. A series of products **50** bearing C-N axial chirality and two central stereocenters were prepared in 40-97% yield, 93 -> 99% ee and > 20:1 dr. Interestingly, Ag_2CO_3 could replace electricity as a stoichiometric oxidant, but $Mn(OAc)_3·2H_2O$ and O_2 could not.

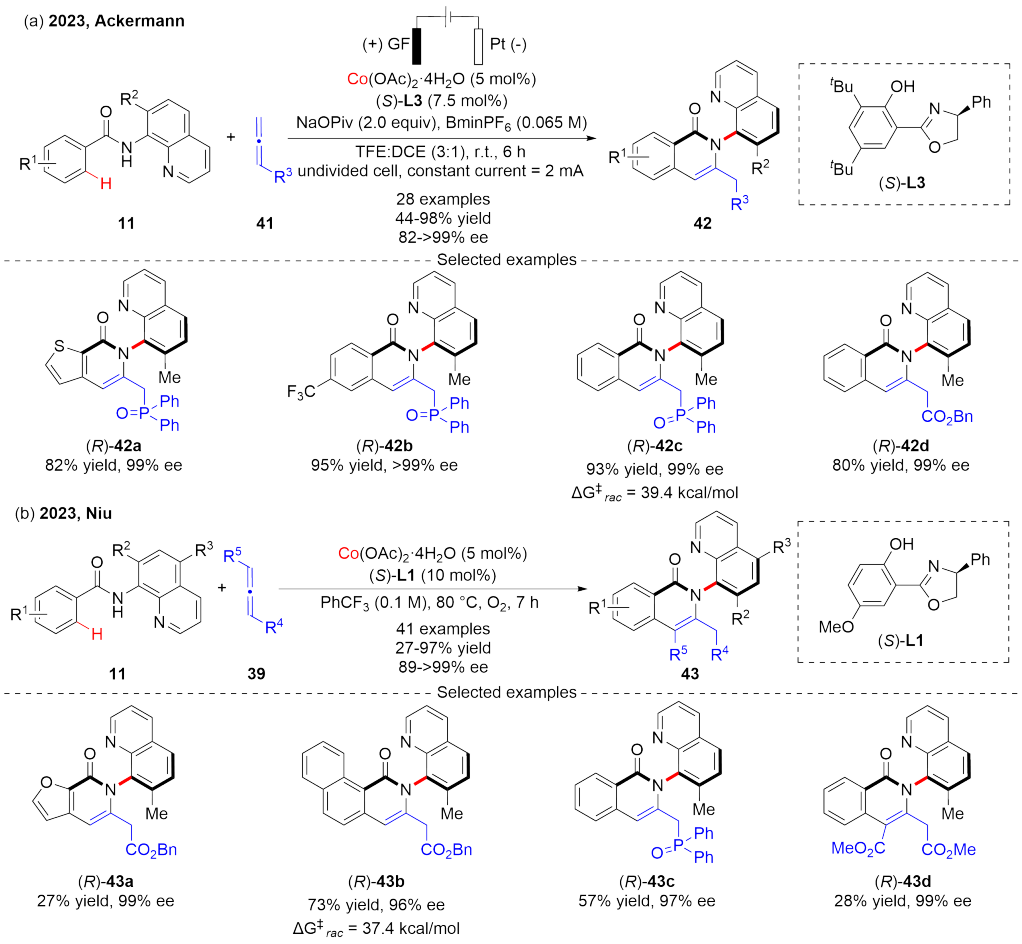

Figure 17. Synthesis of chiral isoquinolinones with C-N axial chirality via intermolecular [4+2] annulation[56,57]. DCE: 1,2-dichloroethane; TFE: 2,2,2-trifluoroethanol.

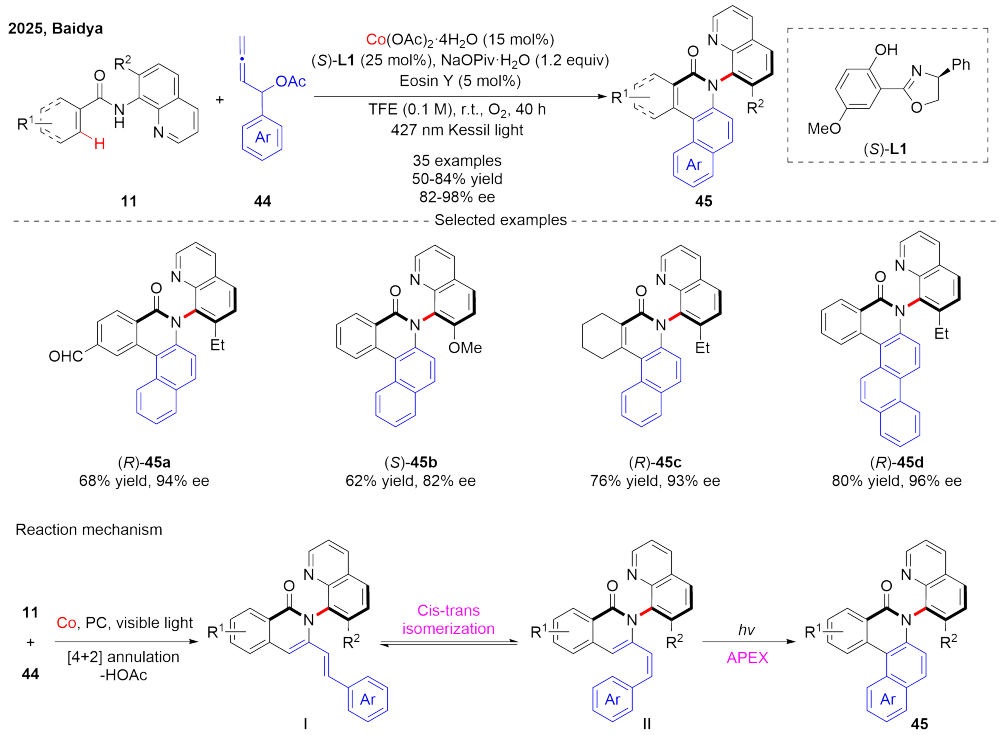

Figure 18. Synthesis of fused polycyclic chiral isoquinolinones with C-N axial chirality via tandem [4+2] annulation/aromatization[58]. TFE: 2,2,2-trifluoroethanol.

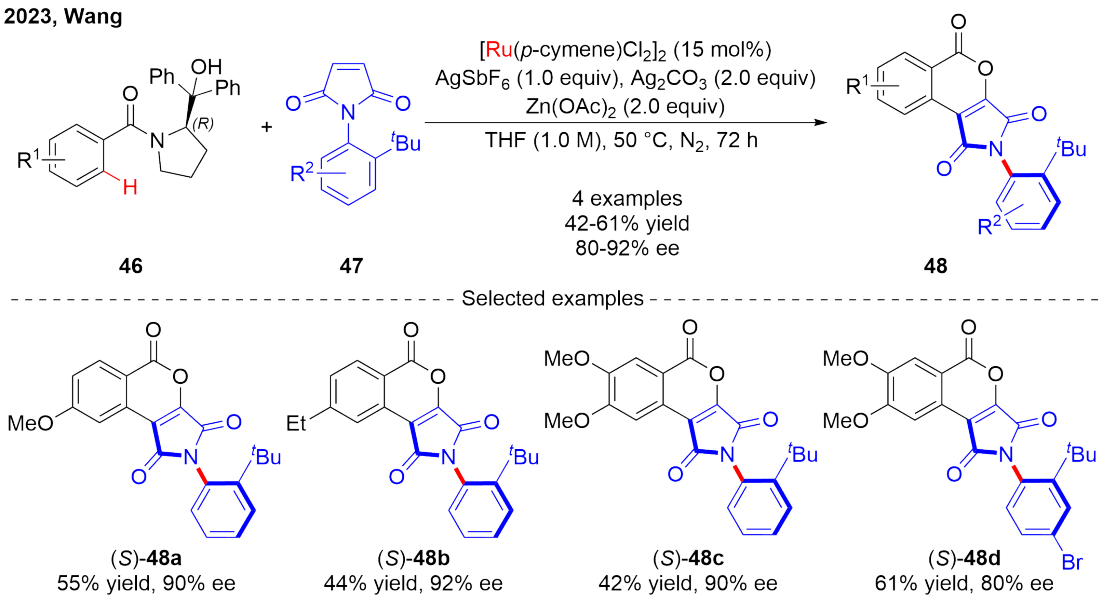

Figure 19. Synthesis of chiral isocoumarins with C-N axial chirality via intermolecular [4+2] annulation by a chiral directing group strategy[60]. THF: tetrahydrofuran.

In 2026, Sharma and coworkers reported an asymmetric [4+2] annulation of *N*-(quinoline-8-yl)benzamide **11** with strained bicyclic alkenes **51**, using $Mn(OAc)_3 \cdot 2H_2O$ as the stoichiometric oxidant (Figure 20b)[62]. With Co^{II}/Salox **L8** as the catalyst, products **52** were obtained in 41-99% yield, with 85 -> 99% ee and 17.1 -> 20:1 dr (**Condition A**). Distinct from Lu's system (Figure 6c), in this case, photocatalysis afforded reduced yields and enantioselectivities (**Condition B**).

In 2025, Miao and coworkers reported the Co^{II}-catalyzed desymmetric [4+2] annulation of diphenylphosphinamides **32** with maleimides **53** with Salox **L1** as the chiral ligand (Figure 21)[63]. This protocol afforded a series of products **54** featuring both C-N axial and *P*-central chirality in 45-89% yield with 92 -> 99% ee and > 20:1 dr. DFT calculations revealed a Co^{III}/Co^{II} catalytic cycle. Stereoselective control of *P*-chirality occurs during C-H activation. The (S_P, S_C)-**TS1** was found to have a 2.89 kcal/mol lower energy barrier than (R_P, S_C)-**TS1'**, consistent with the experimental observations. Intermediate **II** undergoes migration insertion and reductive elimination to generate intermediate **III** as detected by HRMS. Intermediate **III**, with a low rotational barrier about the C-N bond, undergoes stepwise oxidation to fix the C-N axial configuration, which is also assisted by the departure of Co^{II}/Salox.

2.2.4 Using (Hetero)aryl Iodides as reactants (Catellani reaction)

In 2021, Zhou and coworkers reported the construction of C-N axial chirality through the Catellani reaction. With palladium (Pd)/norbornene (**NBE1**) as the catalyst, the reaction of aryl iodides **55** and aryl bromides **56** proceeded smoothly, affording C-N axially chiral phenanthridinones **57** in 42-97% yield with 87 -> 99% ee (Figure 22)[64]. Stoichiometric K_2CO_3 is required to neutralize the *in situ* generated acid HX. DFT calculations revealed that the reaction involves conversion from C-C to C-N axial chirality. The C-H activation occurs after oxidative addition of the aryl iodides **55** and migratory insertion of **NBE1**. Subsequent oxidative addition of the aryl bromide **56** generates an intermediate **II** bearing C-C axial chirality. Following N-H deprotonation and reductive elimination, the C-C axial chirality is converted into the C-N axial chirality, affording the C-N axially chiral phenanthridinone **57**. Steric hindrance between the methyl group and NBE favors the formation of (*S*)-C-C axis, whereas that between the methyl group and the *tert*-butyl group drives the conversion of the (*S*)-C-C axis to the (*R*)-C-N axis.

Subsequently, Zhou used iodoheterocycles **58** as substrates in the reaction with aryl bromides **56** under Pd/**NBE1** catalysis, affording polycyclic C-N atropisomers **59** in 55-98% yield with 21-98% ee (Figure 23)[65].

2.3 [3+2] annulation reaction

In 2021, Li and coworkers reported a [3+2] annulation of anilines **60** with alkynes **12** using chiral $CpRh^{III}$ catalyst **C4** to construct C-N axially chiral indoles **61** (Figure 24a)[66]. The R^1 substituent on the isoquinoline directing group was essential to enhance the atropostability of the C-N chiral axis. The products **61** were prepared in 24-89% yield with 74-96% ee and 7:1 -> 20:1 rr (regioisomeric ratio).

Wang and coworkers employed a H_8-BINOL-derived chiral $BenRu^{II}$ catalyst **C5** in the [3+2] annulation of anilines **60** with alkynes **12**,[67] delivering C-N axially chiral products **61** in 14-97% yield with 72-98% ee (Figure 24b). In this reaction, $Cu(OAc)_2$ served not only as a stoichiometric oxidant but also as a chloride-abstraction reagent to activate catalyst **C5**. Na_2CO_3 could neutralize the HOAc generated in the reaction, thereby improving the yield.

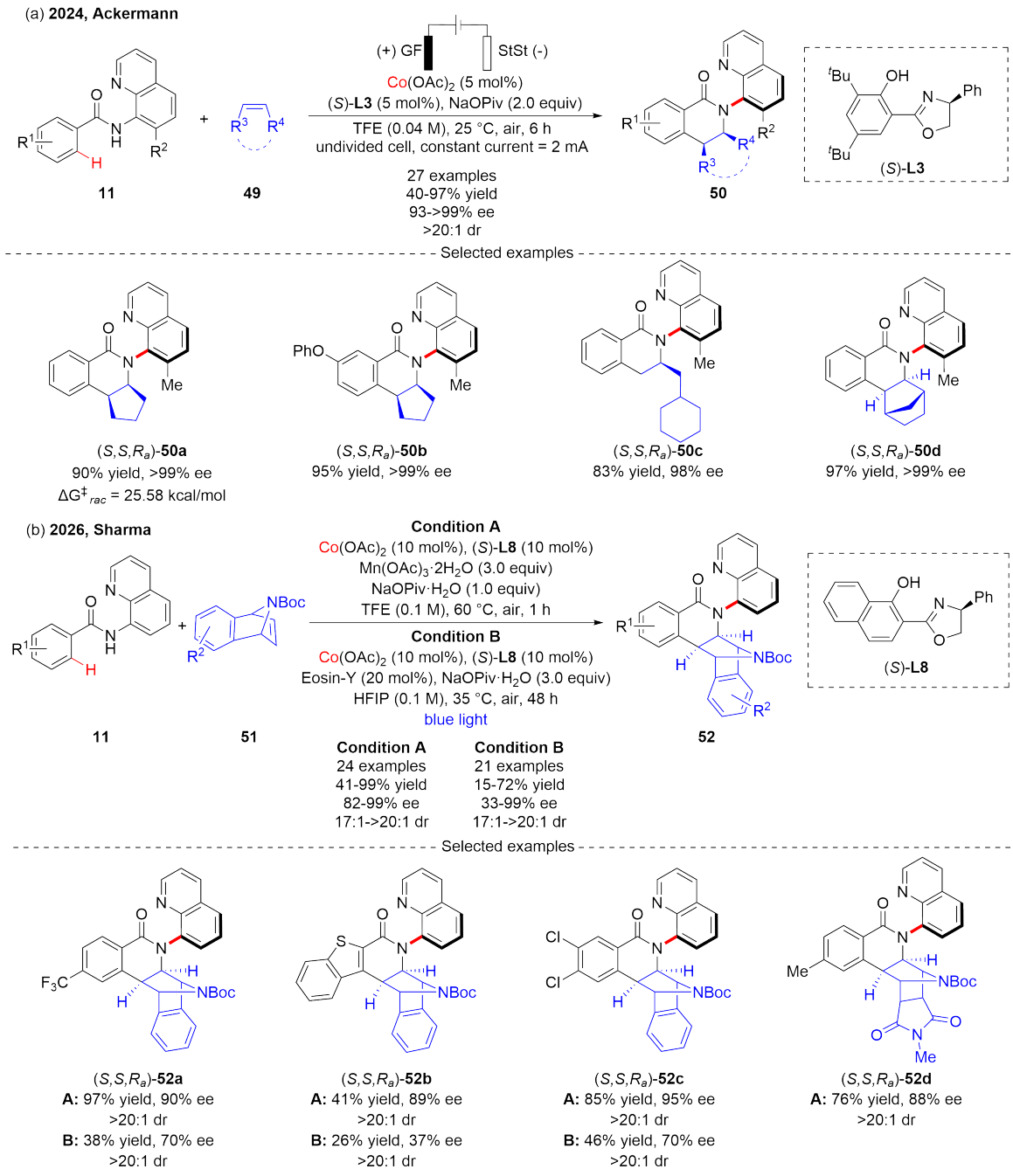

Figure 20. Synthesis of chiral dihydroisoquinolinones bearing a C-N chiral axis with *N*-(quinolin-8-yl)benzamides and alkenes via [4+2] annulation[61,62]. HFIP: hexafluoroisopropanol; TFE: 2,2,2-trifluoroethanol.

Almost simultaneously, Ackermann and colleagues realized electrochemical [3+2] annulation of anilines **60** and alkynes **12** with chiral BenRu^{II} catalyst **C5**, affording products **61** in good yields and high enantioselectivities (47–99% yield and 72–94% ee) (Figure 24c)[68]. The use of electrochemistry eliminated the need for the stoichiometric oxidant. Notably, this work constitutes the first application of a chiral BenRu^{II} catalyst in electrocatalysis.

In 2021, Li and coworkers reported an asymmetric [3+2] annulation of nitrones **62** with alkynes **8**, catalyzed by CpRh^{III} catalyst **C3** (Figure 25)[69]. The products **63**, bearing both a C–N chiral axis and a stereogenic center, were obtained in 67–91% yield, 91–95% ee and > 20:1 dr (six examples). Notably, the introduction of an acid additive induces inversion of the stereocenter (from *R* to *S*) while also enhancing both the yield and enantioselectivity. Compared with other asymmetric [3+2] annulations, this reaction achieves stereocontrol over two chiral elements.

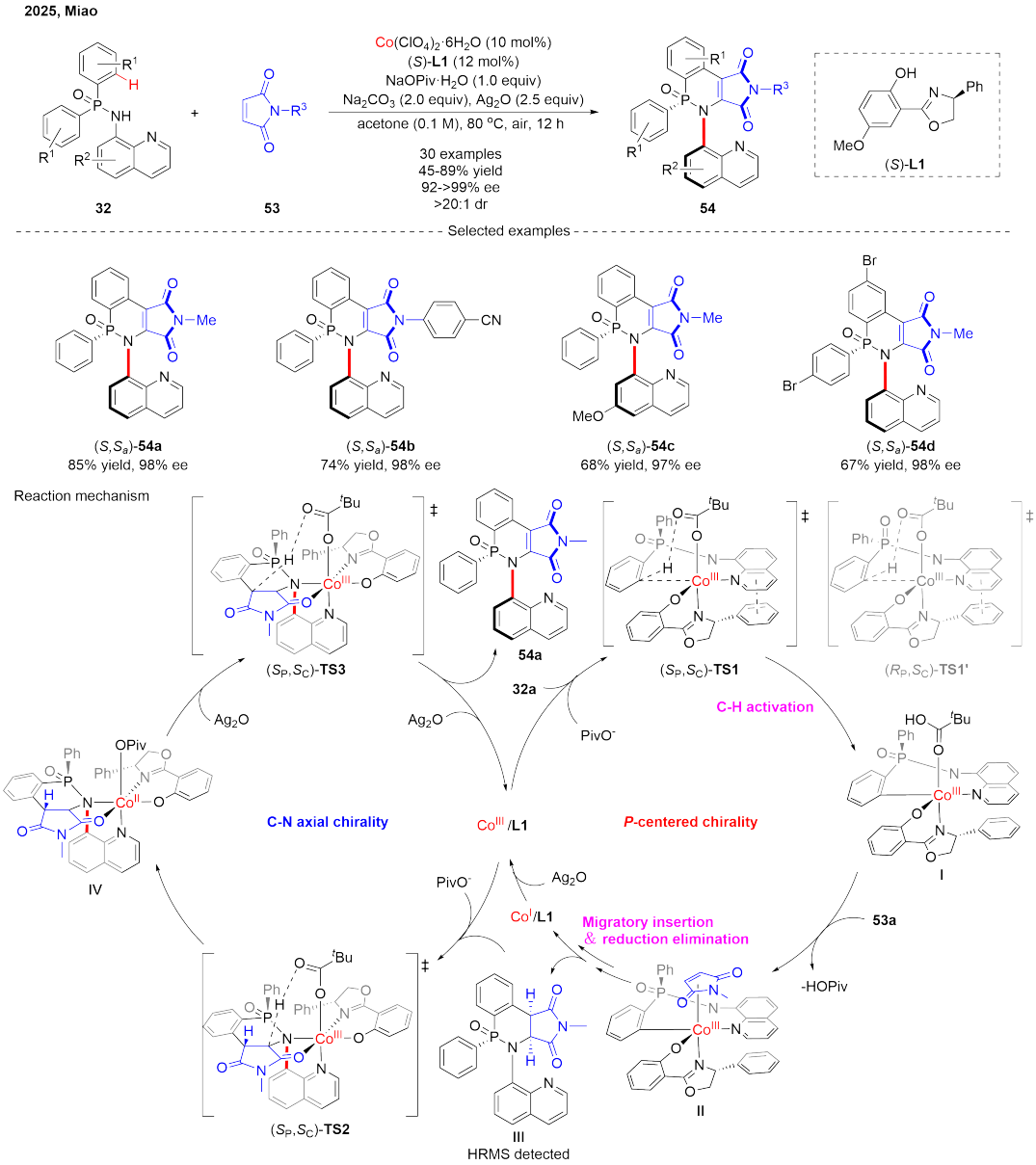

Figure 21. Desymmetric [4+2] annulation of diphenylphosphinamides with maleimides[63].

2.4 [4+1] annulation reaction

In 2023, Niu and coworkers reported an efficient atroposelective C–H activation/[4+1] annulation of *N*-(quinoline-8-yl)benzamide **11** and isonitriles **64** with the Co^{II}/Salox **L1** catalyst (Figure 26)[70]. This reaction afforded 3-iminoisoindolinones **65** bearing a C–N chiral axis in 51–98% yield with 74 -> 99% ee. The reaction proceeds via C–H activation and migratory insertion of isocyanide to generate a six-membered metallacyclic intermediate **I**, which then undergoes reductive elimination to deliver the target product. Notably, O_2 was used as an oxidant.

2.5 [3+3] annulation reaction

Constructing C–N axial chirality via a [3+3] annulation is rarely reported. In 2023, Li and coworkers reported an enantiodivergent [3+3] annulation of benzamide **66** with CF_3-imidoyl sulfoxonium ylides (TFISYs) **67** using the chiral $CpRh^{III}$ catalyst **C6** (Figure 27)[71]. This reaction afforded C–N axially chiral biaryls in 31–85% yield with 73–99% ee for **68** and 36–65% yield with 56–91% ee for **68'**. Notably, the product configuration could be inverted simply by alternating the solvent (*R* configuration in DCM; *S* configuration in hexafluoroisopropanol (HFIP)). DFT calculations reveal that the σ-bond metathesis serves as the enantiodetermining step, and the TS architecture is solvent-dependent. In DCE, a neutral TS is involved, wherein the combined steric repulsion and H···F interaction render (*S*)-**TS1** higher in energy than (*R*)-**TS1**. In HFIP, by contrast, a cationic TS prevails, and steric hindrance between the substrate and the chiral ligand makes (*R*)-**TS2** energetically less favorable than (*S*)-**TS2**.

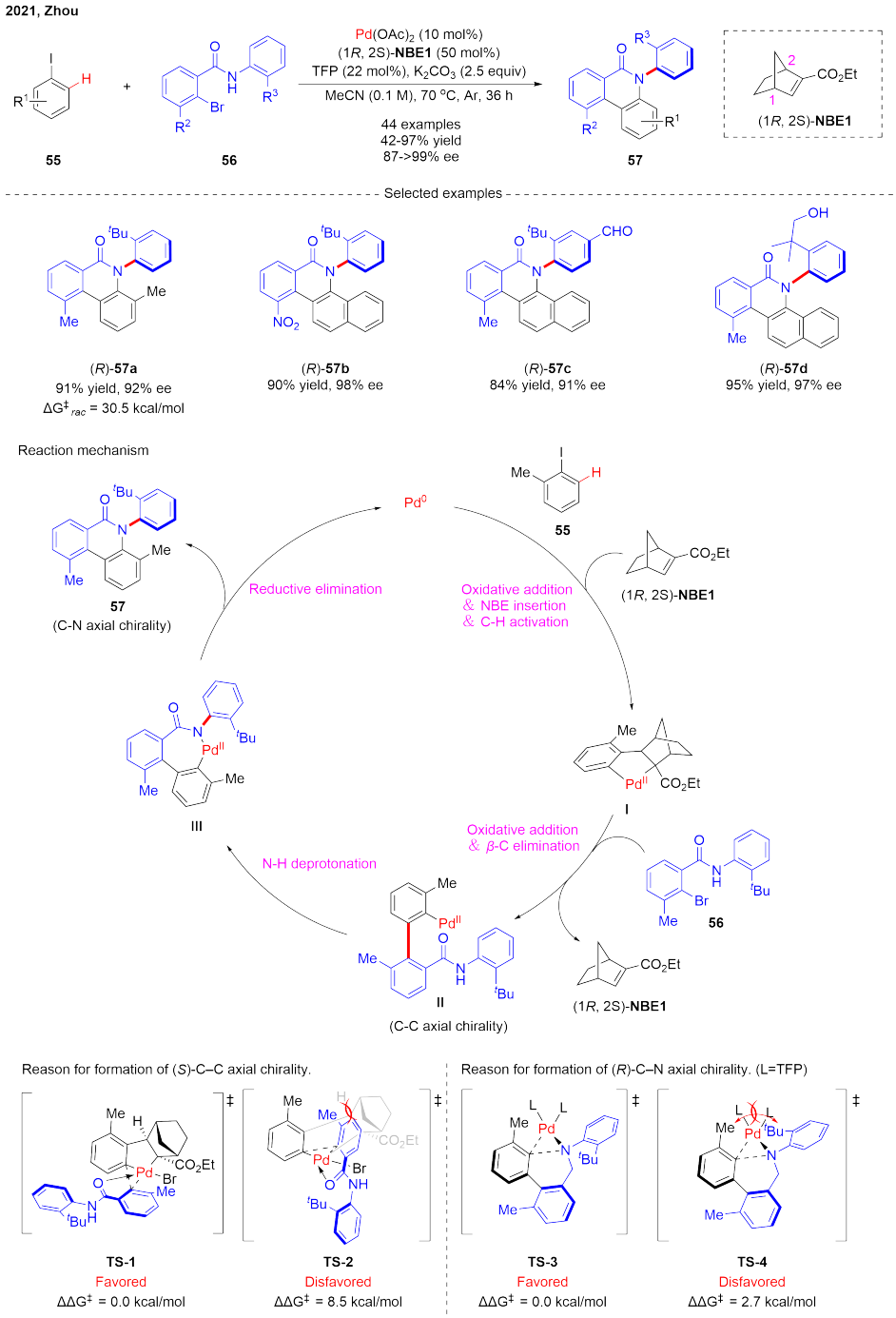

Figure 22. Synthesis of chiral phenanthridinones bearing a C-N chiral axis with aryl iodides and aryl bromides via Catellani reaction[64]. TFP: tri(2-furyl)phosphine.

3. Asymmetric C-H Activation/Alkynylation Reaction

Construction of C-N axial chirality via C-H activation/alkylation is possible. In 2019, Shi and coworkers reported an asymmetric C-H activation/alkylation reaction with heteroarenes **69** and bromoalkynes **70** by a chiral transient directing group strategy (Figure 28)[18]. In the presence of $Pd(OAc)_2$ and *tert*-leucine **transient directing group (TDG)1**, C-N axially chiral products **71** were formed in 43-87% yield with 64-99% ee. Eight examples were demonstrated.

Later, Shi extended Pd^{II}-catalyzed asymmetric C-H activation/alkylation to construct C-N axially chiral *N*-aryl peptoids with the inexpensive chiral ligand **L10** (Figure 29)[72]. The reaction of *N*-aryl peptoids **72** bearing a bulky side arm with bromoalkynes **70** gave chiral products **73** in 11-99% yield with 61-99% ee. Restricted rotation about the amide C-N bond gave rise to *E*/*Z* isomers in ratios ranging from 2:1 to 33:1. The reaction acidity is a critical factor affecting both yield and enantioselectivity, with 3 equiv of Ag_2CO_3 being optimal.

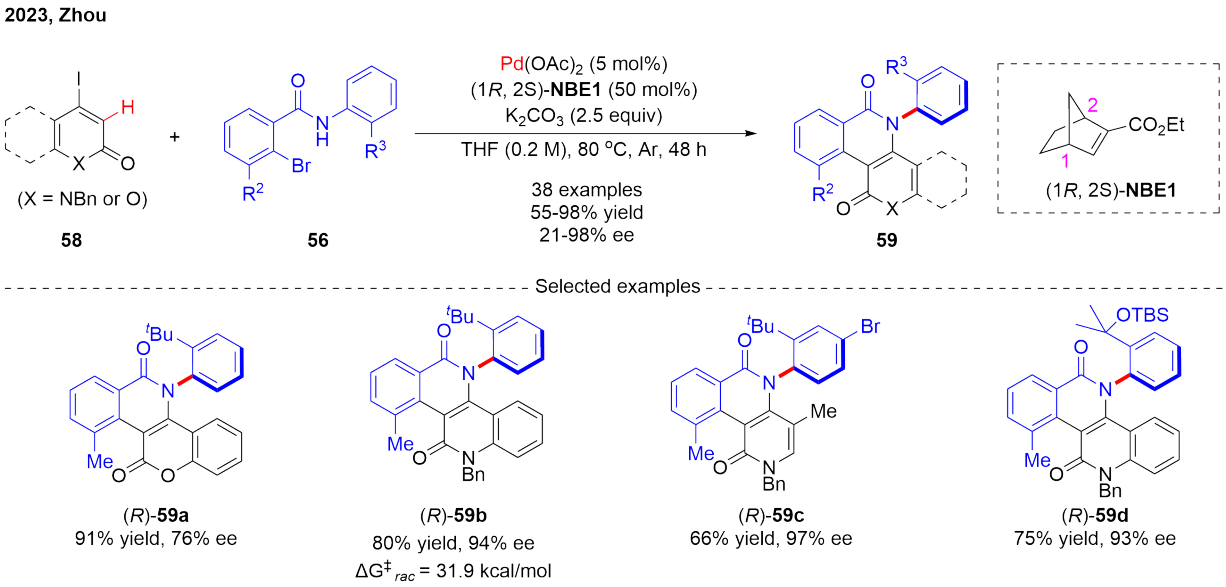

Figure 23. Synthesis of polycyclic C-N atropisomers with iodoheterocycles and aryl bromides via Catellani reaction[65]. THF: tetrahydrofuran.

In 2026, Li and coworkers succeeded in constructing a remote C-N chiral axis that lies three bonds away from the reaction site (Figure 30)[73]. With chiral CpRh **C3** as the catalyst, *N*-aryl-1,8-naphthalimides **74** smoothly coupled with bromoalkynes **70** to deliver the C-N axially chiral products **75** in 43-84% yield with 55-99% ee. It was found that increasing the Ag_2CO_3 loading from 40 to 80 mol% led to a gradual increase in enantioselectivity from 70% ee to 92% ee, accompanied by an increase in the yield of the bis-alkynylation byproduct from 3% to 21%. Notably, the chiral acid additive **A2** proved essential for achieving high enantioselectivity. When $[Cp^*RhCl_2]_2$ was used as the catalyst, both the *S*- and *R*-configured **A2** afforded the product **75** with 7% ee. However, when the chiral catalyst **C3** was employed, *S*-configured **A2** led to much higher enantioselectivity than its *R*-configured counterpart (90% ee *vs.* 67% ee). This implies the existence of a chiral matching effect.

4. Asymmetric C-H Activation/Alkenylation Reaction

Construction of C-N axial chirality by asymmetric C-H activation/alkenylation can be achieved via two strategies: (a) Heck-type reactions with alkenes, and (b) addition reactions to alkynes. Current advances have predominantly focused on Heck-type C-H alkenylation. Its mechanism involves C-H activation, migratory insertion of alkenes, and β-H elimination (Figure 31).

In 2019, Xie and coworkers developed a Pd-catalyzed atroposelective C-H activation/alkenylation of *N*-aryl heterocycles **76** with alkenes **77** by desymmetrization, dynamic kinetic resolution or kinetic resolution (Figure 32)[20]. Assisted by L-valine **TDG2**, the desymmetrization or dynamic kinetic resolution proceeded well. A broad range of *N*-arylindoles **76** and alkenes **77**, including polarized unsaturated alkenes, 4-nitrostyrene and even internal alkenes, were tolerated, affording diverse C-N axially chiral products **78** in 35-77% yield with 84-99% ee. In contrast, L-*tert*-Leucine **TDG1** proved to be optimal for the kinetic resolution of *N*-arylindoles **79** and alkenes **77**, affording chiral products **80** in 37-48% yield with 97-99% ee, together with enantioenriched recovered **79** (35-46% yield with 45-94% ee). The selectivity factors are high (*s* = 155-459).

Later, Ackermann and coworkers employed electrocatalysis in the Pd/**TDG1**-catalyzed kinetic resolution of *N*-arylindoles **81** with alkenes **77** (Figure 33)[74]. The C-N axially chiral indoles **82** were obtained in 21-41% yield with 92-99% ee. Notably, electrocatalysis significantly reduced the reaction time compared with the use of benzoquinone (BQ) or silver trifluoroacetate (AgTFA) as chemical oxidants.

In 2026, Li and coworkers reported the alkenylation of *N*-aryl-1,8-naphthalimides **74** with alkenes **83**, constructing a remote C-N chiral axis that lies three bonds away from the reaction site (Figure 34)[73]. Using chiral CpRh **C3** as the catalyst, the products **84** were obtained in 40-67% yield with 80-98% ee. Similar to the aforementioned asymmetric alkynylation (Figure 30), chiral acid **A2** was essential to ensure high enantioselectivity.

In 2020, Shi and coworkers described the construction of C-N axially chiral amides through Pd-catalyzed C-H alkenylation of *N*-aryl peptoids **72** with alkenes **83** via dynamic kinetic resolution (Figure 35)[75]. In the presence of $Pd(OAc)_2$ and chiral ligand **L10**, a broad range of C-N axially chiral products **85** were prepared in 37 -> 99% yield and 84 -> 99% ee. Stoichiometric AgOAc was required as the oxidant. Rotation barriers around the amide C-N bonds lead to isomeric products (*E*:*Z* = 2.3:1 -> 20:1). Notably, this work represented one of the first examples of constructing C-N axially chiral anilides through C-H activation.

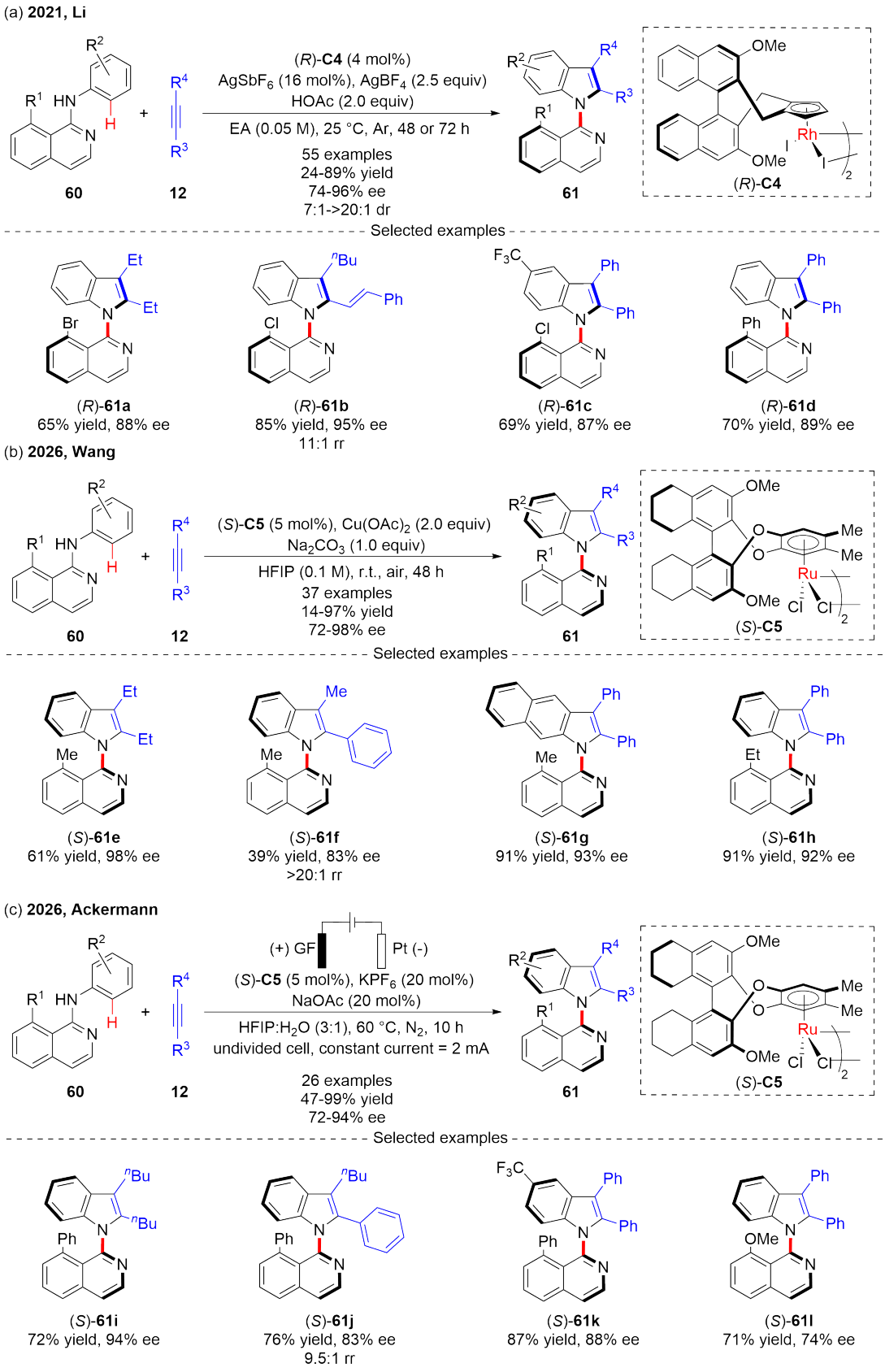

Figure 24. Synthesis of chiral indoles bearing C-N chiral axis with anilines and alkynes via [3+2] annulation[66-68]. HOAc: acetic acid; HFIP: hexafluoroisopropanol; EA: ethyl acetate.

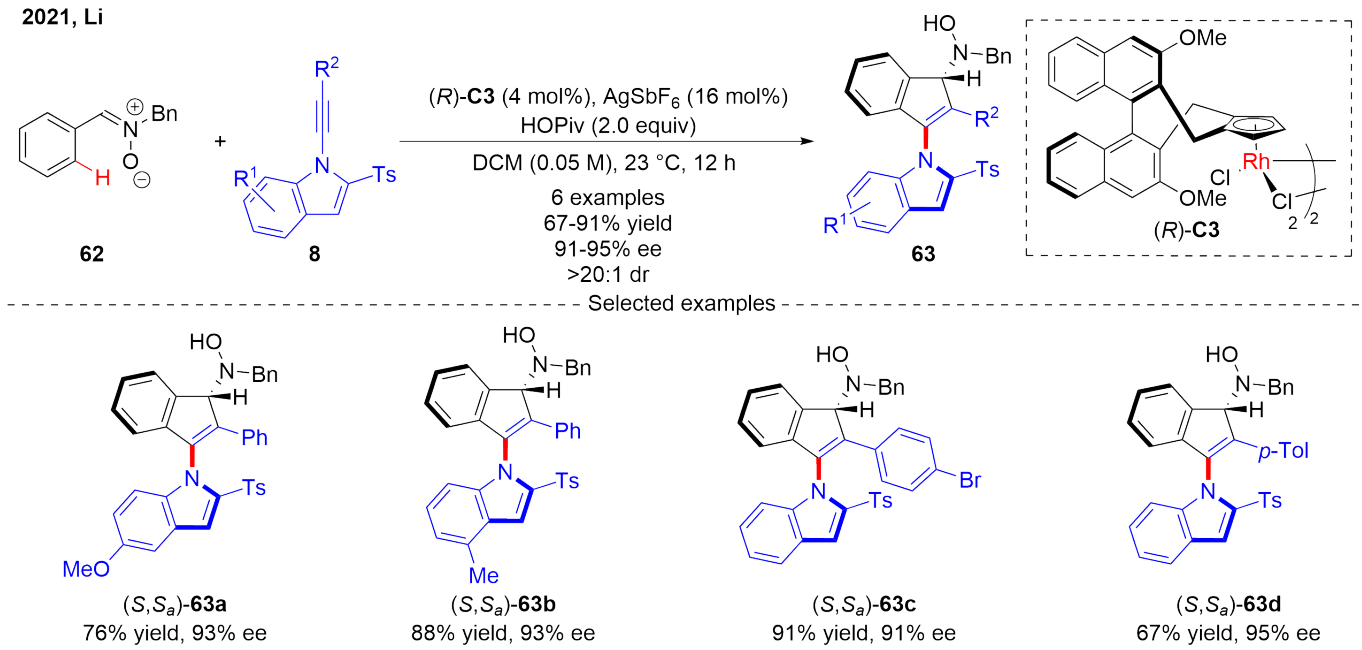

Figure 25. Synthesis of C-N axially and centrally chiral indenes with nitrones and alkynes via [3+2] annulation[69]. DCM: dichloromethane.

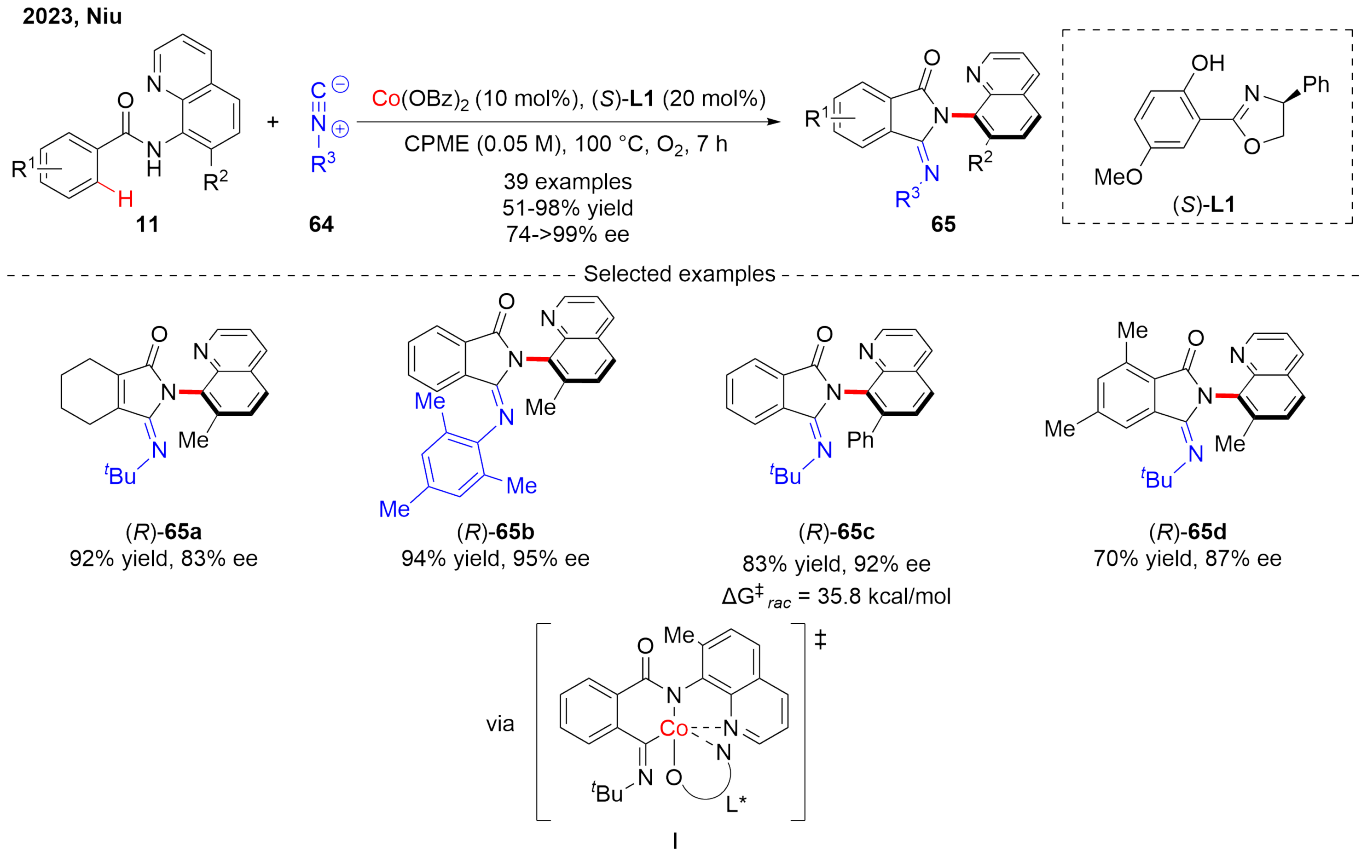

Figure 26. Synthesis of 3-iminoisoindolinones bearing a C-N chiral axis with *N*-(quinoline-8-yl)benzamides and isonitriles via [4+1] annulation[70]. CPME: cyclopentyl methyl ether.

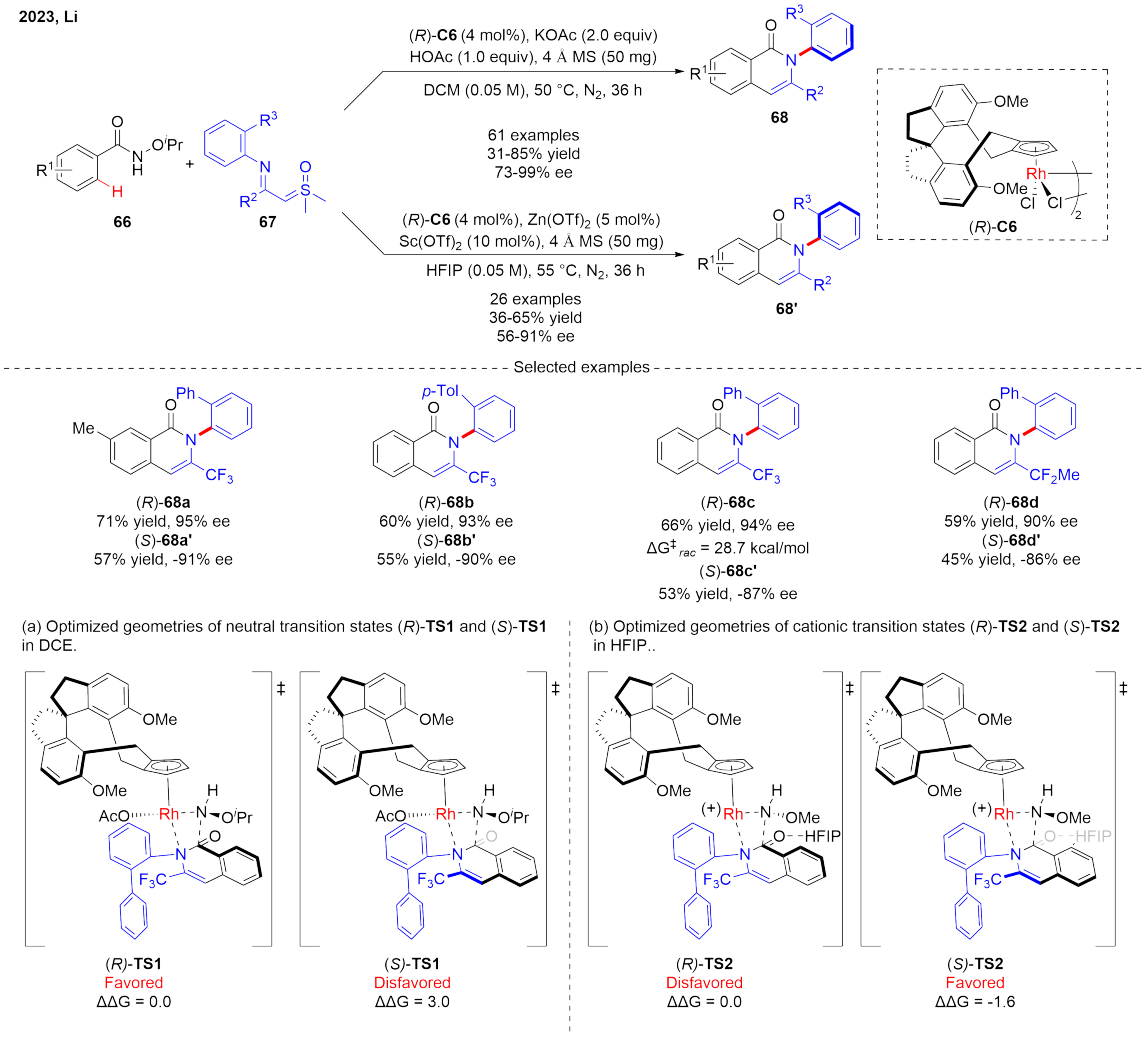

Figure 27. Synthesis of chiral isoquinolones bearing a C-N chiral axis with secondary benzamides and TFISYs via [3+3] annulation[71]. HFIP: hexafluoroisopropanol; DCM: dichloromethane; HOAc: acetic acid; TFISYs: CF_3-imidoyl sulfoxonium ylides.

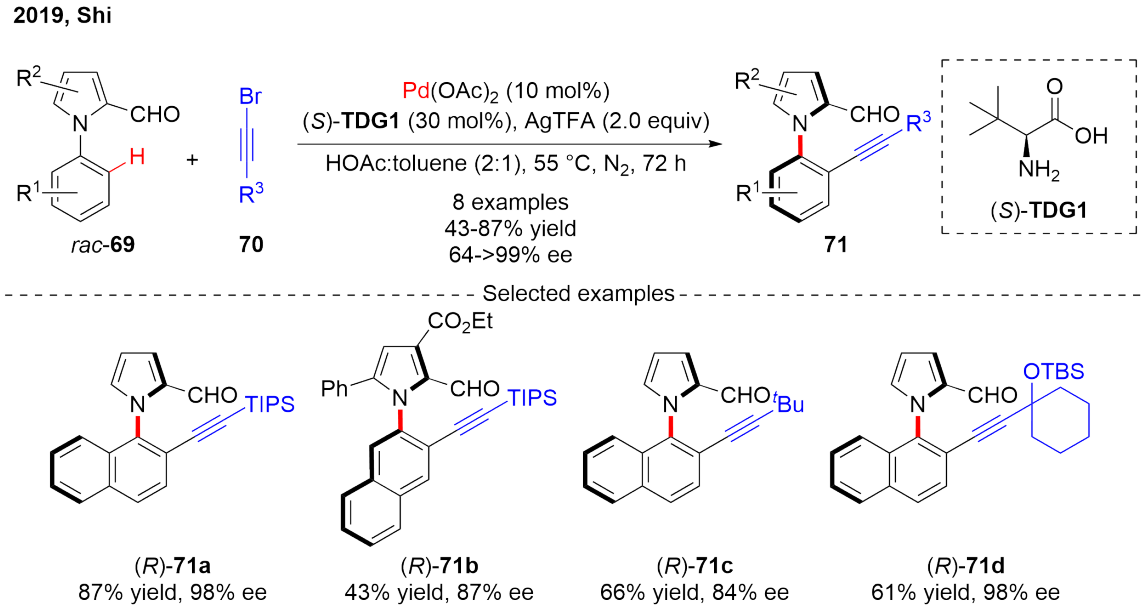

Figure 28. Synthesis of C-N axially chiral compounds via C-H activation/alkylation[18]. HOAc: acetic acid; TDG: transient directing group.

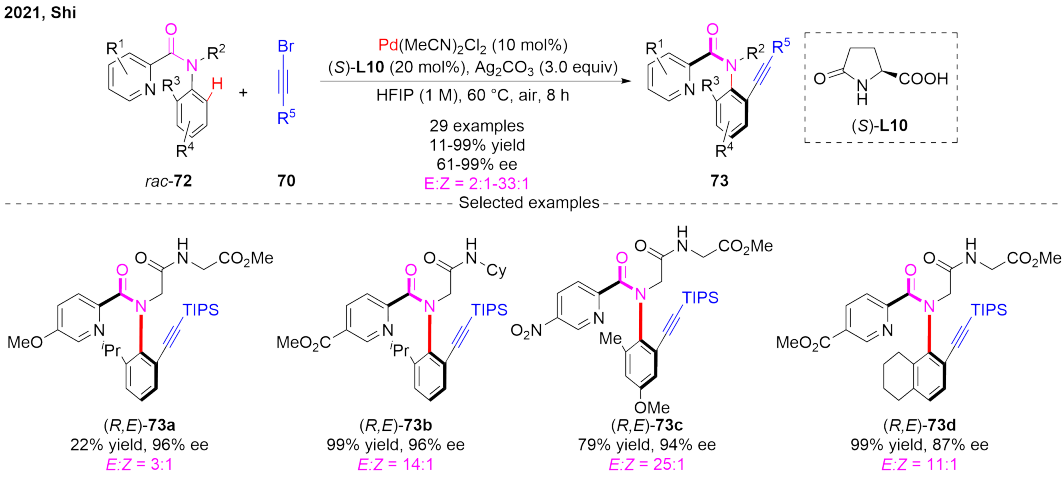

Figure 29. Synthesis of chiral atropisomers bearing a C-N chiral axis with racemic *N*-aryl peptoids and bromoalkynes[72]. HFIP: hexafluoroisopropanol.

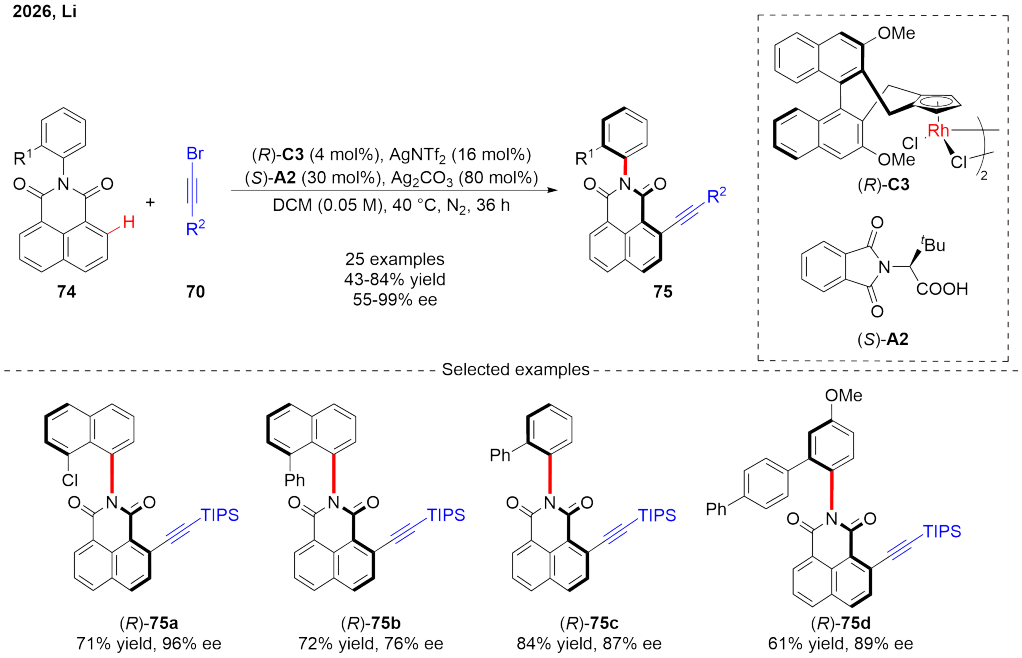

Figure 30. Construction of remote C-N chiral axis by asymmetric alkynylation of *N*-aryl-1,8-naphthalimides with bromoalkynes[73]. DCM: dichloromethane.

In 2022, Ackermann and coworkers presented a thioether-directed asymmetric C-H activation of *N*-arylindoles **86** and alkenes **83** catalyzed by Pd/**L11**, affording the C-N axially chiral products **87** in 54-89% yield and 85-99% ee (Figure 36a)[76]. Subsequently, Shi and coworkers developed the free amine-directed asymmetric C-H activation of *N*-arylindoles **88** and alkenes **83** catalyzed by Pd^{II}/chiral phosphoric acid **L12**, giving the target products **89** in 31-91% yield with 73-96% ee (Figure 36b)[77]. Due to the small steric hindrance of the amino group, the C-N rotational barrier of the product is low ($\Delta G^{\ddagger}_{rac}$ = 28.6 kcal/mol for **89d** in ^{i}PrOH at 80 °C). Later, Li and coworkers reported a $Pd(OAc)_2$/chiral acid **L10**-catalyzed, phosphoxy-directed C2 alkenylation of *N*-arylindoles **90** with alkenes **83**, affording a range of C-N axially chiral products **91** in 37-92% yield with 73 -> 99% ee (Figure 36c)[78]. Of the above three analogous examples, Shi and Li used stoichiometric metal oxidants, whereas Ackermann used air.

In 2021, Li and coworkers reported the enantioselective reaction of (hetero)arenes **92** with alkynes **8** using the chiral $CpRh^{III}$ catalyst **C3**, affording tetrasubstituted chiral olefins **93** via a unique migration of the directing group (Figure 37)[79]. Zinc carboxylate *rac*-**Zn1** was identified as an effective additive. Diverse C-N axially chiral acrylamides **93** were prepared in 54-93% yield and 80-99% ee. DFT calculations suggested that the *N*-aminocarbonyl migration proceeds via the β-nitrogen elimination of intermediate **I** to generate an isocyanate intermediate **II**. Subsequently, intermediate **II** underwent migratory insertion of isocyanate followed by protonation to give the product. This reaction is redox neutral, which obviates the need for external oxidants and thus significantly improves atom economy.

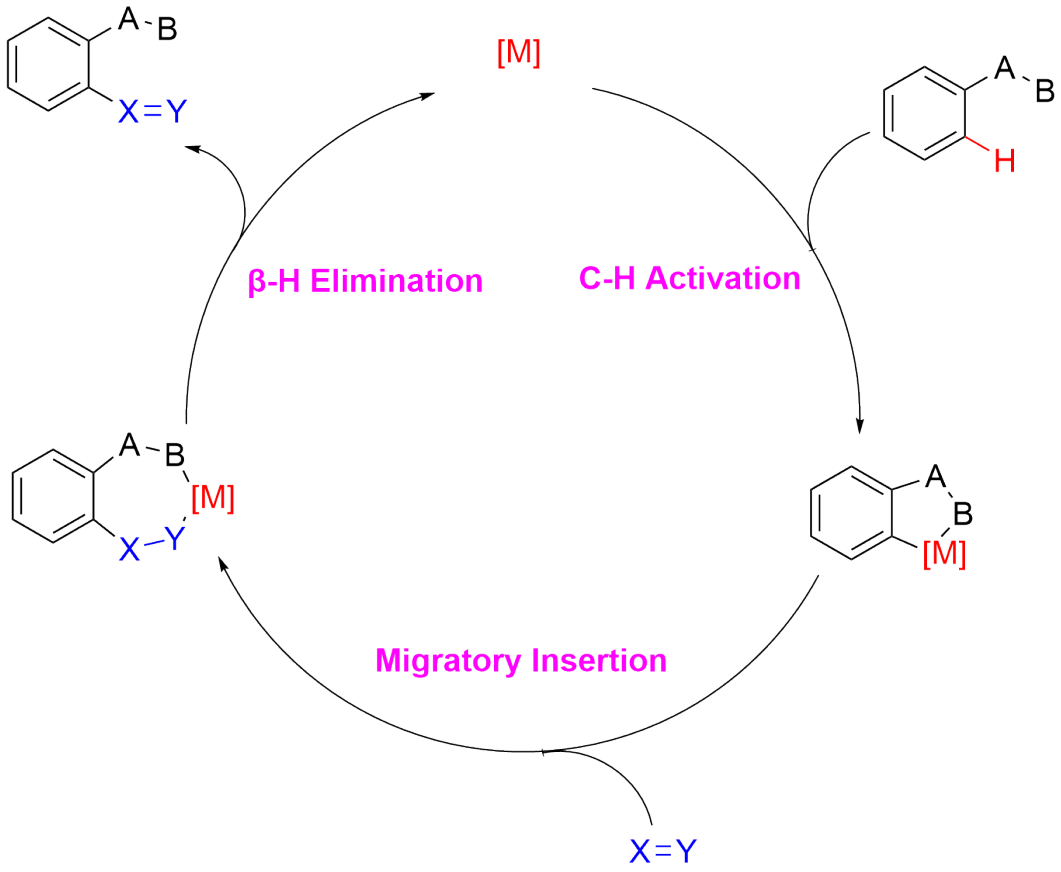

Figure 31. General mechanism of Heck-type C-H alkenylation reaction.

5. Asymmetric C-H Activation/Alkylation Reaction

To construct C–N axial chirality, alkenes serve not only as reactants in annulation and alkenylation reactions, but also participate in alkylation reactions. In 2021, Li and coworkers demonstrated simultaneous construction of central and axial chirality in the reaction of benzamides **94** with *N*-arylmaleimides **47** catalyzed by chiral CpRh **C7** (Figure 38)[80]. A broad range of benzamides **94** and *N*-arylmaleimides **47** were compatible, giving chiral products **95** in 40–98% yield with 81 -> 99% ee and > 19:1 dr. Mechanistically, during the coordination of *N*-arylmaleimides **47** with the C–H activation intermediate, the *exo*-type intermediates **III** and **IV** are disfavored due to the steric repulsion between the *N*-aryl ring and the *tert*-butyl on the Cp ligand. The configuration of the final product is governed by the steric interaction between the *N*-aryl substituent and the NR_2 group in the *endo*-type intermediates **I** and **II**, with intermediate **II** being more conducive to the reaction.

With the chiral transient directing group strategy, Shi and coworkers realized the asymmetric C–H activation/alkylation of benzaldehydes **96** with *N*-arylmaleimides **47** catalyzed by $[Ru(p\text{-cymene})Cl_2]_2$ and **TDG3** (Figure 39)[81]. A series of chiral products **97** with both C–N axial and central chirality were obtained in 27–99% yield with 16–98% ee and 2:1–18:1 dr. Notably, several additives are requisite to ensure the ideal reaction outcomes.

In 2022, Ackermann and coworkers reported a chiral imidazolidine carboxylic acid (CICA) ligand, which could be readily prepared from chiral diphenylethylenediamine in a single step. The chiral acid **L13** was successfully applied to the Ru^{II}-catalyzed asymmetric C–H alkylation of *N*-isoquinolyl indoles **98** with alkenes **83** (Figure 40a)[82]. The diastereoselectivity and regioselectivity are uniformly high (> 20:1 dr and b:l > 20:1). The C–N axially chiral products **99** were obtained in 35–93% yield and 30–96% ee.

Later, Ackermann and coworkers developed a data-driven transfer learning workflow that employed machine learning (ML) to predict catalytic performance (Figure 40b)[83]. By leveraging statistical data from a related transformation as the knowledge source, the ML model capitalized on delta learning to deliver accurate and extrapolative enantioselectivity predictions. Guided by this knowledge-transfer model, virtual screening of a broad set of 360 chiral carboxylic acids (CCA) led to the identification of a new ligand **L14** featuring an intriguing furyl moiety. Intriguingly, the robustness of **L14** was subsequently validated in Co^{II}-catalyzed C–H alkylation of *N*-isoquinolyl indoles **98** with alkenes **83**, which afforded a diverse array of C–N axially chiral indoles **99** in 47–95% yield with 82–95% ee, 4.6:1 to > 19:1 dr and > 19:1 b:l.

Notably, taking advantage of chiral BenRu^{II} catalyst **C8**, Wang and coworkers also successfully accomplished the C-H alkylation of *N*-isoquinolyl indoles **98** with alkenes **83** in 2025. A broad range of products **99** bearing both central and axial chirality were smoothly obtained in 48-99% yield with 91-99% ee, > 20:1 dr and > 20:1 b:l (Figure 40c)[84]. Substitution of HOAc by NaOAc resulted in complete loss of reactivity, indicating the essential role of the proton source.

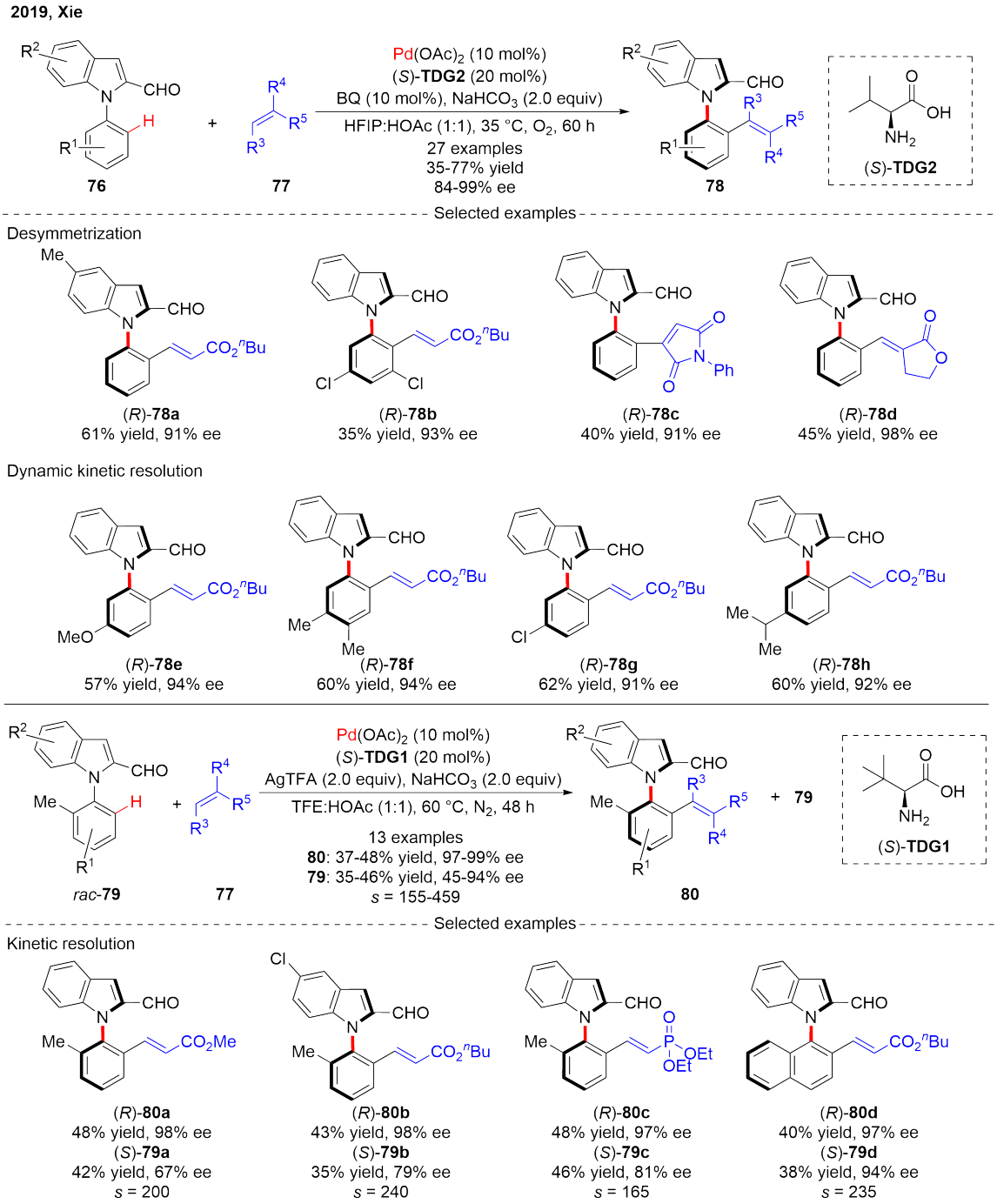

Figure 32. Synthesis of C-N axially chiral indoles via C-H activation/alkenylation of *N*-aryl heterocycles with alkenes[20]. HFIP: hexafluoroisopropanol; HOAc: acetic acid; TFE: 2,2,2-trifluoroethanol; TDG: transient directing group.

Ackermann and coworkers reported an alkylation of *N*-aryl-indoles **100** with alkenes **83** by an Fe/**L15** catalyst, affording the products **101** bearing both central and C-N axial chirality in 25-95% yield, with 86-99% ee and 9:1 -> 19:1 dr (Figure 41)[85]. The imine moiety in **100** acted as the directing group. The Grignard reagent was added to deprotonate the *N*-heterocyclic carbene (NHC) precursor **L15** to form the NHC ligand. A more electron-donating and less sterically demanding methoxy group at the ortho position, together with a bulky substituent at the meta position, proved beneficial to the stereocontrol ability of the ligand.

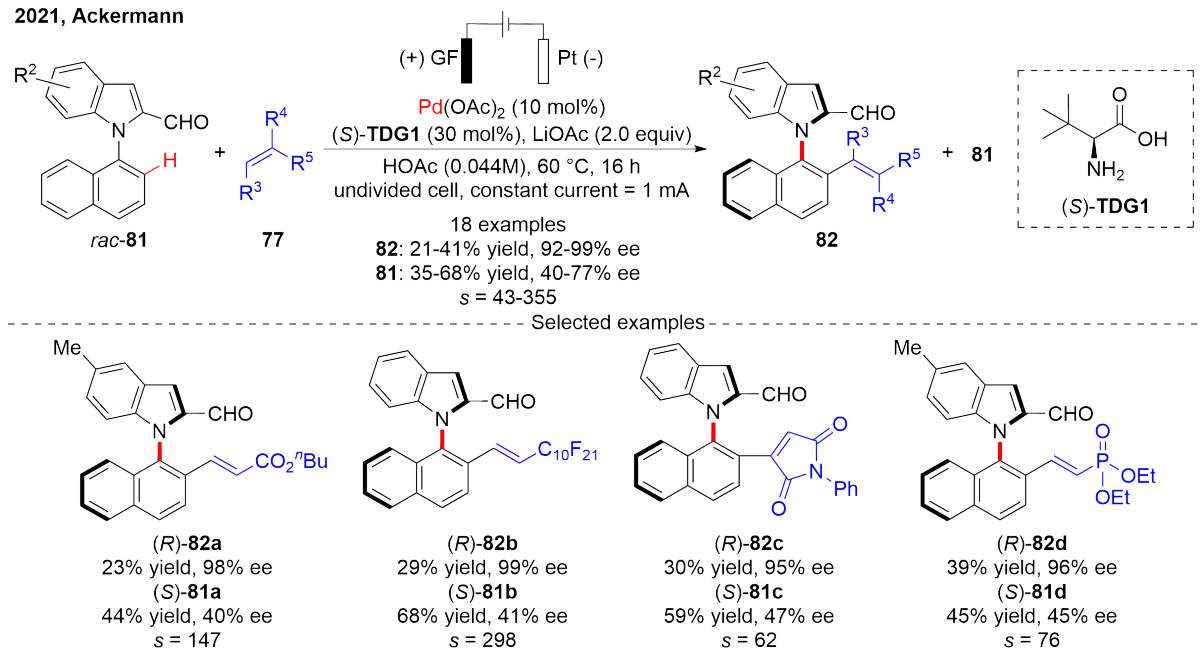

Figure 33. Synthesis of C-N axially chiral indoles with racemic *N*-arylindoles and alkenes by electrocatalysis[74]. HOAc: acetic acid; TDG: transient directing group; LiOAc: lithium acetate.

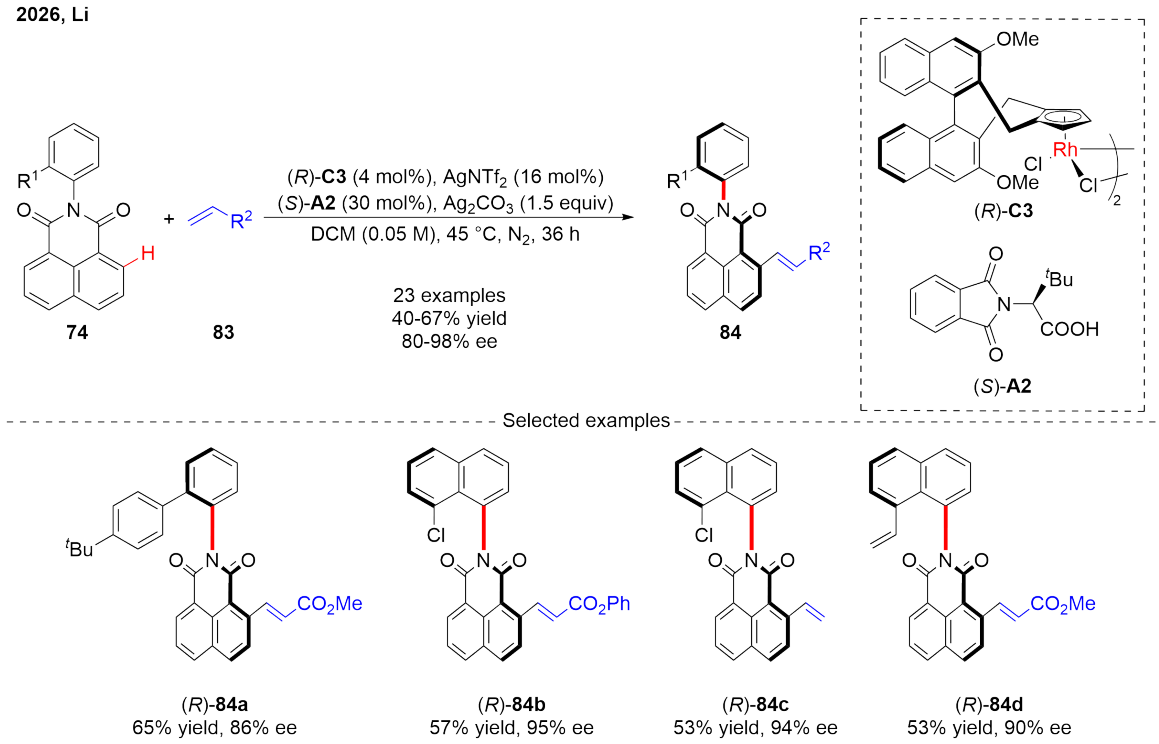

Figure 34. Asymmetric alkenylation of *N*-aryl-1,8-naphthalimides with alkenes[73]. DCM: dichloromethane.

In 2023, Li and coworkers reported an asymmetric C-H alkylation of pyridones **102** with *N*-$ArSO_2$, *O*-allyl hydroxyamines **103**, affording chiral products **104** bearing a C-N chiral axis and a chiral center in 62-91% yield with 89-98% ee and > 20:1 dr (Figure 42)[86]. This reaction was also extended to the kinetic resolution of *rac*-**102**, delivering product **104** in 42-52% yield with 93-99% ee and > 20:1 dr. In the proposed reaction mechanism, intermediate **I** forms via Rh-catalyzed C-H activation of **102** and coordination of **103**. Migratory insertion affords intermediate **II**. Subsequently, PivOH promotes N-O bond cleavage with concomitant formation of rhodium nitrenoid **III**. Finally, migratory insertion of nitrenoid furnishes product **104**.

In 2024, Rong and co-workers reported an Ir/chiral bisphosphine **L16**-catalyzed asymmetric alkylation of 2-aryl pyridines **105** with *endo*- or *exo*-*N*-aryl maleimides **106**/**106′** (Figure 43)[87]. The reaction delivered both *endo*-**107** and *exo*-**107′** in high yields with excellent stereocontrol. Notably, the products possess seven chiral axes/centers, including both C-C and C-N axial chirality. The *endo* products were obtained in 40-99% yield with 82-99% ee and > 20:1 dr. The *exo* products were formed in comparable yields (43-99%) but with higher enantioselectivities (93-97% ee) and similarly high dr (> 20:1). UV-vis, photoluminescence, CD, and CPL spectra of representative products showed promising optical properties, making them potential candidates for chiral organic light-emitting materials.

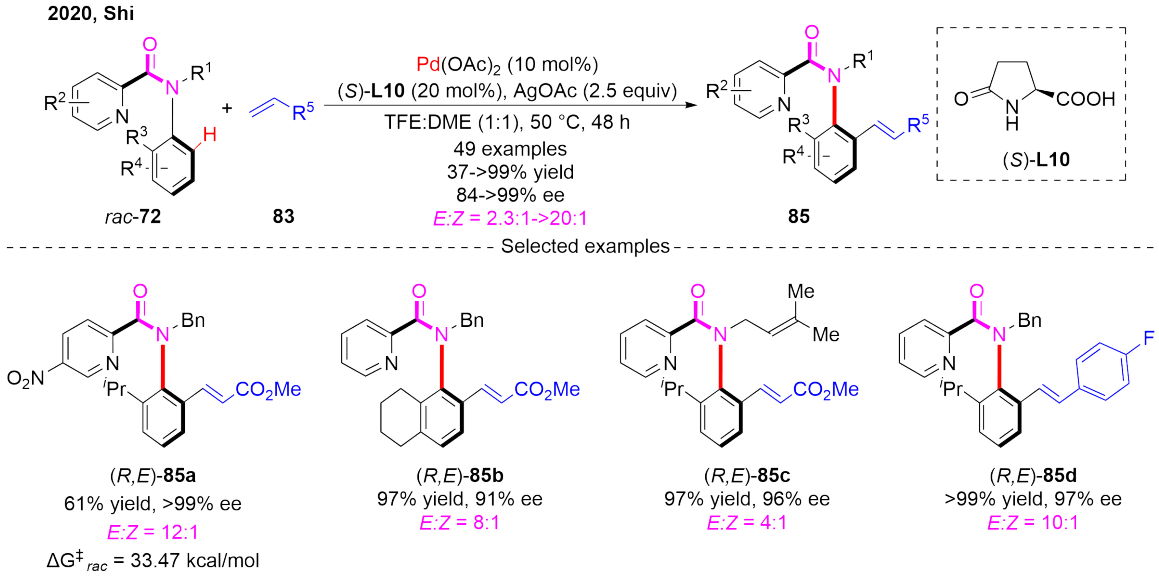

Figure 35. Synthesis of C-N axially chiral amides with racemic *N*-aryl peptoids and alkenes[75]. TFE: 2,2,2-trifluoroethanol; DME: 1,2-dimethoxyethane glyme; AgOAc: silver acetate.

In 2021, Shi and coworkers developed a Pd^{II}-catalyzed C-H alkylation of *N*-aryl peptoids **72** with alkenes **108** to construct C-N axial chirality (Figure 44)[88]. Using the chiral amino acid **L10** as the chiral ligand, chiral products **109** were obtained in 30-90% yield with 5-97% ee. Rotational barriers around the amide C-N bond resulted in isomeric products (*E*:*Z* = 1.4:1-11:1). The reaction proceeded via migratory insertion of 1,1-disubstituted alkenes **108** into the C-H activation intermediate followed by β-hydride elimination. With Ag_2SO_4/$Cu(OAc)_2$ as oxidants, reactivity was markedly enhanced while enantioselectivity slightly decreased.

6. Asymmetric C-H Activation/Arylation Reaction

While C(sp^2)-H activation has been widely employed to construct C-N axially chiral frameworks, C(sp^3)-H activation has rarely been used for this purpose. In 2021, Gong and coworkers achieved a highly efficient Pd-catalyzed kinetic resolution of atropisomeric thioanilides **110** with aryl boronic acids **111** via asymmetric C(sp^3)-H arylation using 1,4-BQ as an external oxidant (Figure 45)[89]. The combination of a Pd catalyst, an anionic chiral Co(III) complex **Co1**, and a matched phosphoramidite ligand **L17** enabled the kinetic resolution, affording the arylated products **112** in 30-55% yield with 82-99% ee and the recovered starting materials **110** in 25-67% yield with 45-99% ee. The addition of 3 Å molecular sieves and H_2O could ensure a higher *s*-factor. This work represents the first example of the construction of C-N axial chirality via C(sp^3)-H activation.

In 2023, Wencel-Delord and coworkers reported the synthesis of chiral indoles **114** bearing both C-C and C-N axes via C-H activation/arylation with *N*-aryl-indoles **100** and aryl chlorides **113** (Figure 46)[90]. Varied yields, enantioselectivities and diastereoselectivities (20-83% yield, 10-98% ee and 1.8:1-32.1:1 dr) have been achieved using Co^{II}/NHC as the catalyst. A proposed mechanism was described. The NHC precursor **L18** is deprotonated by Grignard reagent and then coordinates with $CoBr_2$ to afford the active catalytic species **I**. C-H activation yields intermediate **II**. Oxidative addition of aryl chlorides **113** furnishes intermediate **III**, which subsequently undergoes reductive elimination to give intermediate **IV**. Further transmetalation with the Grignard reagent regenerates catalyst **I**, releasing imine product **114′** bearing a C-N chiral axis. Finally, acidic work-up hydrolyzes the imine to the final product **114**.

7. Asymmetric C-H Activation/Borylation Reaction

Transition metal-catalyzed asymmetric C-H borylation has emerged as a powerful tool for the efficient synthesis of chiral organoboron compounds. However, this strategy has predominantly been employed for the highly enantioselective construction of central chirality[91]. In 2023, Xu reported a desymmetric borylation of *N*-aryl phthalimides **115** bearing a prochiral C-N axis using an

Ir/**L19** catalyst system, delivering the products **116** (Figure 47)[92]. As **116** proved to be unstable and could not be purified by column chromatography, it was converted into the hydroxyl derivatives **117** before isolation. This reaction exhibited high chemoselectivity, with no borylation at the *N*-aryl ring being observed. The products **117** were obtained in good yield and enantioselectivity (56-85% yield and 74-97% ee).

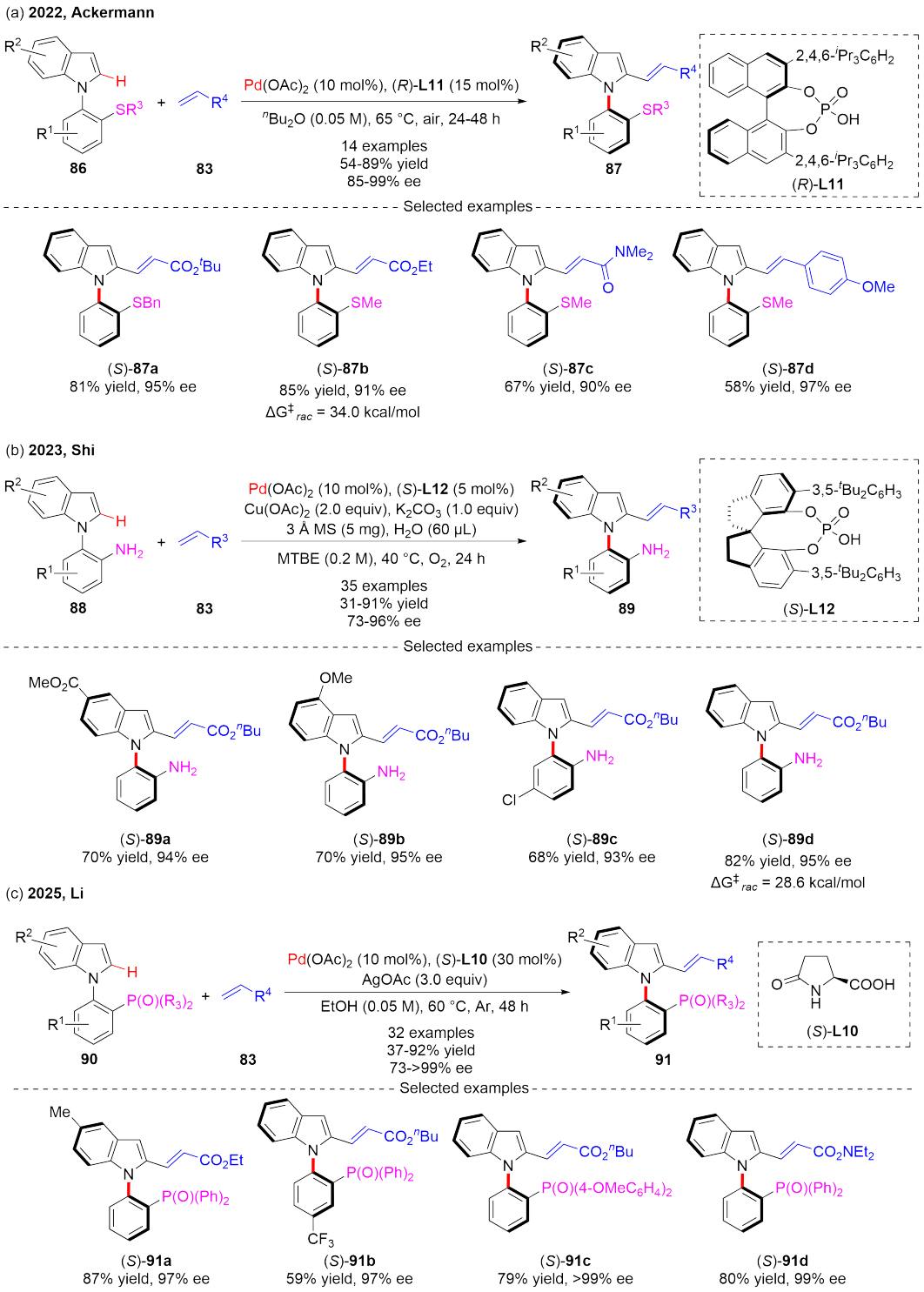

Figure 36. Asymmetric synthesis of C-N axially chiral indoles with thioether, free amine or phosphoxy as directing groups[76-78]. EtOH: ethanol; MTBE: methyl tert-butyl ether.

8. Asymmetric C-H Activation/Imidoylation Reaction

C-H imidoylation serves as an efficient strategy for the construction of heterocycles, typically employing imidoyl chlorides or isocyanides as substrates. However, the development of asymmetric C-H imidoylation remains underdeveloped, with only a handful

of examples reported for the construction of central[93-96], C-C axial[97], helical[98] and inherent[99] chirality. In 2024, Luo and coworkers reported a C-H imidoylation of indole-derived aryl isocyanides **118** with aryl iodides **55**, affording the C-N axially chiral products **119** in 79-91% yield with 83-93% ee (nine examples) (Figure 48)[97].

9. Conclusion and Outlook

This review comprehensively summarizes advances in constructing C-N axial chirality via transition metal-catalyzed C-H activation reactions since 2019. It encompasses a wide range of reaction types, including various annulations and C-H functionalizations. Annulation reactions include [2+2+2], [4+2], [3+2], [4+1] and [3+3] annulations. The [4+2] variant is the most reported. The [3+3] and [4+1] annulations remain less explored and thus warrant far greater attention. C-H functionalization has focused largely on C-C bond formations, including alkynylations, alkenylations, alkylations, arylations, borylations and imidoylations. Future efforts may prioritize the construction of carbon-heteroatom bonds. Diverse metal catalysts have been developed, including Co, Rh, Pd, Ru, Ir, and Fe catalysts. Notably, the high performance of cobalt catalysts is very impressive, and they are frequently paired with Salox ligands. Moreover, both electrocatalysis and photocatalysis have demonstrated great promise in C-H activation reactions toward C-N axial chirality construction. Interestingly, some C-N axially chiral compounds have been found to be promisingly useful in the development of chiral ligand/organocatalyst and optically active materials. To assist readers, detailed information regarding the reaction conditions, reaction outcomes, the largest reaction scale, and representative rotational energy barriers about the C-N chiral axes is summarized in Table 1.

Despite these advances, several challenges remain. First, reports on acyclic C-N axial chirality are scarce. Second, application of this strategy in total synthesis remains limited. Third, most reported examples require high catalyst loadings (10-20 mol% relative to the metal atom) and oxidant loadings (1.0-3.0 equiv of Mn^{III}, Cu^{II}, or Ag^{I} salts). Fourth, only about half of the reports include scale-up experiments, with the largest scale typically ranging from 1.0 to 5.0 mmol in most cases. Continued efforts are needed to reduce catalyst loadings, employ greener oxidants (e.g., O_2, electricity), and develop more cost-effective, efficient, and scalable synthetic methods that can be practically applied to the synthesis of useful functional molecules.

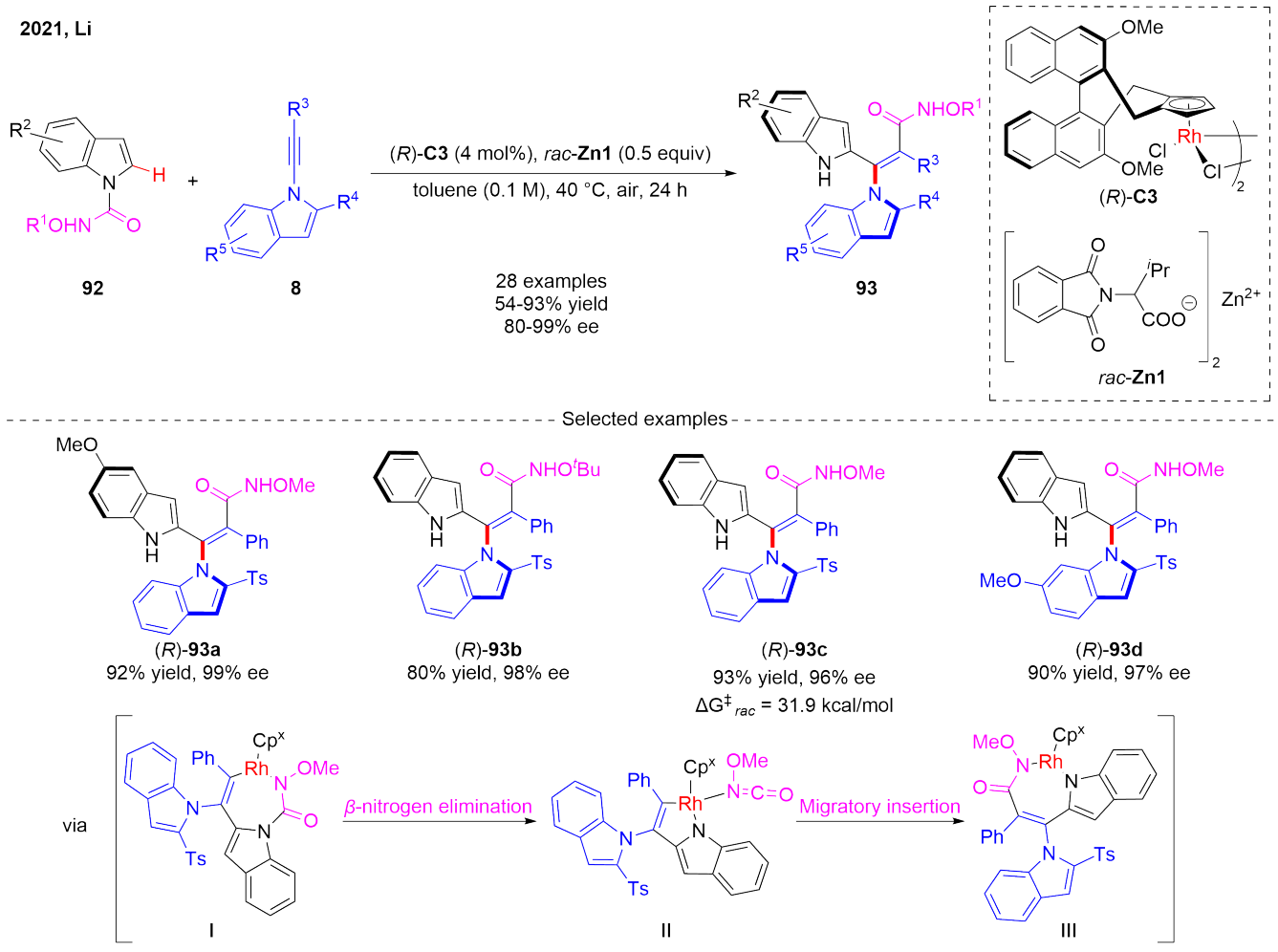

Figure 37. Synthesis of C-N axially chiral acrylamides from (hetero)arenes and alkynes[79].

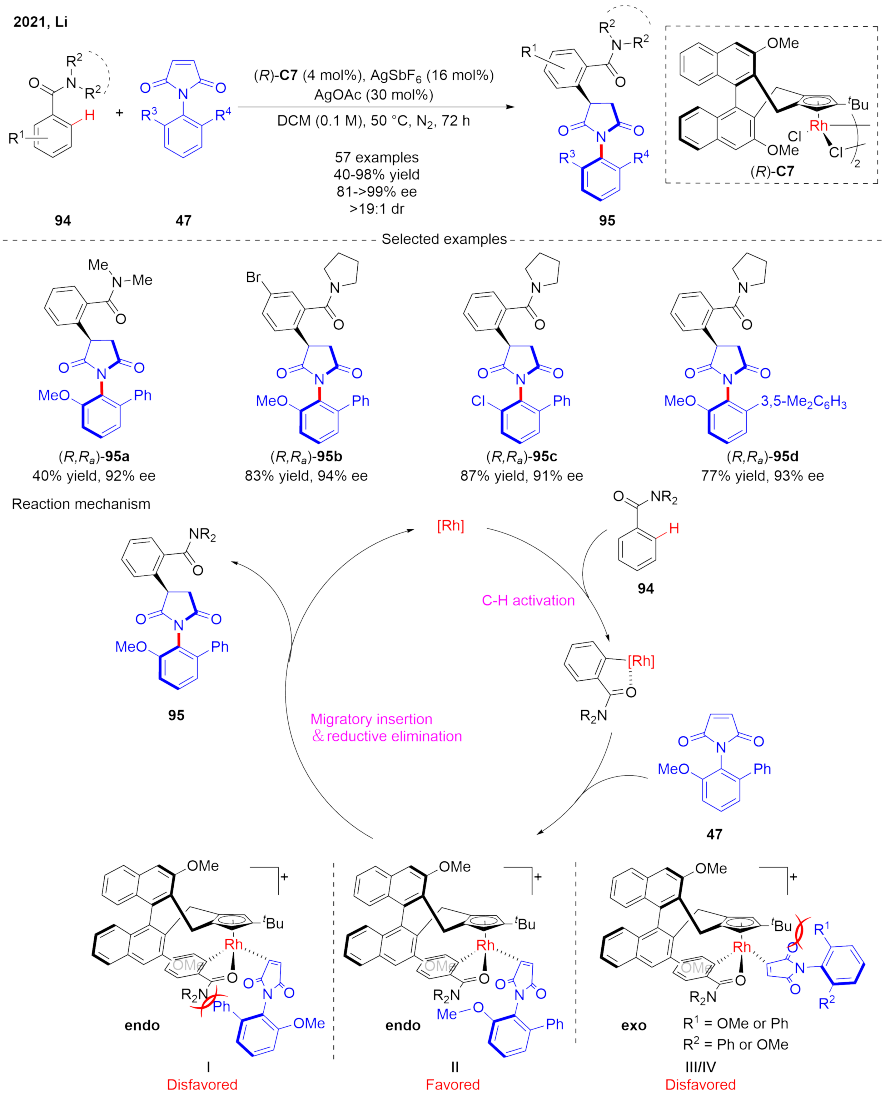

Figure 38. Synthesis of chiral benzamides bearing a C-N chiral axis and chiral center with benzamides and *N*-arylmaleimides[80]. DCM: dichloromethane.

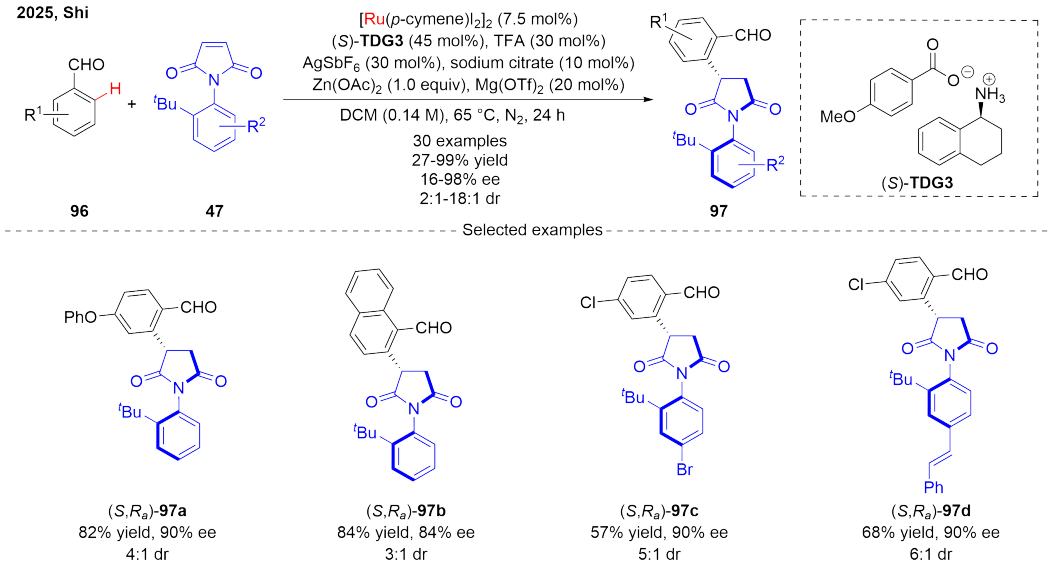

Figure 39. Asymmetric alkylation of benzaldehydes with *N*-arylmaleimides[81]. DCM: dichloromethane; TDG: transient directing group; TFA: trifluoroacetate.

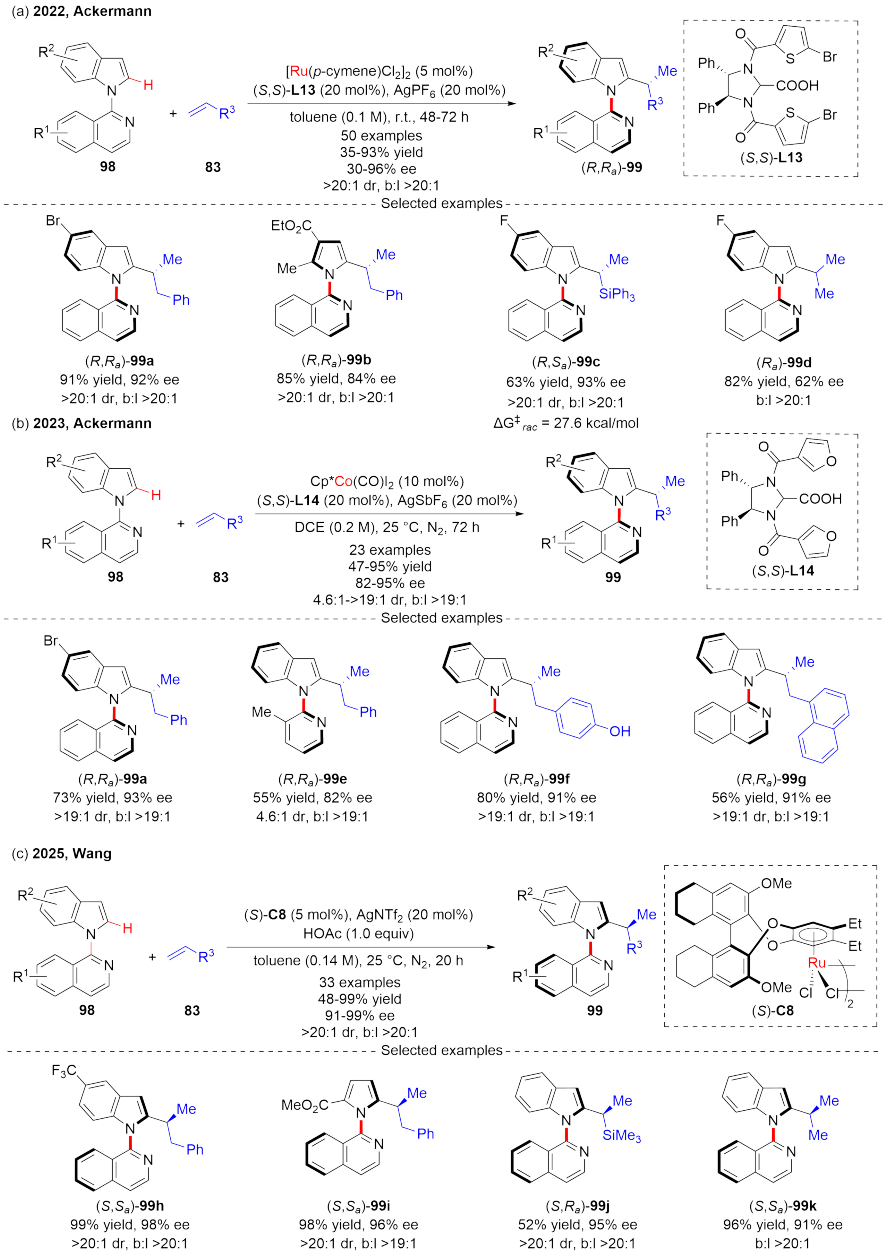

Figure 40. Synthesis of chiral indoles bearing a C-N chiral axis and a chiral center with *N*-isoquinolyl indoles and alkenes[82-84]. DCE: 1,2-dichloroethane; HOAc: acetic acid.

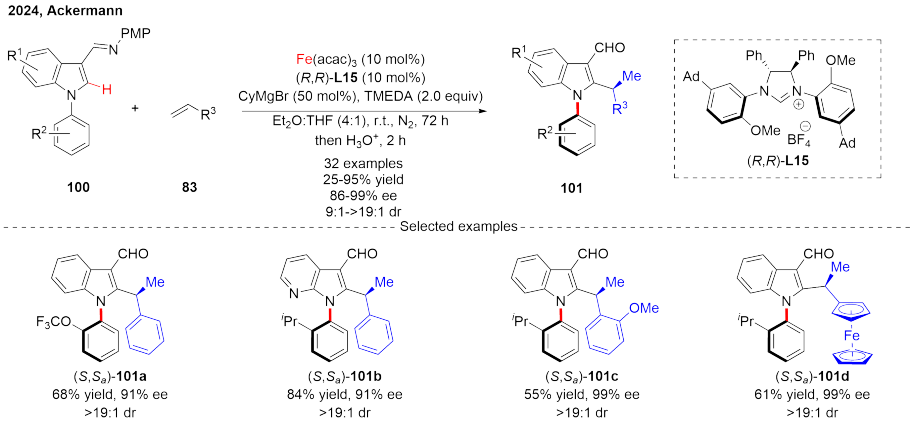

Figure 41. Iron-catalyzed asymmetric C-H activation/alkylation reaction of *N*-aryl-indoles and alkenes[85].

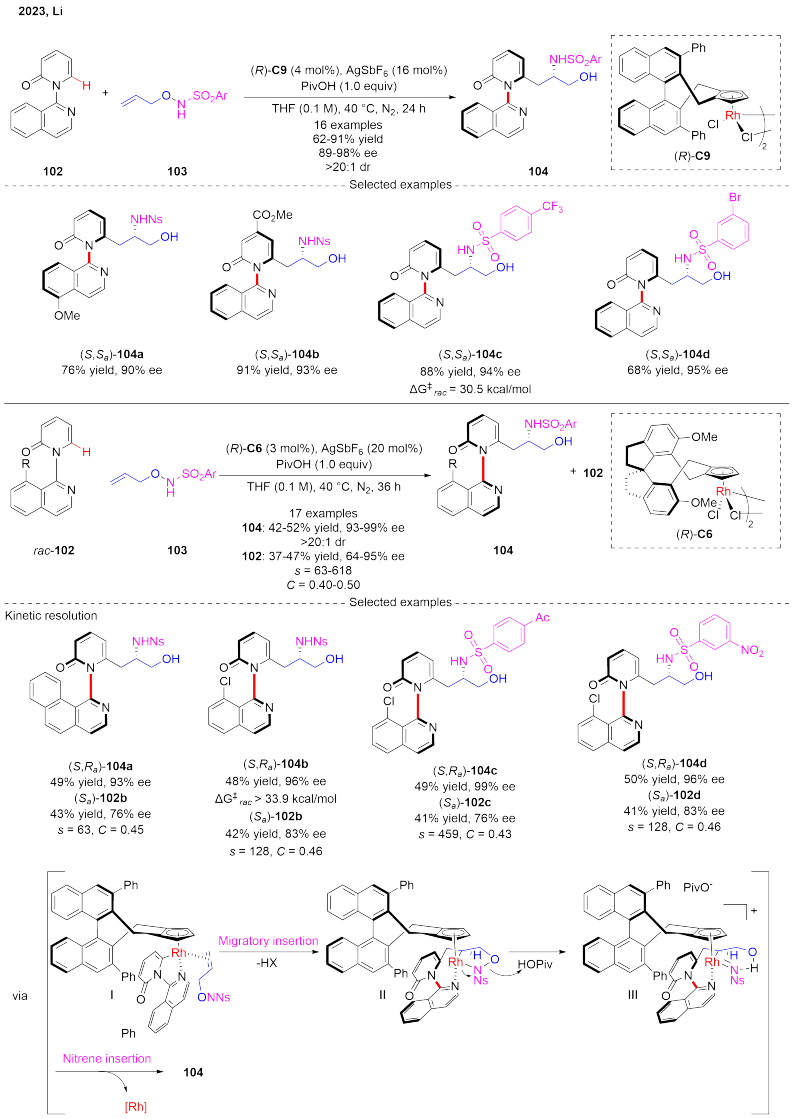

Figure 42. The asymmetric alkylation of pyridones with *N*-ArSO$_2$, *O*-allyl hydroxyamines[86]. THF: tetrahydrofuran.

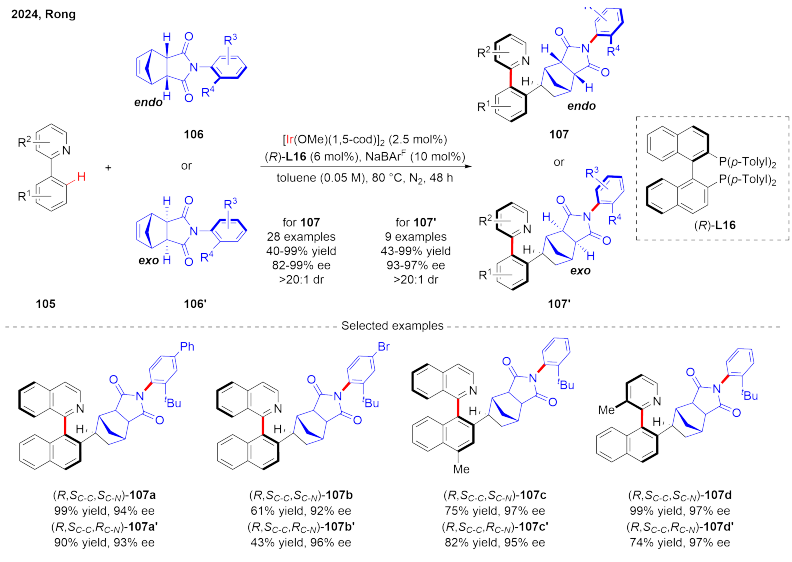

Figure 43. The asymmetric alkylation of 2-aryl pyridines with N-aryl maleimides[87].

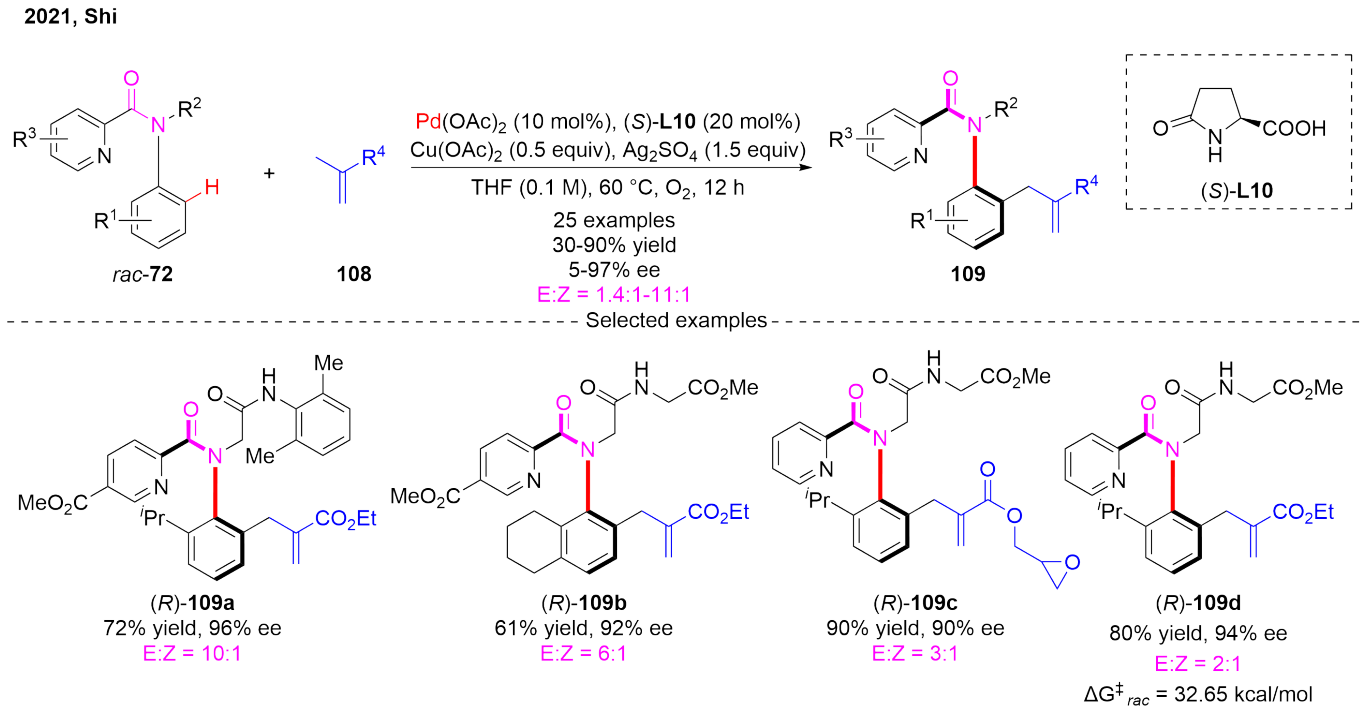

Figure 44. Synthesis of C-N axially chiral *N*-aryl peptoids by asymmetric C-H alkylation with 1,1-disubstituted alkenes[88]. THF: tetrahydrofuran.

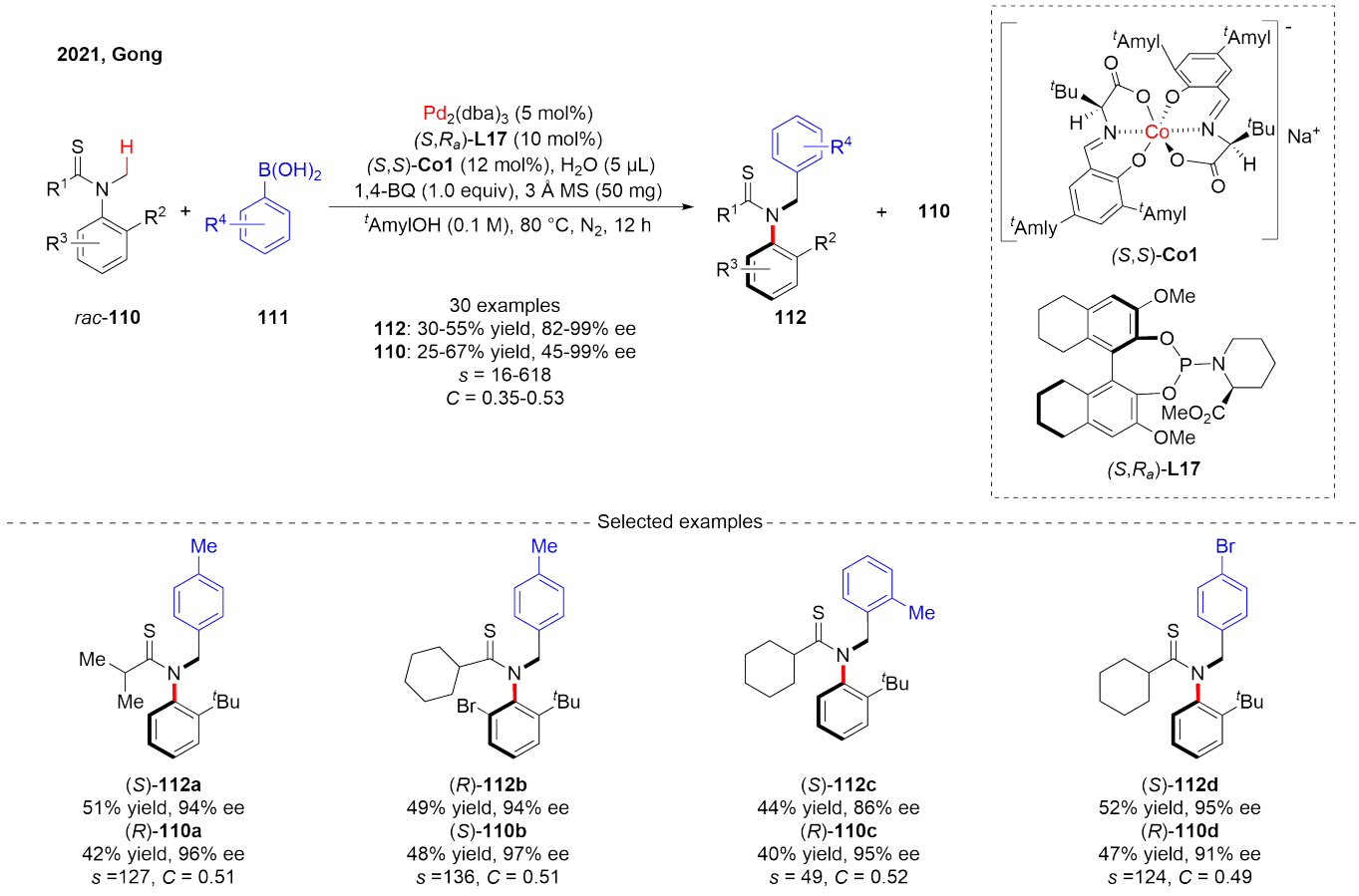

Figure 45. Kinetic resolution of C-N axially chiral thioanilides with aryl boronic acids via asymmetric C(sp^3)-H arylation[89]. BQ: benzoquinone.

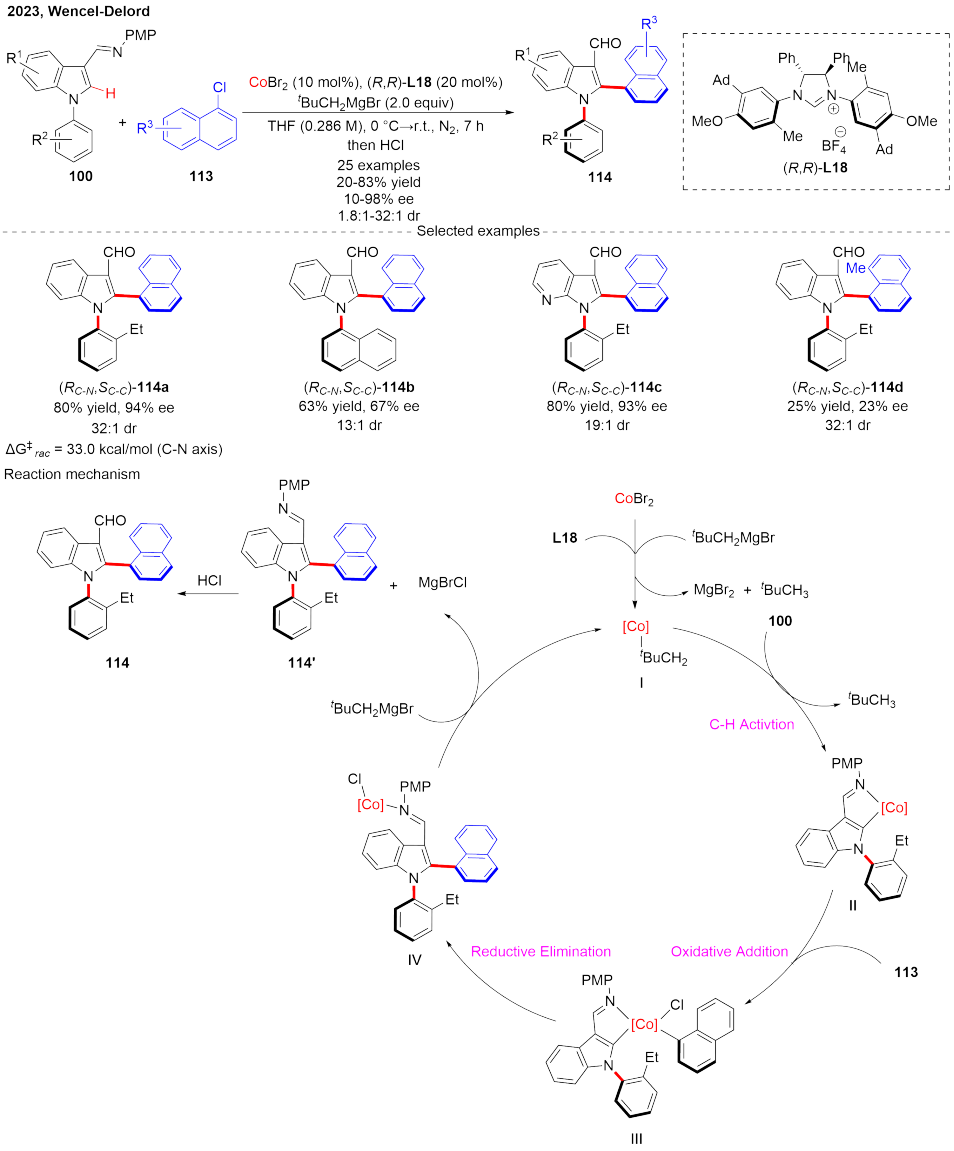

Figure 46. Synthesis of chiral atropisomeric indoles bearing C-N and C-C chiral axes with *N*-aryl-indoles and aryl chlorides [90]. THF: tetrahydrofuran.

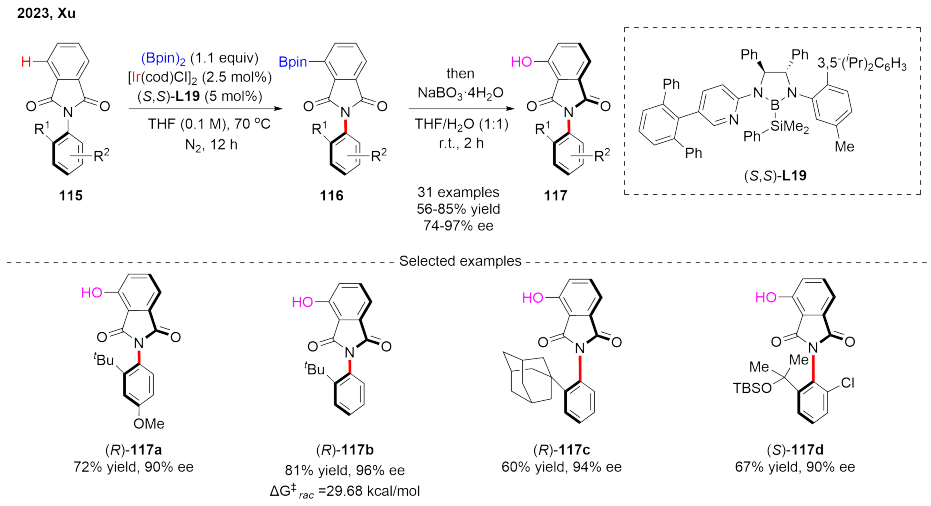

Figure 47. Asymmetric desymmetric borylation of *N*-aryl phthalimides[92]. THF: tetrahydrofuran.

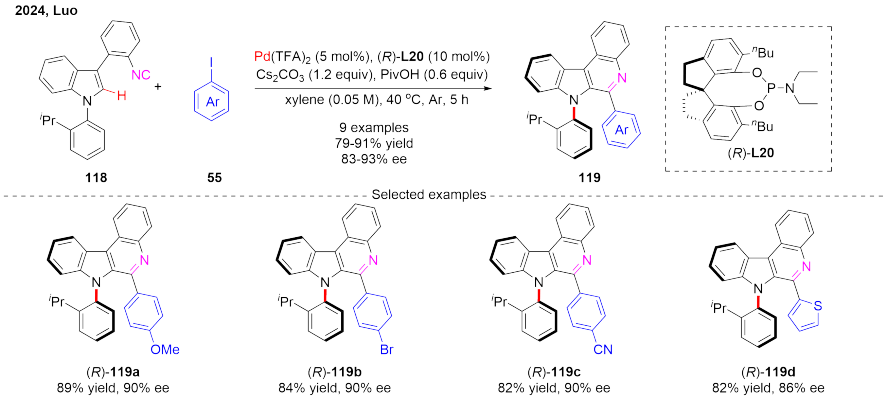

Figure 48. Asymmetric C-H imidoylation of isocyanides with aryl iodides[97]. TFA: trifluoroacetate.

Table 1. Summary of asymmetric C-H activation reactions for the construction of C-N axial chirality.

Entry	Product	Reaction type	Catalyst (mol%)	Ligand (mol%)	Oxidant (equiv)	Additive (equiv)	Solvent	Temperature (℃)	Yield (%)	ee (%)	Examples	Largest scale reported (mmol)	$\Delta G^{\ddagger}_{rac}$ (kcal/mol)
1[7]		[2+2+2]	**C1** (5)	\	Ag_2O (1.1)	$AgNTf_2$ (0.2), $^{i}PrCO_2H$ (2.2)	DCE	70	17-99	8-99	39	2.5	\
2[12]			**C2** (2.5)	\	Ag_2O (1.1)	$AgPF_6$ (0.1), DMBA (2.2)	DCM	45	45-95	78-94	20	0.1	\
3[13]	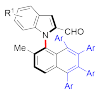		$Pd(OAc)_2$ (10)	**TDG1** (30)	AgTFA (2.0)	NaOAc (3.0)	HFIP/HOAc	70	25-40	95-98	4	0.1	\
4[37]		[4+2]	**C3** (4)	\	\	**A1** (1.0), $TlPF_6$ (0.16) $Zn(OTf)_2$ (0.1)	DCM	30	54-85	77-98	23	1.0	> 34.1 for **10a** (toluene, 100 ℃)
5[38]			$Co(OAc)_2$·$4H_2O$ (10)	**L1** (20)	O_2	\	dioxane	100	7-98	86-98	50	3.0	37.7-39.4 (DMSO, 160 ℃)
6[41]			$Co(NO_3)_2$·$6H_2O$ (10)	**L1** (15)	air	NaOPiv (2.0), **PC1** (0.02)	HFIP	r.t.	31-99	73-98	43	0.2	\
7[42]	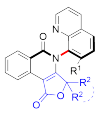		$Co(OAc)_2$·$4H_2O$ (10)	**L2** (15)	electricity	$AdCO_2H$ (3.0), $BminPF_6$ (0.05 M)	$^{i}PrOH$	60	81-95	99	8	0.2	48.3 for **15a** (calculated by DFT)
8[43]			$Co(OAc)_2$·$4H_2O$ (10)	**L3** (20)	$Mn(OAc)_3$·$2H_2O$ (1.0)	NaOPiv·H_2O (1.0)	CH_3OH	100	20-96	91->99	46	3.0	33.3-34.1 (DMSO, 130 ℃)
9[44]			$Co(OAc)_2$·	**L3** (10)	electricity	NaOPiv·H_2	TFE	60	35-97	88-98	38	2.0	34.30-36.32

		$4H_2O$ (10)			O (2.0)						(DMSO, 130-150 ℃)
10[40]		$CoSO_4$·$7H_2O$ (10)	**L4** (20)	$Mn(OAc)_3$·$2H_2O$ (1.0)	NaOPiv·$2H_2O$ (2.0)	^{n}PrOH	50	24-99	41->99	23	4.0	27.6-29.8 (calculated by DFT)
11[45]	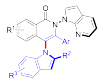	**C3** (3)	\	AgOAc (2.0)	$AgSbF_6$ (0.12), 4-$CF_3C_6H_4CO_2H$ (1.0)	**S1**	80	32-82	88-99	19	0.1	\
12[46]	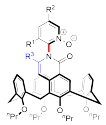	$Co(OAc)_2$·$4H_2O$ (10)	**L5** (15)	O_2	NaOPiv·H_2O (2.0)	PhF	80	40-94	81-96	32	1.5	33.7-34.7 (dioxane, 120 ℃)
13[47]	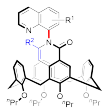	$Co(OAc)_2$·$4H_2O$ (10)	**L6** (10)	$Mn(OAc)_3$·$2H_2O$ (2.0)	NaOPiv·H_2O (2.0)	EtOH	70	60-99	99->99	49	1.2	\
14[48]	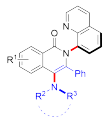	$Co(OAc)_2$·$4H_2O$ (10)	**L7** (25)	electricity	NaOPiv (2.0), $BminPF_6$ (0.06 M)	^{i}PrOAc/ ^{n}heptane/ TFE	60	37-82	16-99	22	0.2	\
15[49]		$Co(OAc)_2$·$4H_2O$ (10)	**L1** (20)	O_2	\	DCE	50	32-93	96->99	36	2.5	35.8-43.2 (decane, 160-200 ℃)
16[50]		$Co(OAc)_2$·$4H_2O$ (20)	**L8** (30)	air	NaOPiv (2.0)	HFIP	r.t.	72-98	93->99	37	0.1	33.5-34.5 (DMSO, 110 ℃)
17[51]	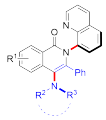	$Co(OAc)_2$·$4H_2O$ (10)	**L3** (15)	air	NaOPiv·H_2O (2.0)	TFE	25	73-93	80-98	25	2.0	>29.7 (TFE, 70 ℃)
18[52]	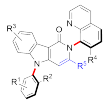	$Co(OAc)_2$·$4H_2O$ (10)	**L6** (10)	$Mn(OAc)_3$·$2H_2O$ (2.0)	NaOPiv·H_2O (2.0)	^{t}BuOH	40	23->99	96->99	60	2.5	\
19[53]	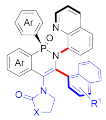	$Co(OAc)_2$·$4H_2O$ (10)	**L9** (10)	$Mn(OAc)_2$·$4H_2O$ (1.0), air	NaOPiv·H_2O (2.0)	^{t}BuOH	40	56-87	88->99	22	0.2	\
20[54]	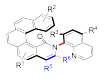	$Co(OAc)_2$·$4H_2O$ (20)	**L3** (20)	O_2	\	HFIP	75	25-92	90->99	44	1.0	37.6 for 36b (dodecane, 150 ℃)
21[43]	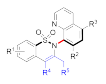	$Co(OAc)_2$·$4H_2O$ (5)	**L3** (5)	O_2	PivOH (1.0)	$(CHCl_2)_2$	100	32-95	77-98	45	3.0	34.4-34.9 (DMSO, 130 ℃)
22[56]	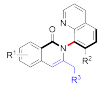	$Co(OAc)_2$·$4H_2O$ (5)	**L3** (7.5)	electricity	NaOPiv (2.0), $BminPF_6$	TFE/DCE	r.t.	44-98	82->99	28	29.7	39.4 for 42c (DMSO, 190 ℃)

					(0.065 M)							
23[57]			$Co(OAc)_2·4H_2O$ (5)	**L1** (10)	O_2	\	$PhCF_3$	80	27-97	89->99	41	4.0	37.1-37.4 (DMSO, 160 ℃)
24[58]	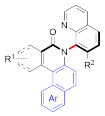		$Co(OAc)_2·4H_2O$ (15)	**L1** (25)	O_2	$NaOPiv·H_2O$ (1.2), Eosin Y (0.05)	TFE	r.t.	50-84	82-98	35	0.2	\
25[60]			$[Ru(p\text{-cymene})Cl_2]_2$ (15)	chiral directing group strategy	Ag_2CO_3 (2.0)	$AgSbF_6$ (1.0), $Zn(OAc)_2$ (2.0)	THF	50	42-61	80-92	4	0.2	\
26[61]			$Co(OAc)_2$ (5)	**L3** (5)	electricity	NaOPiv (2.0)	TFE	25	40-97	93->99	27	0.2	25.58 for (*d8*-toluene, 90-110 ℃)
27[62]	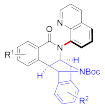		$Co(OAc)_2·4H_2O$ (10)	**L8** (10)	$Mn(OAc)_3·2H_2O$ (3.0)	$NaOPiv·H_2O$ (1.0)	TFE	60	41-99	82-99	24	0.2	\
28[63]			$Co(ClO_4)_2·6H_2O$ (10)	**L1** (12)	Ag_2O (2.5)	$NaOPiv·H_2O$ (1.0), Na_2CO_3 (2.0)	acetone	80	45-89	92->99	30	2.9	\
29[64]			$Pd(OAc)_2$ (10)/ **NBE1** (50)	TFP (22)	\	K_2CO_3 (2.5)	MeCN	70	42-97	87->99	44	4.0	30.5-38.5 (calculated by DFT)
30[65]			$Pd(OAc)_2$ (10)/ **NBE1** (50)	\	\	K_2CO_3 (2.5)	THF	80	55-98	21-98	38	0.1	31.9 for **59b** (toluene, 100 ℃)\
31[66]	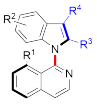	[3+2]	**C4** (4)	\	$AgBF_4$ (2.5)	$AgSbF_6$ (0.16), HOAc (2.0)	EA	25	24-89	74-96	55	0.1	\
32[67]			**C5** (5)	\	$Cu(OAc)_2$ (2.0)	Na_2CO_3 (1.0)	HFIP	r.t.	14-97	72-98	37	2.5	\
33[68]			**C5** (5)	\	electricity	KPF_6 (0.2), NaOAc (0.2)	$HFIP/H_2O$	60	47-99	72-94	26	0.1	\
34[69]	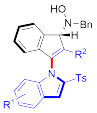		**C3** (4)	\	\	$AgSbF_6$ (0.16), HOPiv (2.0)	DCM	23	67-91	91-95	6	1.0	\
35[70]		[4+1]	$Co(OBz)_2$ (10)	**L1** (20)	O_2	\	CPME	100	51-98	74->99	39	4.0	35.8-37.3 (DMSO, 140 ℃)
36[71]		[3+3]	C6 (4)	\	\	KOAc (2.0), HOAc	DCM	50	31-85	73-99	61	0.1	28.7->37.0 (iPrOH or

					(1.0)4 Å MS (50 mg)							toluene, 70-120 ℃)
37[18]		Alkynylation	$Pd(OAc)_2$ (10)	**TDG1** (30)	\	AgTFA (2.0)	HOAc/toluene	55	43-87	64->99	8	0.1	\
38[72]			$Pd(MeCN)_2Cl_2$ (10)	**L10** (20)	\	Ag_2CO_3 (3.0)	HFIP	60	11-99	61-99	29	2.5	\
39[73]	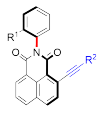		**C3** (4)	\	\	$AgNTf_2$ (0.16), **A2** (0.3), Ag_2CO_3 (0.8)	DCM	40	43-84	55-99	25	0.1	\
40[20]		Alkenylation	$Pd(OAc)_2$ (10)	**TDG2** (20)	O_2	BQ (0.1), $NaHCO_3$ (2.0)	HFIP/HOAc	35	35-77	84-99	27	0.1	\
41[74]			$Pd(OAc)_2$ (10)	**TDG1** (30)	electricity	LiOAc (2.0)	HOAc	60	21-41	92-99	18	0.2	\
42[73]	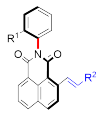		**C3** (4)	\	Ag_2CO_3 (1.5)	$AgNTf_2$ (0.16), **A2** (0.3)	DCM	45	40-67	80-98	23	0.1	\
43[75]	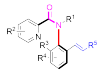		$Pd(OAc)_2$ (10)	**L10** (20)	AgOAc (2.5)	\	TFE/DME	50	37->99	84->99	49	0.1	29.72-33.47 (^{i}PrOH, 80-110 ℃)
44[76]			$Pd(OAc)_2$ (10)	**L11** (15)	air	\	$^n Bu_2O$	65	54-89	85-99	14	0.1	34.0 for **87b** (calculated by DFT)
45[77]			$Pd(OAc)_2$ (10)	**L12** (5)	$Cu(OAc)_2$ (2.0)	K_2CO_3 (1.0), 3 Å MS (5 mg) H_2O (60 μL)	MTBE	40	31-91	73-96	35	5.0	28.6 for **89d** (^{i}PrOH, 80 ℃)
46[78]			$Pd(OAc)_2$ (10)	**L10** (30)	AgOAc (3.0)	\	EtOH	60	37-92	73->99	32	5.0	\
47[79]	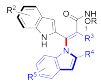		**C3** (4)	\	\	**Zn1** (0.5)	toluene	40	54-93	80-99	28	0.1	31.9 for **93c** (toluene, 100 ℃)
48[80]	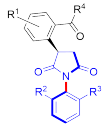	Alkylation	**C7** (4)	\	\	$AgSbF_6$ (0.16), AgOAc (0.3)	DCM	50	40-98	81->99	57	0.1	\
49[81]			[Ru(*p*-cymene)I_2]$_2$ (7.5)	**TDG3** (45)	\	TFA (0.3), $AgSbF_6$ (0.3), sodium citrate	DCM	65	27-99	16-98	30	7	\

					(0.1), $Zn(OAc)_2$ (1.0), $Mg(OTf)_2$ (0.2)							
50[82]			[Ru(*p*-cymene)$Cl_2]_2$ (5)	**L13** (0.2)	\	$AgPF_6$ (0.2)	toluene	r.t.	35-93	30-96	50	0.1	27.1-27.6 (*d8*-toluene, 70-80 ℃)
51[83]			Cp*Co(CO)I_2 (10)	**L14** (20)	\	$AgSbF_6$ (0.2)	DCE	25	47-95	82-95	23	0.1	\
52[84]			**C8** (5)	\	\	$AgNTf_2$ (0.2), HOAc (1.0)	toluene	25	48-99	91-99	33	3.5	\
53[85]			$Fe(acac)_3$ (10)	**L15** (10)	\	CyMgBr (0.5), TMEDA (2.0) (then H_3O^+)	Et_2O/THF	r.t.	25-95	86-99	32	4.0	\
54[86]			**C9** (4)	\	\	$AgSbF_6$ (0.16), PivOH (1.0)	THF	40	62-91	89-98	16	0.1	\
55[87]			[Ir(OMe)(1,5-cod)]$_2$ (2.5)	**L16** (6)	\	$NaBAr^F$ (0.1)	toluene	80	40-99	82-99	28	3.5	\
56[88]			$Pd(OAc)_2$ (10)	**L10** (20)	$Cu(OAc)_2$ (0.5) Ag_2SO_4 (1.5)	\	THF	60	30-90	5-97	25	4.0	32.65 for **109d** (*p*-xylene at 125 °C.)
57[89]	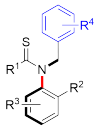	Arylation	$Pd_2(dba)_3$ (5)	**L17** (10)	1,4-BQ (1.0)	**Co1** (0.12), H_2O (5 μL) 3 Å MS (50 mg)	^{t}AmylOH	80	30-55	82-99	30	0.1	\
58[90]			$CoBr_2$ (10)	**L18** (20)	\	^{t}BuCH_2MgBr (2.0) (then HCl)	THF	0 ℃→r.t.	20-83	10-98	25	3.0	33.0 for **114a** (calculated by DFT)
59[92]	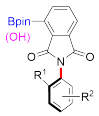	Borylation	[Ir(cod)Cl]$_2$ (2.5)	**L19** (5)	\	(then $NaBO_3 \cdot 4H_2O$)	THF	70	56-85	74-97	31	17.9	29.68 for 117b (toluene, 100 ℃)
60[97]	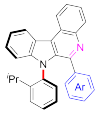	Imidoylation	$Pd(TFA)_2$ (5)	**L20** (10)	\	Cs_2CO_3 (1.2), PivOH (0.6)	xylene	40	79-91	83-93	10	0.1	\

TDG: transient directing group; AgTFA: silver trifluoroacetate; AgOAc: silver acetate; TFE: 2,2,2-trifluoroethanol; DCE: 1,2-dichloroethane; HFIP: hexafluoroisopropanol; TFP: 3,3,3-trifluoropropene; NBE: norbornene; THF: tetrahydrofuran; EA: ethyl acetate; DCM: dichloromethane; CPME: cyclopentyl methyl ether; BQ: benzoquinone; LiOAc: lithium acetate; DME: 1,2-dimethoxyethane glyme; TFA: trifluoroacetate; Pd: palladium; TMEDA: tetramethylethylenediamine.

Declarations

Authors contribution

Ji J: Investigation, writing-original draft, writing-review & editing.
Wang J: Conceptualization, funding acquisition, supervision, writing-review & editing.

Conflicts of interest

The authors declare that they have no conflicts of interest.

Ethical approval

Not applicable.

Consent to participate

Not applicable.

Consent for publication

Not applicable.

Availability of data and materials

Not applicable.

Funding

We thank the National Key R&D Program of China (Grant No. 2022YFA1504303), the National Natural Science Foundation of China (Grant No. 22371310), and GBRCE for Functional Molecular Engineering for financial support.

Copyright

© The Author(s) 2026.

References

1. Bringmann G, Tasler S, Endress H, Kraus J, Messer K, Wohlfarth M, et al. Murrastifoline-F: First total synthesis, atropo-enantiomer resolution, and stereoanalysis of an axially chiral N,C-coupled biaryl alkaloid. J Am Chem Soc. 2001;123(12):2703-2711. [DOI][PubMed]
2. Jiang HL, Luo XH, Wang XZ, Yang JL, Yao XJ, Crews P, et al. New isocoumarins and alkaloid from Chinese insect medicine, Eupolyphaga sinensis Walker. Fitoterapia. 2012;83(7):1275-1280. [DOI]
3. Bringmann G, Gulder T, Reichert M, Meyer F. Ancisheynine, the first N,C-coupled naphthylisoquinoline alkaloid: Total synthesis and stereochemical analysis. Org Lett. 2006;8(6):1037-1040. [DOI][PubMed]
4. Mino T, Nishikawa K, Asano M, Shima Y, Ebisawa T, Yoshida Y, et al. Chiral N-1-adamantyl-N-trans-cinnamylaniline type ligands: Synthesis and application to palladium-catalyzed asymmetric allylic alkylation of indoles. Org Biomol Chem. 2016;14(31):7509-7519. [DOI]
5. Abdellah I, Boggio-Pasqua M, Canac Y, Lepetit C, Duhayon C, Chauvin R. Towards the limit of atropochiral stability: H-MIOP, an N-heterocyclic carbene precursor and cationic analogue of the H-MOP ligand. Chem Eur J. 2011;17(18):5110-5115. [DOI]
6. Gan KB, Zhong RL, Zhang ZW, Kwong FY. Atropisomeric phosphine ligands bearing C-N axial chirality: Applications in enantioselective Suzuki-Miyaura cross-coupling towards the assembly of tetra-*ortho*-substituted biaryls. J Am Chem Soc. 2022;144(32):14864-14873. [DOI]
7. Mannschreck A, von Angerer E. The metolachlor herbicide: An exercise in today's stereochemistry. J Chem Educ. 2009;86(9):1054. [DOI]
8. Bock LH, Adams R. Stereochemistry of phenyl pyrroles. XIX. J Am Chem Soc. 1931;53(9):3519-3522. [DOI]
9. Hammer H, Bader BM, Ehnert C, Bundgaard C, Bunch L, Hoestgaard-Jensen K, et al. A multifaceted GABAA receptor modulator: Functional properties and mechanism of action of the sedative-hypnotic and recreational drug methaqualone (quaalude). Mol Pharmacol. 2015;88(2):401-420. [DOI][PubMed][PMC]
10. LaPlante SR, Edwards PJ, Fader LD, Jakalian A, Hucke O. Revealing atropisomer axial chirality in drug discovery. ChemMedChem. 2011;6(3):505-513. [DOI][PubMed]
11. LaPlante SR, Fader LD, Fandrick KR, Fandrick DR, Hucke O, Kemper R, et al. Assessing atropisomer axial chirality in drug discovery and development. J Med Chem. 2011;54(20):7005-7022. [DOI]
12. Lanman BA, Parsons AT, Zech SG. Addressing atropisomerism in the development of sotorasib, a covalent inhibitor of KRAS $G^{12}C$:

Structural, analytical, and synthetic considerations. Acc Chem Res. 2022;55(20):2892-2903. [DOI][PubMed][PMC]
13. Perreault S, Chandrasekhar J, Patel L. Atropisomerism in drug discovery: A medicinal chemistry perspective inspired by atropisomeric class I PI3K inhibitors. Acc Chem Res. 2022;55(18):2581-2593. [DOI][PubMed]
14. Wang Z, Meng L, Liu X, Zhang L, Yu Z, Wu G. Recent progress toward developing axial chirality bioactive compounds. Eur J Med Chem. 2022;243:114700. [DOI]
15. Wu YJ, Liao G, Shi BF. Stereoselective construction of atropisomers featuring a C-N chiral axis. Green Synth Catal. 2022;3(2):117-136. [DOI]
16. Kitagawa O, Kohriyama M, Taguchi T. Catalytic asymmetric synthesis of optically active atropisomeric anilides through enantioselective N-allylation with chiral Pd-tol-BINAP catalyst. J Org Chem. 2002;67(24):8682-8684. [DOI][PubMed]
17. Terauchi J, Curran DP. N-Allylation of anilides with chiral palladium catalysts: The first catalytic asymmetric synthesis of axially chiral anilides. Tetrahedron Asymmetry. 2003;14(5):587-592. [DOI]
18. Zhang S, Yao QJ, Liao G, Li X, Li H, Chen HM, et al. Enantioselective synthesis of atropisomers featuring pentatomic heteroaromatics by Pd-catalyzed C-H alkynylation. ACS Catal. 2019;9(3):1956-1961. [DOI]
19. Li H, Yan X, Zhang J, Guo W, Jiang J, Wang J. Enantioselective synthesis of C-N axially chiral N-aryloxindoles by asymmetric rhodium-catalyzed dual C-H activation. Angew Chem Int Ed. 2019;58(20):6732-6736. [DOI]
20. Zhang J, Xu Q, Wu J, Fan J, Xie M. Construction of N-C axial chirality through atroposelective C-H olefination of *N*-arylindoles by palladium/amino acid cooperative catalysis. Org Lett. 2019;21(16):6361-6365. [DOI][PubMed]
21. Liao G, Shi BF. Synthesis of axially chiral compounds via transition metal-catalyzed atroposelective C-H functionalization. Acc Chem Res. 2025;58(9):1562-1579. [DOI][PubMed]
22. Xiao X, Chen B, Yao YP, Zhou HJ, Wang X, Wang NZ, et al. Construction of non-biaryl atropisomeric amide scaffolds bearing a C-N axis via enantioselective catalysis. Molecules. 2022;27(19):6583. [DOI]
23. Wei J, Zhu M, Zhang B, Li K, Zhang X. Recent advances in atroposelective synthesis of axially chiral heterobiaryl featuring indole frameworks. Tetrahedron. 2023;149:133716. [DOI]
24. Xiang SH, Ding WY, Wang YB, Tan B. Catalytic atroposelective synthesis. Nat Catal. 2024;7(5):483-498. [DOI]
25. Mei GJ, Koay WL, Guan CY, Lu Y. Atropisomers beyond the C-C axial chirality: Advances in catalytic asymmetric synthesis. Chem. 2022;8(7):1855-1893. [DOI]
26. Rodríguez-Salamanca P, Fernández R, Hornillos V, Lassaletta JM. Frontispiece: Asymmetric synthesis of axially chiral C-N atropisomers. Chem Eur J. 2022;28(28):e202282861. [DOI]
27. Yang T, Zhang Y, Dou Y, Yang D, Niu JL. Earth-abundant cobalt-catalyzed enantioselective C-H functionalizations. Sci China Chem. 2026;69(2):659-679. [DOI]
28. Ackermann L. Metalla-electrocatalyzed C-H activation by earth-abundant 3d metals and beyond. Acc Chem Res. 2020;53(1):84-104. [DOI][PubMed]
29. Liao G, Zhang T, Lin ZK, Shi BF. Transition metal-catalyzed enantioselective C-H functionalization via chiral transient directing group strategies. Angew Chem Int Ed. 2020;59(45):19773-19786. [DOI]
30. Chen Z, Zhang F. Recent progress on catellani reaction. Tetrahedron. 2023;134:133307. [DOI]
31. Li T, Leng D, Niu JL, Hu XH, Loh TP. Recent advances in the synthesis of C-N/N-N atropisomers via asymmetric annulation. Top Curr Chem (Cham). 2026;384(1):6. [DOI][PubMed]
32. Umeda N, Tsurugi H, Satoh T, Miura M. Fluorescent naphthyl- and anthrylazoles from the catalytic coupling of phenylazoles with internal alkynes through the cleavage of multiple C-H bonds. Angew Chem. 2008;120(21):4083-4086. [DOI]
33. Li SS, Qin L, Dong L. Rhodium-catalyzed C-C coupling reactions via double C-H activation. Org Biomol Chem. 2016;14(20):4554-4570. [DOI]
34. Doraghi F, Karimtabar MS, Ghasemi M, Larijani B, Mahdavi M. Transition metal-catalyzed dual C-H activation/annulation reactions involving internal alkynes. Chem Rec. 2024;24(7):e202400069. [DOI][PubMed]
35. Yan X, Jiang J, Wang J. A class of readily tunable planar-chiral cyclopentadienyl rhodium(III) catalysts for asymmetric C-H activation. Angew Chem Int Ed. 2022;61(23):e202201522. [DOI]
36. Zhang J, Xu Q, Fan J, Zhou L, Liu N, Zhu L, et al. Pd(ii)-Catalyzed enantioconvergent twofold C-H annulation to access atropisomeric aldehydes: A platform for diversity-oriented-synthesis. Org Chem Front. 2021;8(13):3404-3412. [DOI]
37. Wang P, Huang Y, Jing J, Wang F, Li X. Rhodium(III)-catalyzed atroposelective synthesis of C-N axially chiral naphthylamines and variants via C-H activation. Org Lett. 2022;24(13):2531-2535. [DOI]
38. Si XJ, Yang D, Sun MC, Wei D, Song MP, Niu JL. Atroposelective isoquinolinone synthesis through cobalt-catalysed C-H activation and annulation. Nat Synth. 2022;1(9):709-718. [DOI]
39. Yao QJ, Chen JH, Song H, Huang FR, Shi BF. Cobalt/salox-catalyzed enantioselective C-H functionalization of arylphosphinamides. Angew Chem Int Ed. 2022;61(25):e202202892. [DOI]
40. Wang BJ, Xu GX, Huang ZW, Wu X, Hong X, Yao QJ, et al. Single-step synthesis of atropisomers with vicinal C-C and C-N diaxes by cobalt-catalyzed atroposelective C-H annulation. Angew Chem Int Ed. 2022;61(39):e202208912. [DOI]
41. von Münchow T, Dana S, Xu Y, Yuan B, Ackermann L. Enantioselective electrochemical cobalt-catalyzed aryl C-H activation reactions. Science. 2023;379(6636):1036-1042. [DOI]
42. Wang LN, Fu YLT, Liao CY, Xiao WJ, Lu LQ. Enantioselectivity synthesis of isoquinolin-1-one derivatives with C-N axial chirality via cobalt-

catalyzed oxidative formal (4+2) cycloaddition: Light or not. Chiral Chem. 2026;2(1):202513. [DOI]
43. Si XJ, Zhao X, Wang J, Wang X, Zhang Y, Yang D, et al. Cobalt-catalyzed enantioselective C-H/N-H annulation of aryl sulfonamides with allenes or alkynes: Facile access to C-N axially chiral sultams. Chem Sci. 2023;14(26):7291-7303. [DOI]
44. Zhang Y, Liu SL, Li T, Xu M, Wang Q, Yang D, et al. *N*,*O*-auxiliary enabled cobaltaelectro-catalyzed atroposelective C-H annulation. ACS Catal. 2024;14(1):1-9. [DOI]
45. Wang Y, Zhu X, Pan D, Jing J, Wang F, Mi R, et al. Rhodium-catalyzed enantioselective and diastereodivergent access to diaxially chiral heterocycles. Nat Commun. 2023;14:4661. [DOI]
46. Li T, Zhang Y, Du C, Yang D, Song MP, Niu JL. Simultaneous construction of inherent and axial chirality by cobalt-catalyzed enantioselective C-H activation of calix[4] arenes. Nat Commun. 2024;15:7673. [DOI]
47. Qian PF, Zhou G, Hu JH, Wang BJ, Jiang AL, Zhou T, et al. Asymmetric synthesis of chiral calix[4] arenes with both inherent and axial chirality via cobalt-catalyzed enantioselective intermolecular C-H annulation. Angew Chem Int Ed. 2024;63(52):e202412459. [DOI]
48. Boos P, Pandit NK, Dana S, von Münchow T, Hashidoko A, Haberstock L, et al. Multiple atropo selectivity by κ^2-*N*, *O*-oxazoline urea ligands in cobaltaelectro-catalyzed C-H activations: Decoding selectivity with data science integration. ChemistryEurope. 2025;3(3):e202500071. [DOI]
49. Zhang Y, Yang C, Meng X, Wu M, Yang D, Song MP, et al. Synthesis of remote C-N diaxially chiral compounds via cobalt-catalyzed atroposelective C-H activation. Org Lett. 2025;27(23):6076-6081. [DOI]
50. Das A, Kumaran S, Maity P, Premkumar JR, Sundararaju B. Cobalt-catalyzed enantioselective and diastereodivergent construction of C-N atropisomers. J Am Chem Soc. 2025;147(30):26226-26237. [DOI][PubMed]
51. Li W, Fu L, Xu Y, Zhou Y, Qu J, Wang B. Atroposelective synthesis of isoquinolinone bearing two distinct C-N axes via cobalt-catalyzed enantioselective C-H activation/annulation. Chem Commun. 2026;62(14):4276-4279. [DOI]
52. Qian PF, Wu YX, Hu JH, Chen JH, Zhou T, Yao QJ, et al. Atroposelective synthesis of pyridoindolones bearing two remote distinct C-N axes through cobalt-catalyzed enantioselective C-H activation. J Am Chem Soc. 2025;147(12):10791-10802. [DOI]
53. Sau S, Ali A, Pradhan K, Naskar P, Gandon V, Sahoo AK. Desymmetrization and atroposelective cobalt catalyzed C-H annulation of phosphinic amides with ynamides. Org Lett. 2026;28(10):3236-3242. [DOI][PubMed]
54. Wu M, Meng X, Zhou Q, Du C, Yang D, Niu JL. Asymmetric synthesis of heterohelicenes via cobalt-catalyzed enantioselective C-H activation. ACS Catal. 2026;16(15):14943-14955. [DOI]
55. Sikandar S, Zahoor AF, Ghaffar A, Anjum MN, Noreen R, Irfan A, et al. Unveiling the chemistry and synthetic potential of catalytic cycloaddition reaction of allenes: A review. Molecules. 2023;28(2):704. [DOI]
56. Lin Y, von Münchow T, Ackermann L. Cobaltaelectro-catalyzed C-H annulation with allenes for atropochiral and *P*-stereogenic compounds: Late-stage diversification and continuous flow scale-up. ACS Catal. 2023;13(14):9713-9723. [DOI]
57. Wang X, Si XJ, Sun Y, Wei Z, Xu M, Yang D, et al. C-N axially chiral heterobiaryl isoquinolinone skeletons construction via cobalt-catalyzed atroposelective C-H activation/annulation. Org Lett. 2023;25(34):6240-6245. [DOI]
58. Koner M, Ballav N, Varma AJ, Ghosh S, Mondal T, Kuniyil R, et al. Multifaceted photocatalysis enables cobalt catalyzed enantioselective C-H activation and APEX reaction for C-N axially chiral molecules. Chem Sci. 2025;16(41):19296-19303. [DOI]
59. Liu J, Xiao X, Lai Y, Zhang Z. Recent advances in transition metal-catalyzed heteroannulative difunctionalization of alkenes via C-H activation for the synthesis of heterocycles. Org Chem Front. 2022;9(8):2256-2279. [DOI]
60. Chen W, Jiang J, Wang J. Asymmetric ruthenium-catalyzed C-H activation by a versatile chiral-amide-directing strategy. Angew Chem Int Ed. 2024;63(6):e202316741. [DOI]
61. von Münchow T, Yi-Ru L, Parmar R, Peters SE, Trienes S, Ackermann L. Cobaltaelectro-catalyzed C-H activation for central and axial double enantio-induction. Angew Chem Int Ed. 2024;63(31):e202405423. [DOI]
62. Sarthi , Chandra D, Kumar R, Sharma AK, Isegawa M, Sharma U. Co/salox-catalyzed enantioselective C-H annulation for one-step generation of C-N axial and C central chirality. Org Lett. 2026;28(20):6177-6183. [DOI]
63. Jiang B, Wang H, Sun X, Qiao Y, Xu X, Miao Z. Cobalt/salox-catalyzed stereoselective C-H functionalization: Enantioselective construction of axially chiral cyclic phosphinamides with P-stereogenic center. Adv Synth Catal. 2025;367(9):e202500021. [DOI]
64. Liu ZS, Xie PP, Hua Y, Wu C, Ma Y, Chen J, et al. An axial-to-axial chirality transfer strategy for atroposelective construction of C-N axial chirality. Chem. 2021;7(7):1917-1932. [DOI]
65. Wu C, Liu ZS, Shang Y, Liu C, Deng S, Cheng HG, et al. Asymmetric two-component alkenyl catellani reaction for the construction of C: N axial chirality. Chin J Chem. 2024;42(7):699-704. [DOI]
66. Sun L, Chen H, Liu B, Chang J, Kong L, Wang F, et al. Rhodium-catalyzed atroposelective construction of indoles via C–H bond activation. Angew Chem Int Ed. 2021;60(15):8391-8395. [DOI]
67. Ji J, Wang J. Chiral η^6-benzene ruthenium(II)-catalyzed asymmetric C-H activation/annulation to construct C-N axially chiral indoles. ACS Catal. 2026;16(10):8884-8889. [DOI]
68. Liu S, Xu J, Rawal P, Oliveira JCA, Ackermann L. Electrochemical enantioselective ruthenium(II)-catalyzed C-H activations to atropostable indoles and chiral spiropyrazolones. J Am Chem Soc. 2026;148(19):19773-19780. [DOI][PubMed][PMC]
69. Wang F, Jing J, Zhao Y, Zhu X, Zhang XP, Zhao L, et al. Rhodium-catalyzed C-H activation-based construction of axially and centrally chiral indenes through two discrete insertions. Angew Chem Int Ed. 2021;60(30):16628-16633. [DOI]
70. Li T, Shi L, Zhao X, Wang J, Si XJ, Yang D, et al. C-N axially chiral heterobiaryl skeletons construction via cobalt-catalyzed atroposelective annulation. Org Lett. 2023;25(28):5191-5196. [DOI]

71. Wang P, Wu H, Zhang XP, Huang G, Crabtree RH, Li X. Sigma-bond metathesis as an unusual asymmetric induction step in rhodium-catalyzed enantiodivergent synthesis of C-N axially chiral biaryls. J Am Chem Soc. 2023;145(15):8417-8429. [DOI]
72. Wu YJ, Xie PP, Zhou G, Yao QJ, Hong X, Shi BF. Atroposelective synthesis of *N*-aryl peptoid atropisomers via a palladium(ii)-catalyzed asymmetric C-H alkynylation strategy. Chem Sci. 2021;12(27):9391-9397. [DOI]
73. Wang J, Yao Y, Wang F, Li X. Atroposelective synthesis of C-N axially chiral biaryls via catalytic C-H functionalization at a remote site. Org Lett. 2026;28(13):4048-4054. [DOI]
74. Dhawa U, Wdowik T, Hou X, Yuan B, Oliveira JCA, Ackermann L. Enantioselective palladaelectro-catalyzed C-H olefinations and allylations for N-C axial chirality. Chem Sci. 2021;12(42):14182-14188. [DOI][PubMed][PMC]
75. Yao QJ, Xie PP, Wu YJ, Feng YL, Teng MY, Hong X, et al. Enantioselective synthesis of atropisomeric anilides via Pd(II)-catalyzed asymmetric C-H olefination. J Am Chem Soc. 2020;142(42):18266-18276. [DOI]
76. Li Y, Liou YC, Chen X, Ackermann L. Thioether-enabled palladium-catalyzed atroposelective C-H olefination for N-C and C-C axial chirality. Chem Sci. 2022;13(14):4088-4094. [DOI]
77. Wang L, Yuan WK, Wang ZK, Luo J, Zhou T, Shi BF. Synthesis of C-N axial chirality *N*-arylindoles via Pd(II)-catalyzed free amine-directed atroposelective C-H olefination. Chin J Chem. 2023;41(21):2788-2792. [DOI]
78. Jin S, Wang Y, Yan JX, Xu T, Ning M, Yuan Q, et al. P(=O)R_2-directed asymmetric catalytic C-H olefination leading to C-N axially chiral targets. Org Lett. 2025;27(12):2838-2844. [DOI]
79. Mi R, Chen H, Zhou X, Li N, Ji D, Wang F, et al. Rhodium-catalyzed atroposelective access to axially chiral olefins via C-H bond activation and directing group migration. Angew Chem Int Ed. 2022;61:e202111860. [DOI]
80. Wang J, Chen H, Kong L, Wang F, Lan Y, Li X. Enantioselective and diastereoselective C-H alkylation of benzamides: Synergized axial and central chirality via a single stereodetermining step. ACS Catal. 2021;11(15):9151-9158. [DOI]
81. Hui XS, Bao LY, Ding Y, Kong KX, Zhou T, Yao QJ, et al. Simultaneous construction of axial and central chirality via Ru(II)-catalyzed enantioselective intermolecular C-H alkylation. CCS Chem. 2026;8(2):793-802. [DOI]
82. Li Y, Liou YC, Oliveira JCA, Ackermann L. Ruthenium(II)/imidazolidine carboxylic acid-catalyzed C-H alkylation for central and axial double enantio-induction. Angew Chem Int Ed. 2022;61(47):e202212595. [DOI][PubMed][PMC]
83. Zhang ZJ, Li SW, Oliveira JCA, Li Y, Chen X, Zhang SQ, et al. Data-driven design of new chiral carboxylic acid for construction of indoles with C-central and C-N axial chirality via cobalt catalysis. Nat Commun. 2023;14:3149. [DOI]
84. Li J, Long D, Liu H, Jiang J, Wang J. Expedient modular assembling of chiral η^6-benzene ligands: Empowering ruthenium-catalyzed asymmetric C-H activation. J Am Chem Soc. 2026;148(1):1963-1976. [DOI]
85. Zhang ZJ, Jacob N, Bhatia S, Boos P, Chen X, DeMuth JC, et al. Iron-catalyzed stereoselective C-H alkylation for simultaneous construction of C-N axial and C-central chirality. Nat Commun. 2024;15:3503. [DOI]
86. Mi R, Ding Z, Yu S, Crabtree RH, Li X. *O*-allylhydroxyamine: A bifunctional olefin for construction of axially and centrally chiral amino alcohols via asymmetric carboamidation. J Am Chem Soc. 2023;145(14):8150-8162. [DOI][PubMed]
87. Hu X, Zhao Y, He T, Niu C, Liu F, Jia W, et al. Access to distal biaxial atropisomers by iridium catalyzed asymmetric C-H alkylation. Chem Sci. 2024;15(33):13541-13549. [DOI]
88. Jia ZS, Wu YJ, Yao QJ, Xu XT, Zhang K, Shi BF. Pd(II)-catalyzed atroposelective C-H allylation: Synthesis of enantioenriched *N*-aryl peptoid atropisomers. Org Lett. 2022;24(1):304-308. [DOI][PubMed]
89. Jiang HJ, Geng RL, Wei JH, Gong LZ. Atroposelective sp^3 C–H coupling for kinetic resolution of thioanilide atropisomers. Chin J Chem. 2021;39(12):3269-3276. [DOI]
90. Luc A, Oliveira JCA, Boos P, Jacob N, Ackermann L, Wencel-Delord J. Double cobalt-catalyzed atroposelective C-H activation: One-step synthesis of atropisomeric indoles bearing vicinal C-C and C-N diaxes. Chem Catal. 2023;3(10):100765. [DOI]
91. Hu J, Ferger M, Shi Z, Marder TB. Recent advances in asymmetric borylation by transition metal catalysis. Chem Soc Rev. 2021;50(23):13129-13188. [DOI][PubMed]
92. Zhao H, Chen L, Xia C, Xu S. Enantioselective C-H borylation for the synthesis of axially chiral *N*-aryl phthalimides. Asian J Org Chem. 2023;12(2):e202200695. [DOI]
93. Wang J, Gao DW, Huang J, Tang S, Xiong Z, Hu H, et al. Palladium-catalyzed enantioselective C(sp^2)-H imidoylation by desymmetrization. ACS Catal. 2017;7(6):3832-3836. [DOI]
94. Grosheva D, Cramer N. Enantioselective access to 1H-isoindoles with quaternary stereogenic centers by palladium(0)-catalyzed C-H functionalization. Angew Chem Int Ed. 2018;57(41):13644-13647. [DOI][PubMed]
95. Wang J, Li L, Chai M, Ding S, Li J, Shang Y, et al. Enantioselective construction of 1*H*-isoindoles containing tri- and difluoromethylated quaternary stereogenic centers via palladium-catalyzed C-H bond imidoylation. ACS Catal. 2021;11(19):12367-12374. [DOI]
96. Wang X, Luo Y, Li J, Wang C, Liu Q, He Y, et al. Parallel kinetic resolution through palladium-catalyzed enantioselective cycloimidoylation: En route to divergent *N*-heterocycles bearing a quaternary stereogenic center. ACS Catal. 2022;12(24):14918-14925. [DOI]
97. Wang X, Xu J, Luo Y, Wang Y, Huang J, Zhu Q, et al. DFT-assisted atroposelective construction of indole-fused *N*-heteroaromatic frameworks through palladium-catalyzed C-H imidoylation. ACS Catal. 2025;15(1):201-210. [DOI]
98. Yu T, Li ZQ, Li J, Cheng S, Xu J, Huang J, et al. Palladium-catalyzed modular synthesis of enantioenriched pyridohelicenes through double imidoylative cyclization. ACS Catal. 2022;12(20):13034-13041. [DOI]
99. Luo Y, Xu Y, Wang X, Zhang Y, Lin J, Li J, et al. Enantioselective synthesis of inherently chiral quinoline-fused calix[4] arenes via palladium-

catalyzed C-H cycloimidoylation. Chin J Chem. 2026;44(6):771-776. [DOI]

Publisher's Note

Science Exploration remains a neutral stance on jurisdictional claims in published maps and institutional affiliations. The views expressed in this article are solely those of the author(s) and do not reflect the opinions of the Editors or the publisher.